Investigating the role of ADORA2B receptors in pyroptosis of inflammatory macrophages through gene knockdown and overexpression

by

Fatima Almira Deuna

A Thesis submitted to the Faculty of Graduate Studies of

The University of Manitoba

in partial fulfillment of the requirements of the degree of

MASTER OF SCIENCE

Department of Physiology and Pathophysiology

University of Manitoba

Winnipeg

Abstract

Adenosine receptors (ARs) regulate the immune response by activating pro- and anti-inflammatory cascades through mechanisms that are not completely defined.[68] Macrophages also play a central role in the regulation of inflammation from initiation to resolution.[4] ARs on macrophages have been shown to direct major functions including macrophage cell death.[46] Pyroptosis is a highly immunogenic cell death induced by inflammasomes that cause cleavage of caspases and gasdermins.[9-13] This process leads to the release of inflammatory cytokines Interleukin 18 (IL-18) and Interleukin -1β (IL-1β).[11] The canonical pathway that leads to pyroptosis involves the NLRP3 (nucleotide-binding domain, leucine-rich–containing family, pyrin domain–containing-3) inflammasome, caspase-1 and gasdermin-D (GSDMD), though other pathways exist.[10] Recently, our lab found that knocking down the Adenosine 2B (A_{2B}) receptor renders macrophages susceptible to pyroptosis.[46] In this thesis, we seek to confirm the role of the NLRP3 inflammasome specifically in pyroptosis observed after A_{2B} receptor knockdown, and whether lost receptor-protein interactions promote this pathway. Results show that in A_{2B} receptor deficient macrophages, NLRP3 inhibition was able to prevent IL-1β secretion and GSDMD cleavage. However, addition of adenosine to macrophages induced GSDMD cleavage that was not sensitive to NLRP3 inhibition. Furthermore, preliminary experiments showed that caspase-4 was activated by adenosine. Proteomic analysis was used to study receptor-protein interactions and pyroptotic proteins were identified in immunoprecipitation assays. A_{2B} coimmunoprecipitation in epithelial cells and macrophages show that A_{2B} receptors enrich and interact with cellular communication, calcium signaling and gap-junction proteins as well as Toll-like receptor signaling, and serine proteases. Results from proteomics and gene ontology analysis have identified possible alternative pathways through which the A_{2B} receptor might influence macrophage pyroptosis.

Acknowledgements

I would like to acknowledge my supervisor, Dr. Robin da Silva, who has continually guided me throughout my experiments and graduate journey and has taught me good science, critical thinking, and effective writing.

I would also like to acknowledge my committee members: Dr. Christopher Pascoe, and Dr. Peter Thompson, who has given me advise and feedback on experiments and my knowledge to be a better scientist.

I would also like to acknowledge our lab Technician, Ms. Peisan Lew, who has taught me technical skills and keeping the laboratory tidy and organized.

Dr. Samantha Pauls has provided us with THP-1 cells, as well as Phorbol-12-myristate-13-acetate, Dr. Xie, for allowing us to use his lab's sonicator, and Dr. Cattini for allowing us to use his lab's cell plate reader and PCR machine.

Dedication

I dedicate this thesis to my family and friends, and my partner who were patient with me throughout my graduate studies, for all the support they have given, for listening to all my stories, for engaging in my ideas and taking care of me.

"Either write things worth reading, or do things worth writing"- Benjamin Franklin

Table of Contents

List of Tables

List of Figures

1.0 Introduction

1.1 Macrophage pyroptosis increases inflammatory response as a defense mechanism

The body eliminates pathogens such as bacteria and viruses through an orchestrated response, collectively known as inflammation. Inflammation includes the detection of stimuli, activation of cellular pathways, increasing expression of pro-inflammatory factors, and recruitment of immune cells to a site of invasion or injury.[1] These immune cells function to engulf invasive pathogens, and process foreign material to communicate with other cells, developing a process to recognize and eliminate the pathogen from the body.[2] Excessive inflammation can cause damage to the host; therefore, the immune response must be regulated and balanced. Our immune system is comprised of various types of immune cells, each playing a role in the inflammatory response.

Macrophages are immune cells specializing in the clearing of cellular debris and pathogens, a process called phagocytosis.[28] Because of this, they are known as the body's first line of defense. Macrophages reside in tissues and can also be derived from circulating monocytes. Monocytes differentiate into macrophages when they sense a danger signal such as a Pathogen Associated Molecular Pattern (PAMP) or a Damage Associated Molecular Pattern (DAMP) through special receptors.[1] Macrophages then engulf the pathogen and create antigens to present to other immune cells which help identify a threat.[3] Through this process, our immune system recognizes and attacks pathogenic cells and not healthy cells.[48] Non-circulating macrophages that are present within tissues are known as "resident macrophages".[4] Resident macrophages have names based on the organs they reside in or given by scientists who describe or discovered them. A few examples include liver macrophages known as Kupffer cells, lung macrophages known as alveolar macrophages, and neuronal macrophages known as microglia.[1]

These macrophages are known to help in tissue maintenance, repair, and remodelling.[71] Macrophages play a central role from initiation to resolution of inflammation and efficiently balance the immune response to maintain homeostasis. The diverse functionality of macrophages is possible through the activation of different macrophage phenotypes.[4]

Macrophages can display different phenotypes based on the stimulus present in the environment, which then direct its function. There are two main macrophage phenotypes: classically or alternatively activated macrophages.[72] Phagocytosis is performed by classically activated macrophages (M1 macrophages) which initiate the inflammatory response. M1 activation is stimulated by lipopolysaccharide (LPS), a component of bacterial cell wall, or distress signals released by infected or injured cells like interferon-γ (IFN-γ), Tumor Necrosis Factor-α (TNF-α), and Granulocyte Macrophage Colony Stimulating Factor (GM-CSF).[6] M1 macrophages release proinflammatory cytokine Interleukin-1β (IL-1β), and TNF-α that attracts other immune cells and signals the presence of the threat.[5] The main function of M1 macrophages is to eliminate the pathogen. On the other hand, alternatively activated macrophages (M2 macrophages) turn off the inflammatory response and initiate the healing process. M2 macrophages are activated by cytokines Interleukin-4 (IL-4), Macrophage Colony Stimulating Factor (M-CSF), Transforming Growth Factor-β (TGF-β), and Interleukin-10 (IL-10).[6] These cytokines signal wound healing and repair through stimulation of extracellular matrix formation.[6] Figure 1 represents stimulating factors and corresponding activated macrophage phenotype. Balancing macrophage activity is crucial to the immune response. Insufficient response can lead to an environment where pathogens continue to grow, whereas too much of an inflammatory response can lead to excessive tissue injury. Such balance is also applied in macrophage cell death. Most programmed cell deaths package cellular components to prevent

overstimulation of the immune response. However, some cell deaths function to increase inflammation.

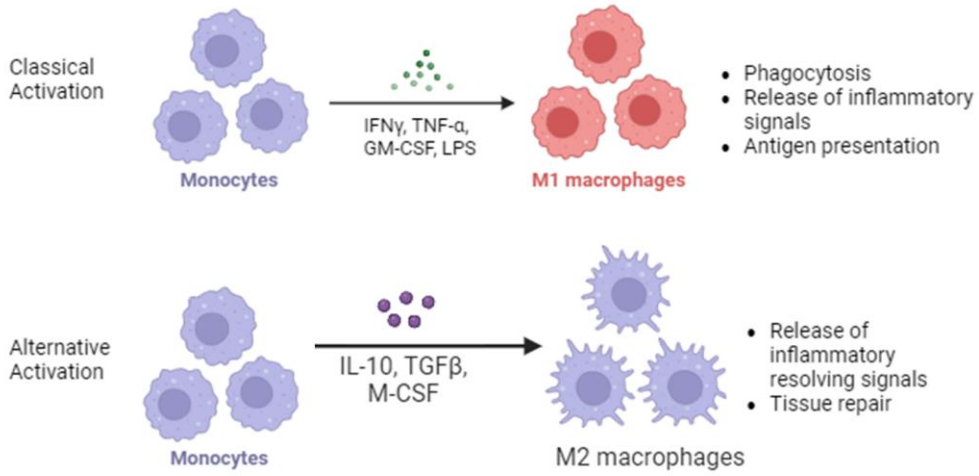

Figure 1: Activators for monocyte differentiation to M1 and M2 macrophage phenotypes and function. Image created using Biorender.

Macrophage pyroptosis is a lytic cell death which specifically functions to increase inflammatory response. Cell death is a tightly regulated process induced by different stimuli and can serve specific physiological functions including elimination of damaged cells, maintaining homeostasis, and immune response.[49] Pyroptosis is an inflammatory cell death characterized by cell membrane pore formation and release of cytokines.[10] Its inflammatory function involves the protease caspase-1, gasdermin D (GSDMD), and proinflammatory cytokines IL-1β, and interleukin-18 (IL-18).[77] Pyroptosis has been predominantly studied in macrophages. Macrophage pyroptosis is described as a protective mechanism for tissues that create an immediate and amplified immune response to a danger signal. Triggered by agents or cellular distress signals, pyroptosis has a role in cancer surveillance and suppression, allergies, autoimmune diseases, tissue injury, and infections.[9,10] A fairly new concept, first described in 1986, there is still much unknown about the mechanisms that regulate pyroptosis and its role in physiology.[10]

Pyroptosis is inflammatory due to the release of relatively large, local amounts of IL-18, and IL-1β.[77] Pyroptosis is known to be initiated through two different cellular pathways: canonical and non-canonical.[10] The canonical pathway is activated when Nod-like receptors with leucin-rich pyrin domains form an inflammasome by associating with an apoptosis associated speck like protein (ASC) containing a caspase activation and recruitment domain.[12] This process is triggered upon recognition of a stimulus, usually a DAMP or PAMP.[11] Unlike other inflammasomes that have very specific activators, the NLRP3 inflammasome has been studied extensively in macrophages and is activated by a variety of stimuli including uric acid, extracellular adenosine triphosphate (ATP), viral pathogens, etc.[102] The active inflammasome recruits and activates caspase-1 which then cleaves GSDMD, IL-18, and IL-1β, thereby activating these molecules. The N-terminal fragment of the cleaved GSDMD protein associates with the plasma membrane and forms pores, causing the release of cellular contents including the cleaved IL-18 and IL-1β.[12,14] These cytokines serve as an inflammatory signal and recruit immune cells to the site. Figure 2 below provides a representation of the canonical pathway.[14] The second cellular pathway that can initiate pyroptosis is triggered by LPS binding to Toll-like receptor 4 (TLR4). TLR4 activation stimulates the transcription and expression of caspases 4 and 5, which then cleave GSDMD, but it also stimulates increase in transcription of NLRP3.[115] Therefore, although not as robust, the non-canonical pathway also activates NLRP3 and caspase-1, causing the release of IL-18 and IL-1β.[13] Figure 2 below represents the activation of the non-canonical pathway. Both pathways protect the cells from invasive pathogens as it creates an increased inflammatory response.

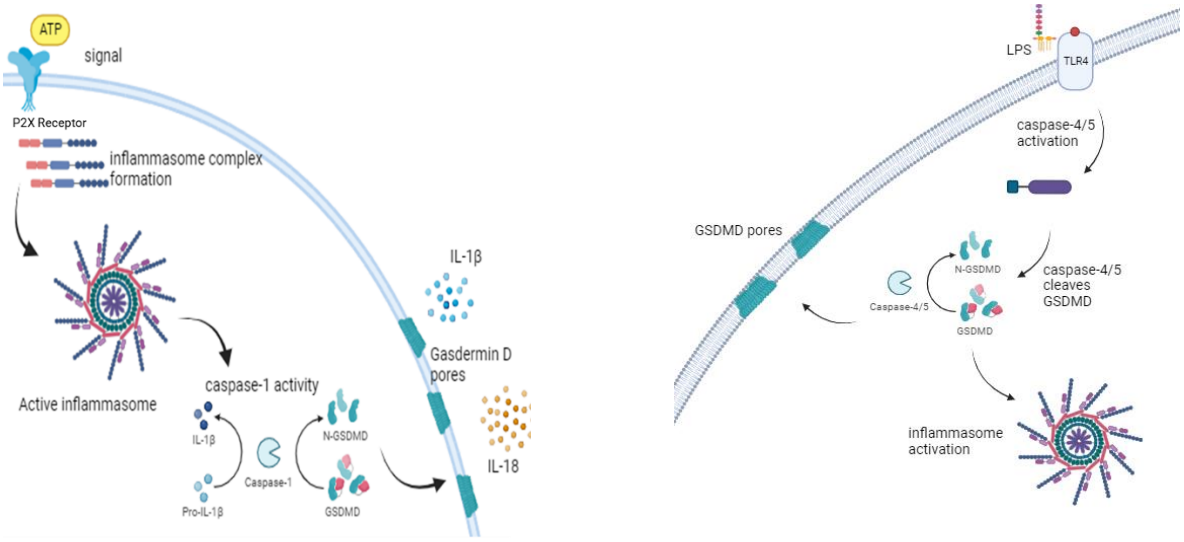

Figure 2: Canonical (left) and noncanonical (right) activation of pyroptosis. Image created using Biorender.

Other inflammasomes, gasdermins, and caspases have also been identified in pyroptosis. NLRP1, Nucleotide-binding domain family, leucine-rich repeat containing, caspase-recruitment domain containing 4 (NLRC4), and Interferon inducible protein (also known as "absent in melanoma 2", AIM2) are able to assemble and form inflammasomes, and are activated by very specific activators.[10] These inflammasomes cleave caspase-1 and activate the canonical pathway of pyroptosis as well.[10, 12] On the other hand, caspase-8 and caspase-3 has also been shown to trigger pyroptosis, apart from caspases-1, -4, and -5. Caspase-8 is activated by TLR3 and TLR4 signalling and cleaves GSDMD.[74-76, 125-127] It is also presumed in the literature that all gasdermins: GSDMA, GSDMB, GSDMC, GSDMD, GSDME and PJVK (pejvakin), have pore-forming potential after cleavage.[76] GSDMD, is cleaved by caspase-1, -4, -5, -11, and -8, GSDME is cleaved by caspase-3, while the proteins responsible for cleavage of other gasdermins have not been identified.[76] The involvement of these proteins in pyroptosis are still being characterized and features of cross talk and various mechanisms of regulation have been proposed.

Understanding the mechanisms through which pyroptosis is modulated by the cell may provide potential therapeutic targets for inflammatory conditions that arise through pyroptosis.

Dysregulation of pyroptosis and NLRP3 activation cause excessive inflammation that is implicated in many conditions such as liver disease, atherosclerosis and Alzheimer's disease. For example, in mice fed with methionine/choline deficient diet, an increased level and activation of caspases and inflammasomes were observed by Wu *et al*.[16] This promoted inflammation, fibrosis, and liver damage, thereby contributing to liver failure.[16] In the heart, factors released by atherosclerotic plaques induces the activation of NLRP3, which increases the incidence of plaque rupture and heart attack.[17] In the brain, an inhibitor of the NLRP3 inflammasome has been shown to attenuate the symptoms and the development of Alzheimer's disease in mice.[18] Finally, Okamoto *et al.* have found that melanoma cells activate NLRP3 and release IL-1β spontaneously, arguing that this release causes many autoinflammatory conditions.[15] These findings demonstrate how pyroptosis can cause excessive inflammation that exacerbate pathological conditions. Interestingly, adenosine and its receptors have recently been linked to pyroptosis are known immune regulators.

1.2 Adenosine Receptors modulate macrophage function and pyroptosis

Adenosine receptors (ARs) are found on the plasma membrane and are expressed by numerous cell types and affect many cellular functions. ARs activate a variety of biological processes essential for cell survival including cell growth and proliferation, vasodilation, neurotransmission, and immunomodulation.[19] Adenosine is formed primarily from the breakdown of ATP. During conditions where there is release of ATP from cells, ectonucleotidases CD39 and CD73 break down ATP and adenosine diphosphate (ADP) to adenosine monophosphate (AMP), and AMP to adenosine respectively.[73] Adenosine levels are highest

during stressful conditions such as hypoxia, ischemia, and inflammation.[65] Adenosine functions as an autocrine and paracrine alarm molecule, with varying effects on inflammation.[68] Some adenosine receptors have been shown to promote inflammatory responses in mast cells, epithelial cells, and smooth muscle cells.[70] On the other hand, in animal models of Multiple Sclerosis (MS) and autoimmune encephalomyelitis, activation of an adenosine receptor ameliorates inflammation.[69] Overall, adenosine's effects on inflammation is unclear and appears to depend on the cell or tissue type involved. Adenosine's wide variety of effects are implemented through its four subtypes.

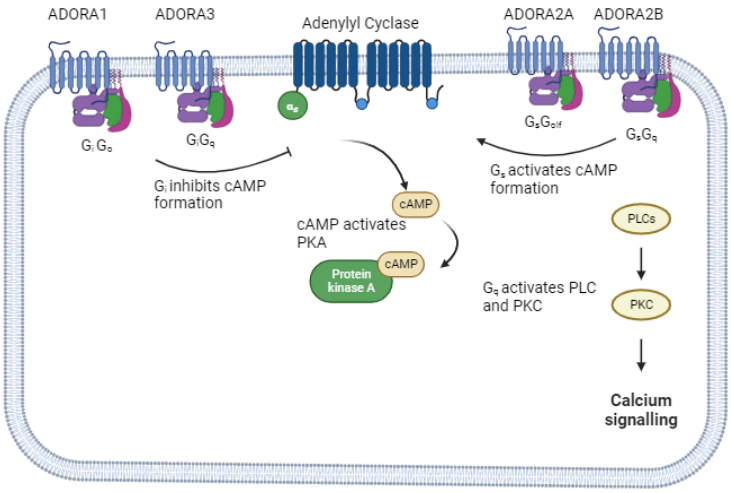

Figure 3: Adenosine receptors and their respective G-proteins signalling mechanisms. Image created through Biorender.

Adenosine exerts its effects through four major types of ARs: ADORA1 (A_1), ADORA2A (A_{2A}), ADORA2B (A_{2B}), and ADORA3 (A_3). These are G-protein coupled receptors (GPCRs) that bind to different G proteins, thereby affecting different signalling cascades. The A_1 receptor interacts with G_i or G_o proteins, A_{2A} interacts with G_s or G_{olf} proteins, A_{2B} interacts with G_s or G_q proteins, and A_3 interacts with G_i or G_q proteins.[20] ARs were thought to primarily exert their influence by either activating or inhibiting the enzyme adenylyl cyclase (AC) through G_s or G_i respectively.[21] Activation of AC triggers the production of a secondary messenger known as

cyclic adenosine monophosphate (cAMP), which activates protein kinase A (PKA).[22] Once activated, PKA phosphorylates numerous enzymes and transcription factors, setting off a cascade of signals that ultimately regulate a wide array of cellular processes, including cell proliferation, growth, arrest and apoptosis. [23, 25] The other main signalling pathway attributed to ARs is that of phospholipase C (PLC), through the G_q protein, that is bound to A_{2B} and A_3 receptors.[24] The PLC pathway affects cellular calcium signalling, and protein kinase C (PKC) which is responsible for gene expression, protein secretion, and inflammatory response in the cell.[26] Figure 3 summarizes the G-proteins linked to the specific ARs and the signalling cascades they activate.

The different AR subtypes can also affect cellular function independently of GPCR signalling through protein-receptor and receptor-receptor interactions.[30-34] For example, A_{2A} and A_{2B} both bind to the same G-protein that increase cAMP signalling, and therefore increase TNF-α production. However, it was found in human primary monocytes that A_{2A} antagonism inhibited TNF-α production, whereas A_{2B} antagonism did not,[59] suggesting that A_{2A} and A_{2B} receptors can induce cellular responses independent of cAMP and GPCR signalling. Protein-protein interactions (PPI) could provide a possible mechanism to explain divergent function of receptors that have the same bound G protein. Protein interactions with ARs provide a more complex signalling mechanism that could be used to fine tune tightly regulated cellular processes such as pyroptosis and macrophage activation. PPI can alter enzyme kinetics, affect substrate binding, create new binding sites, inactivate/suppress a protein, change the specificity of a protein and more.[42] For example, in the striatum, A_{2A} receptors interact with Dopamine-D_2 receptors, which decrease the affinity and activation of D_2 receptors.[60] Another example of AR PPI effects are A_1 and A_{2A} receptor heteromers.[96] Once in the heteromeric form, the receptors respond like a concentration dependent switch.[61] At higher concentrations, A_{2A} receptors are activated, whereas

in lower concentrations, A_1 receptors are activated.[61] AR PPI's have vast effects in cellular signalling dependent on cell type (Table 1). Interestingly, the A_{2A} receptor has been shown to physically interact with Cathepsin D. Blocking Cathepsin D activity increased A_{2A} activity, leading to increased inflammation in peritoneal macrophages.[62] These examples show that AR PPIs could possibly affect macrophage function and immune response.

Table 1: Effects of interacting proteins with each AR, found in different cell types.

Adenosine receptor	**Interacting protein**	**Cell Type**	**Effect**
ADORA1	Adenosine Deaminase (ADA) Dopamine receptors Neurobin	Epithelial Neurons and fibroblasts Brain	Increased efficiency in receptor signaling D_1 depress A_1 effects Anti-convulsant[66] Unknown
ADORA2A	Ubiquitin-specific protease 4 (USP4) Cathepsin D mGlu5 receptor	endothelial Peritoneal macrophages Striatum[71]	Quality control of A_{2A} expression from ER[67] Increased inflammation[62] Unknown
ADORA2B	Snap receptor 23 (SNARE-23) P105 APIP	Endothelial Endothelial Cardiomyocytes	Plasma membrane recruition[65] Anti-inflammatory[63] Cardioprotection[64]
ADORA3	N/A		

Adenosine plays a big role in directing macrophage function in inflammation, but the mechanisms are still unclear. Table 2 below outlines the effects of each AR subtype on macrophages.

Table 2: Summary of adenosine receptor effects on macrophages.[24, 27, 28, 29]

Adenosine receptor	**Reported effect on macrophages**
ADORA1	Osteoclast and multinucleated giant cell monocyte differentiation[27] Enhances Fcγ- mediated phagocytosis[28]
ADORA2A	Downregulates classical activation[27] Promotes angiogenesis through Vascular Endothelial Growth Factor (VEGF)[27] Decreased TNF-α production Decrease in macrophage apoptosis[27]

	Suppresses Fcγ- mediated phagocytosis[28] Synergistic upregulation of VEGF with Toll Like Receptors(TLRs)[29]
ADORA2B	Upregulates alternative activation[27] Promotes angiogenesis through VEGF[27] Monocyte to dendritic cell[27] Suppression of TNF-α[24] Suppresses macrophage proliferation[28] Suppresses Fcγ- mediated phagocytosis[28] IL-6 release[28]
ADORA3	Promotes angiogenesis through VEGF[27] Prevents oxidative burst[28]

The AR subtypes have been shown to affect pyroptosis differently. For example, through an unknown mechanism, A_1 receptors suppress caspase-1, and IL-18 release in pyroptosis.[35] Similarly, the A_3 receptors were shown to inhibit NLRP3, GSDMD, and caspase-1.[36,40] Conversely, A_{2A} has been shown to activate pyroptosis through the cAMP/PKA pathway in one study, and A_{2A} activation is required for sustained inflammation.[37, 52] Additionally, inactivation of A_{2A} receptor leads to decreased NLRP3 activation, implying that A_{2A} activity is necessary for the activation of NLRP3.[54] Many aspects of adenosine's link to pyroptosis are still being elucidated.

A_{2B}'s effects on inflammation and pyroptosis are mixed and appear to vary based on cell type. A_{2B} has been linked, alongside A_{2A}, to pro-inflammatory effects and pyroptotic activation in lung injury.[55] On the other hand, A_{2B} receptor regulates CD73 which inhibits GSDMD and NLRP3 inflammasome in hematopoietic stem cells through heme-oxygenase-1 activation.[38, 39] As listed in Table 2, A_{2B} receptors promote alternative activation of macrophages, angiogenesis through VEGF, suppression of TNF-α, and suppression of phagocytosis, all of which are anti-inflammatory in nature.[50] A_{2B} activation can protect the heart in ischemia [41] and A_{2B} expression is higher in inflammatory macrophages than in macrophages resolving inflammation.[59] Furthermore, knocking down the A_{2B} receptor causes macrophages to become prone to pyroptosis, implying an important role of the A_{2B} receptor in the protection of the cell during

inflammation.[46] This result is a novel discovery that provides a new target for mediating pyroptosis and regulating inflammation through the A_{2B} receptors.

1.3 Elucidating the role of A_{2B} in macrophage pyroptosis

The objective of this thesis is to elucidate the mechanism by which the A_{2B} receptor regulate inflammatory macrophage pyroptosis observed in the study by Eudy and da Silva.[46] There are two aims in this study of adenosine receptor function: (1) Determine whether the NLRP3 inflammasome is specifically involved in A_{2B} knockdown associated pyroptosis and (2) Identify A_{2B} receptor-protein interactions in macrophages. A two-part project was designed: A_{2B} knockdown macrophages were treated with specific NLRP3 small molecule inhibitor MCC950 to identify the inflammasome's involvement in this pathway; and A_{2B} overexpression, coimmunoprecipitation, and proteomics were used to study potential protein-protein interactions. This study employed western blotting, polymerase chain reaction (PCR) and Enzyme-linked immunosorbent assay (ELISA) to study protein, mRNA, and cytokine expressions respectively. We hypothesized that (1) A_{2B} inhibits pyroptosis with a mechanism involving the NLRP3 inflammasome, and (2) A_{2B} interacts with a multitude of proteins during inflammation that could be mediating this pyroptosis.

Protein knockdown studies can be limited by compensatory mechanisms within the cells. In Eudy and da Silva's study, knocking down the A_{2B} receptor alone caused macrophages to increase pyroptotic markers cleaved caspase-1, and GSDMD.[46] However, the mechanisms responsible for this observation were not clear. Combining two techniques, protein knockdown and small molecule inhibition, allowed us to specifically target possible compensatory mechanisms. MCC950 is reported to be a specific NLRP3 inhibitor that decrease inflammation,

through inhibiting the ATPase activity of NLRP3.[51] If MCC950 is able to attenuate the effects of A_{2B} knockdown in pyroptosis, this mechanism could be linked to NLRP3 activation. Through these methods we aimed to confirm the involvement of NLRP3 in A_{2B} knockdown induced pyroptosis.

The second part of the project involved overexpression of HA-tagged A_{2B} receptor to study receptor-protein interactions in THP-1 macrophages. In vector design, an HA-tag was added to the N terminus of A_{2B} to facilitate downstream immunoprecipitation of the receptor, along with interacting proteins. Aside from the previously described interacting proteins in Table 1 above, A_{2B} has also been shown to coimmunoprecipitate with netrin-1,[56] Dopamine receptor D2 (DRD2)[57], and metabotropic glutamate receptors (mGluR) to name a few. [58, 32] Interestingly, the A_{2B} receptor interacts with ezrin, sodium/hydrogen exchanger isoform 3 regulator 2 (E3KARP), and snare protein 23 (SNAP-23), which have been associated with programmed cell death, apoptosis.[82] A_{2B} stimulation increased ezrin-E3KARP interaction, which was not observed in simple cAMP stimulation using forskolin.[43] Therefore, it is implied that this is not occurring through GPCR-cAMP activation. Furthermore, E3KARP has been shown to decrease cell death by modulating mGluR5 signalling which has been shown to increase neuronal cell death through PLC activation.[44, 62] Similarly, upregulation of Ezrin protected leukemia cells from ursolic acid mediated cell death.[45] These proteins have not been coimmunoprecipitated with A_{2B} and in our research, proteins ezrin, E3KARP and SNAP23 were potential candidates to coimmunoprecipitate with A_{2B}. This would have shown a possible mechanism of A_{2B}'s cell protective function. Proteomics is an evolving and emerging field of biology and not many studies have been done on adenosine receptors.[34] Additionally, AR protein-protein interactions have not been studied extensively in macrophages. Using proteomic analysis, we sought to

identify putative co-immunoprecipitated proteins with A_{2B} to provide evidence that these proteins are interacting. However, these interactions need to be confirmed and potential mechanisms need to be further studied.

Understanding the role of A_{2B} in macrophage pyroptosis can contribute to our scientific knowledge of immune regulation, cell death, and inflammation. A_{2B} receptors are not fully understood and its effects on pyroptosis is a novel discovery. Through this research we clarified the link of the NLRP3 inflammasome to A_{2B} and found proteins that may interact with the A_{2B} receptor in macrophages.

2.0 Materials and Methods

2.1 Cell culture

THP-1 cells obtained from American Type Culture Collection (ATCC, Virginia, USA), were maintained in RPMI-1640 media (GIBCO, New York, USA) supplemented with 10% (v/v) Fetal Bovine Serum (FBS, GIBCO), 0.25µg/mL Amphotericin B (Alfa Aesar, Massachusetts, U.S.A.) 10µg/mL Gentamycin (Fisher Bioreagents, Pennsylvania, USA), and 0.05µM 2-mercaptoethanol (Alfa Aesar). Cells were grown in T75 flasks (ThermoFisher Scientific, Massachusetts, U.S.A.) and incubated at 37°C and 5% CO_2.

To change media, cell suspensions were transferred from T75 flasks to 15mL centrifuge tubes (Corning, Arizona, USA) and centrifuged at 100 x g for 1 min using Sorvall ST8 Centrifuge (ThermoFisher Scientific), forming a cell pellet. 75% of the supernatant was aspirated, and new, warmed media was added to resuspend the cells before transferring back to T75 flasks. The cell density was kept between $1x10^5$ cells/mL and $9x10^5$ cells/mL. Media was changed every 1-2 days, depending on cell density.

For cell counts, 100µL of 0.4% Trypan Blue stain (GIBCO) and 100µL of cell suspension were mixed in sterilized microcentrifuge tubes and allowed to sit for 1-2 minutes. 10µL of this mixture was placed on the hemocytometer (Hausser Scientific, Pennsylvania, USA), and cells within each of the four quadrants were counted and total number of cells were calculated.

THP-1 monocytes were grown and maintained until ready for passaging or there is enough for experiments. Cells were differentiated into macrophages by adding Phorbol-12-myristate-13-acetate (PMA) with a final concentration of 5µL/mL, and incubating in 37°C, 5% CO_2 for 48 hours. After which, the cells phenotypically change from suspension cells to adherent cells as

macrophages. Media was removed, the cells were washed twice with warmed Phosphate Buffer Saline (PBS, GIBCO), and new media was added on the macrophages for experiments.

2.2 A_{2B} siRNA Knockdown

Cells were plated at $1.2x10^6$ cells/well in 6-well plates and differentiated into macrophages as described above. New media was added for transfection: RPMI-1640 supplemented with 10% FBS. Antibiotics were not added in this media as it will interrupt the transfection process.

2.2.1 siRNA transfection and PMA differentiation

Validated ADORA2B (A_{2B}) siRNA Silencer Select (AMBION, Pennsylvania, USA) with the sequence (sense: 5'- AGACUUCCGCUACACUUUUTT- 3', antisense: 5'- AAAAGUGUAGCGGAAGUCUCG) and Lipofectamine 3000 (ThermoFisher Scientific) was used to knockdown the A_{2B} receptor. Following the product protocol, all chemicals were allowed to reach room temperature before transfection procedure. The transfection procedure was optimized by testing a variety of siRNA concentrations, Lipofectamine volumes, and time incubation periods and measuring transfection efficiency through qPCR. Results of this optimization is shown in section 3.1, Figures 4-7. After optimization, the procedure is as follows: 5nM of A_{2B} siRNA or scramble siRNA were diluted into 250µL OptiMEM media (GIBCO) for each well that need to be transfected. Similarly, 5µL of Lipofectamine 3000 was diluted in 250µL OptiMEM for each well that needed to be transfected. The Lipofectamine and siRNA solutions are combined according to Table 3 below. This solution was allowed to incubate for 10 mins at room temperature before it was added to the wells in a drop wise manner. The cells were then incubated in 37°C, 5% CO_2 for 36 hours before treatment.

Table 3: Final volumes of the transfection solutions per well on a 6-well plate.

Solution	Knockdown cells	Scramble cells

siRNA	4.5µL of 5µM A_{2B} siRNA	4.5µL of 5µM scramble siRNA
Lipofectamine 3000	5µL	5µL
OptiMEM	500µL	500µL

2.2.2 Treatments

36 hours after transfection, media was aspirated and replaced with new, warmed 2 mL of RPMI-1640 (without FBS or antibiotics). Ten different treatment conditions were applied to both the A_{2B} siRNA knockdown and the scramble treated cells for a total of 20 groups. The treatment groups are listed on Table 4 below. Treatments were consisted of lipopolysaccharide (Sigma Aldrich, Missouri, USA), adenosine (Sigma Aldrich), ATP (Sigma Aldrich), and MCC950 (Millipore Sigma, Darmstadt, Germany). To be consistent, all treatment solutions were diluted to a final concentration of 1% (v/v) Dimethyl sulfoxide (DMSO, Fisher Bioreagents), and the vehicle group was treated with a 1% (v/v) DMSO diluted in PBS solution. Concentrations of treatments were identified through a mix of references and optimizing dosage through experiments. LPS and adenosine were identified previously by our lab.[46] ATP concentration was optimized and shown in Figure 8, and MCC950 concentration was identified through the literature,[77] and this was shown to work in Figure 9 below. Cells were incubated in treatment for a total of 4 hours.

Table 4: Treatments for the Scramble and Knockdown transfected THP-1 cells.

Group	**Scramble or Knockdown**
1	Vehicle (1% DMSO)
2	LPS (5ng/mL)
3	Adenosine (1mM)
4	ATP (3mM)
5	MCC950 (1µM)

6	LPS (5ng/mL) + MCC950 (1μM)
7	LPS (5ng/mL) + Adenosine (1mM)
8	LPS (5ng/mL) + ATP (3mM)
9	LPS (5ng/mL) + Adenosine (1mM) + MCC950 (1μM)
10	LPS (5ng/mL) + ATP (3mM) + MCC950 (1μM)

LPS addition: For groups 7-10, LPS was added first and incubated for 3 hours in 37°C and 5% CO_2. After which, the media was aspirated and replaced before adding Ade, ATP, MCC950, or a combination of these drugs, and incubated for 1 hr in 37°C and 5% CO_2.

MCC950 Addition: For group 6, MCC950 was added before LPS to test MCC950's inhibition of LPS priming. For groups 9 and 10, MCC950 was added after LPS priming for 3 hours, and before Adenosine or ATP, to test MCC950's ability to inhibit the effects of the specific drug being tested.

After treatment, 1mL of media was collected in labelled microcentrifuge tubes for the IL-1β Human ELISA kit (Invitrogen, Ontario, Canada). The rest of the media was aspirated, and cells were washed with PBS twice. 50μL of Radioimmunoprecipitation assay buffer (RIPA buffer) supplemented with protease and phosphatase, or 400μL RNAzol RT (Sigma Aldrich), was added to each well of adhered cells for western blotting or PCR, respectively. Cells were scraped, and the lysates were collected in microcentrifuge tubes. Both media and cell lysates were stored in -80°C until ready for analysis.

2.2.3 Western blotting

2.2.3.1 Making gels and solutions

12% TGX Stain-Free FastCast Acrylamide Kit (Bio-rad, California, U.S.A.) was used to make gels. Following the protocol, the resolving portion of the gel was made by mixing equal parts resolver solution A and B provided in the kit and adding Tetramethylethylenediamine (TEMED, Fisher Bioreagents) to a final concentration of 0.05% (v/v) and 0.5% (v/v) of 10% Ammonium Persulfate (APS, Fisher Bioreagents). This solution was poured into 1.5mm glass plates and allowed to polymerize for 15-30 mins. After which, the stacker gel was made in a similar way, mixing equal parts stacker solution A and B and adding a final concentration of 0.1% (v/v) TEMED and 0.5% (v/v) 10% APS. This was poured on top of the resolving gel, then allowed to polymerize for 15-30 mins with a comb in place to make 10- or 15-well gels.

2.2.3.2 Sample preparation

Samples were sonicated to break down the cell membrane and release proteins from the cells. Protein samples in RIPA buffer were sonicated three times for 5 pulses, making sure there is time in between for the sample to cool, and prevent overheating. The sonicated samples were then transferred to new labelled microcentrifuge tubes for protein concentration tests.

Following the protocol, Pierce Bicinchoninic acid (BCA) Protein Assay Kit (ThermoFisher Scientific) was used to quantify the proteins present in the sonicated samples. Standards were made from the 2mg/mL protein aliquot provided in the kit. 1mg, 0.5mg, 0.25mg, 0.1mg, 0.05mg, and 0.025mg/mL were the concentrations used to make the standard curve. Samples were diluted 5x with MilliQ water. 10µL aliquots of either standard or sample were added into the wells of a 96-well microplate. Working reagent was made by mixing 50 parts

Reagent A with one part Reagent B, provided in the kit. 200µL of working reagent is added onto each well and mixed in a shaker. The mixture was allowed to sit for 30 mins at 37°C. Nanodrop One (ThermoFisher Scientific) was used to measure the absorbance of each sample at 562nm. An installed BCA assay measurement program was used in the Nanodrop One software where protein concentrations were calculated by the computer from absorbance values. A final concentration of 1µg/µL of loading sample was made by calculating how much volume of sample to add to 4x Laemmli buffer (Bio-rad) and 2-mercaptoethanol (9 parts Laemmli: one part 2-mercaptoethanol). The final volume of the sample was 25% Laemmli, thereby diluting the 4x to 1x.

2.2.3.3 Gel electrophoresis

Mini-PROTEAN tetra cell (Bio-rad) was used to run the gel electrophoresis. Gels were placed on the running module and into the buffer tank which was then filled with enough 1x Sodium dodecyl sulfate (SDS) Running buffer. 30µg of sample were loaded per well and 10µL of the standard ladder was also loaded on one of the wells for reference. The tank was connected to a power supply (PowerPac Basic, Bio-rad) and ran at 150mV, 400mA until samples have entered the stacking gel, and then the charge was increased to 250mV and ran until the samples reach the bottom of the gel. The Stain-free™ stain was activated in gels fosr 45 seconds on the ChemiDoc MP (Bio-rad) using UV trans illumination (520/110nm) before transferring to a membrane.

2.2.3.4 Transfer to membrane and blocking

0.45µm low fluorescence Polyvinylidene difluoride (PVDF) membranes (Bio-rad) were cut and soaked in methanol for 30 secs and washed with MilliQ water three times before soaking

into 1x Tris-glycine transfer buffer. Filter papers were also cut and soaked in this transfer buffer before the transfer procedure. The gel, membrane and filter papers were layered onto the Power blotter XL (Invitrogen) machine in the following order: filter paper, membrane, gel, and another filter paper. A pre-installed transfer program was selected, which applied 25 mV, 2.5 A, for 10 mins. After, the membranes were rinsed in MilliQ water, pictures were taken as a stain free blot using the ChemiDoc. The membranes were then blocked with either 5% (w/v) Bovine Serum Albumin (BSA, Sigma Aldrich) or 5% (w/v) skim milk dissolved in 1x Tris-Buffered Saline with 0.1% (v/v) Tween-20 (TBST, Fisher Bioreagents), at room temperature. The timing of incubation can be found on Table 5 below. After blocking, the blots were washed with TBST for 10 mins 3 times, before incubation with antibodies.

Table 5: Blocking procedure used for specific target proteins after transfer to PVDF membrane.

Target Protein	**Length of Incubation and Blocking Reagent**
Caspase-1	15 mins in 5% BSA
GSDMD	15 mins in 5% BSA
NLRP3	1 hr in 5% Skim Milk
β-actin	1 hr in 5% Skim Milk
A_{2B}	15 mins in 5% BSA
Caspase-4	15 mins in 5% BSA

2.2.3.5 Primary and secondary antibodies

Primary antibodies were diluted in either BSA or skim milk in TBST in varying dilutions and percentages, with 0.05% (v/v) sodium azide (ThermoFisher Scientific) to prevent bacterial growth in the solution. Table 6 below indicates the antibody, dilution factor, and incubation period of each primary antibody used. Each antibody was validated by testing band signals with a serial dilution of proteins to ensure the protein load is within linear range. During incubation

with the primary antibody, enough solution was placed on the container to ensure the entire membrane is covered well, and this was placed on a plate shaker for agitation while incubating.

Table 6: Dilution factors an incubation time for primary antibodies used.

Antibody	Dilution factor	Incubation
A_{2B} (Millipore Sigma)	1:1000	Overnight at 4°C
GSDMD (Cell Signaling Technologies)	1:200	Overnight at 4°C
Caspase- 1 (Cell Signaling Technologies)	1:500	Overnight at 4°C
NLRP3 (Cell Signaling Technologies)	1:1000	Overnight at 4°C
β-actin (Cell Signaling Technologies)	1:1000	Overnight at 4°C
Caspase-4	1:500	Overnight at 4°C

After primary antibody incubation, three 10 min washes of TBST was performed then 1:5000 incubation with Anti-rabbit Horse radish peroxidase (HRP, cell signalling) as a secondary antibody in 5% of the Blocking reagent used for 2 hours at room temperature. After this, three 10 min washes of TBST were performed before a 10 min incubation with enhanced chemiluminescence (ECL) solution, made with of equal parts Clarity Western ECL substrate Luminol/enhancer solution (Bio-rad) and Peroxide solution (Bio-rad). The container was covered in foil to prevent light exposure and placed on a shaker while incubating. After which, the membranes were imaged using ChemiDoc MP, a chemiluminescent and colorimetric exposures were taken, and bands were analyzed using Image Lab Software (Bio-rad). Multiple exposures of the blots were acquired at different lengths of time to ensure the bands were not saturated.

2.2.3.6. Analyzing western blot images

ImageLab software was used to analyze the densities of bands observed as a measure of relative quantities. All bands were normalized to β-actin, and overall lane proteins from the stain free blot. Graphpad Prism was used to perform statistical analysis.

2.2.4. Polymerase Chain Reaction (PCR)

2.2.4.1 Harvesting RNA from samples

Samples in RNAzol was thawed in ice and 0.16mL of Nuclease free water (GIBCO) was added to each tube of RNAzol sample. The tubes were vortexed for 15s and allowed to stand at room temperature for 15 minutes. These samples were then placed in the centrifuge to spin for another 15 minutes at 12 000 x g, at 4°C. After which, the supernatant is collected, and mixed with equal volume of isopropanol, which precipitated the RNA. This solution was mixed well and allowed to stand for 10 mins at room temperature before it was spun in the centrifuge at 12 000 x g for 10 mins at 4°C to pull down the RNA as a white pellet. The supernatant was disposed of carefully using a pipetter, and the pellet was washed with 75% ethanol twice. Washing was performed by adding 0.27mL of 75% ethanol to the pellet and spun in the centrifuge at 8000 x g, for 3 mins at room temperature. After the second wash, the ethanol was removed, and the pellet was dissolved in 20µL of RNAse free water. The concentration and quality of these samples were checked with the Nanodrop spectrophotometer, by looking at the absorbance values at both 260nm and 280nm.

2.2.4.2 RNA cleanup

The 260/280 ratio reading acquired from the Nanodrop is considered pure at ~2.0 for RNAs. Samples with a ratio below this were cleaned using an RNEasy kit (QIAGEN). Following the protocol, the 20µL RNA samples were topped up with 80µL of RNAse free water to total 100µL. 350µL of Buffer RLT provided by the kit was added, along with 250µL of 100% ethanol, totalling 700µL of solution in the tube. The solution was mixed properly and then transferred into RNEasy mini spin columns provided by the kit and spun in the centrifuge at 12 000 x g for 15s at 22°C. The spin columns have a collection tube underneath and the buffer flows through the columns into these tubes while the RNA attaches to the column. The solution in the collection tube is known as "flow through", and this was discarded. 500µL of Buffer RPE provided by the kit was then added to the spin columns, and this was also spun at 12 000 x g for 15s at 22°C. The flowthrough was discarded and 500µL of Buffer RPE was added again to the column, and this was centrifuged at 12 000 x g for 2 minutes at 22°C. The spin column was then placed into a 1.5mL collection tube, and 15µL of RNAse free water was added into the column and spun for 1 min at 12 000 x g. The RNA from the spin column would dissolve into the RNAse free water hence the RNA would be in the flowthrough. These were kept in the tube and tested for concentration and quality using the Nanodrop Spectrophotometer once more before cDNA synthesis.

2.2.4.3 cDNA synthesis

Using the concentration provided by Nanodrop, calculations were done to identify how much volume is needed to make 2000ng of cDNA, assuming all RNA will be converted to cDNA 1:1. cDNA was synthesized using High-Capacity cDNA Reverse Transcription Kit (ThermoFisher Scientific). A master mix was made using the kit, by mixing 2µL RT buffer, 2µL RT random

primers, 0.8µL dNTP mix (100mM), 4.2µL Nuclease free water, and 1µL of MultiScribe Reverse transcriptase, for each RNA sample that need to be converted to cDNA. The calculated volume of 2000ng of RNA samples were topped up with the appropriate amount RNAse free water to total 10µL, and 10µL of master mix was added. Additionally, one sample was made by pooling RNA from all negative controls into one to make 2000ng of cDNA, this was used to create the standard curve in the following step. Samples were vortexed to mix well and centrifuged to bring all liquid to the bottom of the tube before placing into the SimpliAmp™ Thermal Cycler (ThermoFisher).

2.2.4.4 PCR

After cDNA synthesis, the samples were prepared and aliquoted into 96-well PCR plates. First, a master mix was made using 10µL SYBR green, 1µL of 10µM forward primer of target RNA, 1µL of 10µM reverse primer of target RNA, and 4µL RNAse free water. At the same time, cDNA samples were diluted 50x. Each well of the PCR plate was filled with 16µL of master mix and 4µL of diluted sample to total 20µL per well. Targets used for these experiments were A_{2B}, and Cyclophilin B (CYCB), that was used as a housekeeping gene. Annealing temperature was set at 60°C. The reaction efficiency was calculated to be greater than 95% for each PCR experiment. Table 7 below show the sequence of the primers used. Standards are made using the pool of negative controls and diluting this 2000ng of cDNA by 10, followed by a serial 1:5 dilution of up to 6 points on the standard curve (200ng, 40ng, 8ng, 1.6ng, 0.32ng, 0.064ng/µL). Each sample and standard were pipetted in triplicate into the 96-well plates. The plate is placed in the PCR machine where it goes to cycle of heating and cooling.

Table 7: Sequence of primers used for PCR acquired from Integrated DNA technologies (IDT, Iowa USA)

	Forward	**Melting Temperature**	**Reverse**	**Melting Temperature**
A_{2B}	5'- GGG CTT CTG CAC TGA CTT CT- 3'	65.2	5'- AAG ATG GAG CTC TGC GTG AG- 3'	64.9
Cyclophilin B	5'- TGC CAT CGC CAA GGA GTA G- 3'	64.8	5'- CTG CAC AGA CGG TC CTC AAA-3'	65.3

2.2.4.5 Enzyme-Linked Immunosorbent Assay (ELISA)

Human IL-1β coated ELISA kit (Invitrogen) was used to quantify the IL-1β secreted in the media of treated cells. Media that was collected and stored in -80℃ was thawed on ice and diluted either 5x or 20x depending on the relative concentrations of IL-1β. Following the protocol, all solutions were allowed to reach room temperature. The 20x Wash and Assay buffer provided in the kit was diluted to 1x using autoclaved MilliQ water. Standards were prepared by diluting the 200pg/mL aliquot provided in the kit. 200pg, 100pg, 50pg, 25pg, 12.5pg, 6.25pg, and 3.13pg/mL were the concentrations used to make the standard curve. On the provided 96-well microplate, 50µL of diluted sample media or standards were added, then 100µL of 1:100 diluted biotin-conjugate solution. The plate was covered in foil, placed on a shaker, and incubated for 2 hours in room temperature. After, the solution was poured out of the wells, and they were washed four times with the wash buffer. 100µL of diluted streptavidin-horseradish peroxidase solution, provided in the kit, was added to the wells. This was incubated for 30 mins and poured out, and again washed four times before 100µL of TMB-substrate was added. During the 25-minute incubation, a blue color was observed to develop. 100µL of stop solution was added to each well, changing the blue hue to yellow. The microplate was then placed in a

microplate reader and the absorbance was read at 450nm, with a reference wavelength of 620nm. The IL-1β concentration per sample was calculated by extrapolating absorbance values from the standard curve and multiplying by the dilution factor.

2.3 Overexpression, Coimmunoprecipitation and proteomics

2.3.1 Lipofectamine 3000 overexpression

Cells were plated to have 1.2 x10^6 cells/well on 6-well plates and differentiated as described before. After which, cells were washed with PBS and media was aspirated and replaced with RPMI-1640 supplemented with 10% FBS. Lipofectamine 3000 was used to transfect the cells with either the stuffer or the A_{2B} plasmids. Optimization of lipofectamine volume and incubation period was performed and results are shown in Figures 23 and 24. The optimized procedure is as follows: 2.5µg of plasmid (A_{2B} or stuffer from Vector Builder, Illinois, USA) was placed in 250µL of OptiMEM. 5µL of Lipofectamine 3000 was added to 250µL of OptiMEM as well. These solutions were mixed and incubated for 10 mins before adding to cells in a drop-wise manner. Cells were incubated for 36 hours before analysis with western blot or PCR, protocol as described above, or coimmunoprecipitation as described below.

2.3.2 Coimmunoprecipitation

Coimmunoprecipitation was performed following the protocol published by Thermofisher for HA tag beads and Immunoprecipitation lysis buffer.

2.3.2.1 Sample preparation:

After Lipofection, the media was aspirated from the 6-well plates, and the cells were washed twice with cold PBS. 400µL of cold lysis buffer (IP buffer, Thermofisher) was added to the cells. Cells were scraped into a microcentrifuge tube, mixed and then centrifuged at ~13,000 × g for 10 mins at 4°C, to pellet cell debris. The supernatant was transferred to a new tube for sonication as described above.

2.3.2.2 Immunoprecipitation

25µL of Pierce Anti-HA Magnetic Beads was placed into a 1.5mL microcentrifuge tube and washed with 175µL of 0.05% TBS-T twice. The sample containing HA-tagged protein was added to the beads and incubated at room temperature for 30 minutes with mixing. The tubes were placed on the magnetic stand, and the supernatant was discarded. 300µL of TBS-T was used to wash the beads twice and once with 300µL of MilliQ water. The beads were kept in 1x TBS and sent to the Manitoba Centre for Proteomics and Systems Biology at the University of Manitoba for proteomic analysis or eluted for western blotting.

2.3.2.3 Basic Elution

100µL of 50mM NaOH was added to the beads and gently vortexed before incubating at room temperature on a rotator for 5 minutes. The tubes were placed on a magnetic stand and the supernatant was transferred to a new tube and beads were discarded. This solution was neutralized by adding 50µL of Neutralization Buffer (1M TRIS, pH 8.5) for each 100µL of eluate. This eluate was then run on western blot following procedures described above.

3.0 Results

In this research, the role of A_{2B} in macrophage pyroptosis was elucidated through receptor knockdown studies and the use of small molecule inhibitor for the NLRP3 inflammasome, MCC950 (shown in section 3.3). Receptor-protein interactions were examined through overexpression, coimmunoprecipitation, and proteomic analysis (shown in section 3.5).

3.1 Optimization of experimental parameters for A_{2B} Knockdown

3.1.1 siRNA concentration

A range of siRNA concentrations were tested to identify the optimal concentration for knockdown. Figure 4 below shows the results of qPCR analysis of the different concentrations. 5nM of A_{2B} siRNA gave the best knockdown at 56.5%.

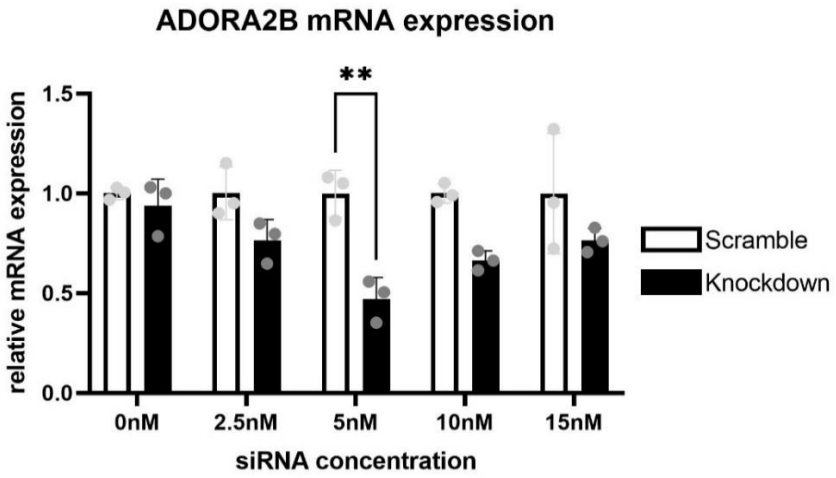

Figure 4: A_{2B} mRNA expression in THP-1 measured by qPCR after knockdown using different siRNA concentrations. Bars represent average mRNA expression and error bars represent standard deviation. 2-way ANOVA was performed to identify statistical difference for n=3.

3.1.2 Time incubation

A range of time incubations were also tested to identify the optimal time for knockdown. Figure 5 below shows the results of qPCR analysis at several time points. This showed that the best knockdown with the least time incubation period was 36 hours. (24 hr- 56.6% knockdown,

36hr- 68.2%, 48hr- 67%, 72hr-53.9%). This also showed that the knockdown was stable over time.

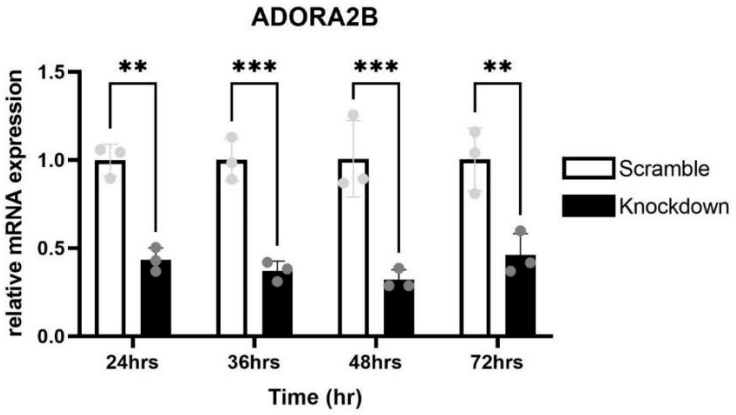

Figure 5: A_{2B} mRNA expression in THP-1 measured by qPCR after knockdown using different time incubations. Bars represent average mRNA expression and error bars represent standard deviation. 2-way ANOVA was performed to identify statistical difference for n=3.

3.1.3 Lipofectamine 3000 volume

A range of Lipofectamine 3000 volumes were tested to identify the optimal volume for knockdown. The most effective volumes are shown in Figure 6 below. qPCR analysis indicated that 5µL of Lipofectamine 3000 is the best, which provided 81.13% knockdown.

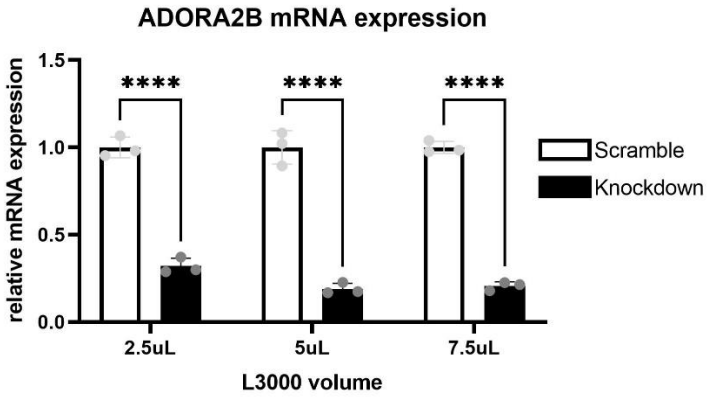

Figure 6: A_{2B} mRNA expression in THP-1 measured by qPCR after knockdown using different Lipofectamine 3000 volumes. Bars represent average mRNA expression and error bars represent standard deviation. 2-way ANOVA was performed to identify statistical difference for n=3.

3.1.4 Protein expression

Western blotting was used to determine protein levels of the A_{2B} receptor after optimizing knockdown procedures. Similar to qPCR, western blot showed an 81% knockdown of A_{2B} receptors. This is sufficient for the purposes of this study.

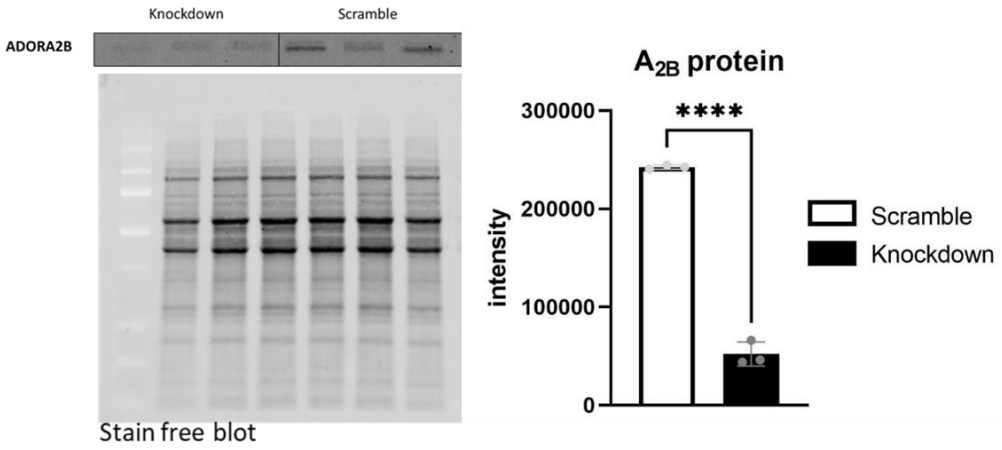

Figure 7: Western blot of A_{2B} receptor at 37 kDa for THP-1 cells treated with optimized knockdown procedure. Densitometry analysis indicates an 81% knockdown of protein. Bars represent average band intensity and error bars represent standard deviation. Student's t-test was performed to identify statistical difference for n=3.

3.2 Optimal Treatment conditions

Treatments used to assess inflammasome activation, induction, and inhibition were first tested and optimized on THP-1 macrophages to ensure that treatments perform their intended purposes.

3.2.1 ATP concentrations

Western blotting was used to assess effective induction of pyroptosis by different ATP concentrations. GSDMD cleavage, an indicator of pyroptosis, can be observed in Figure 8. 3mM and 5mM ATP treatments exhibit effective cleavage of GSDMD. 3 mM ATP was used for further experiments to limit toxic osmotic burden.

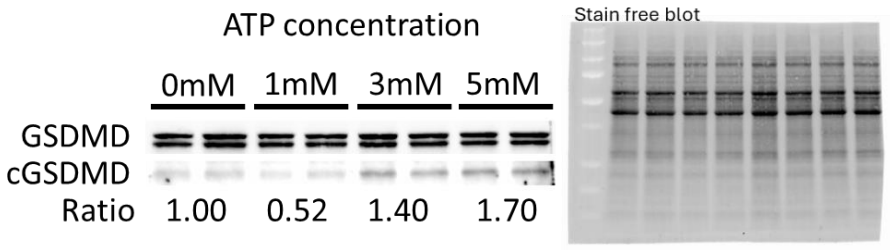

Figure 8: Western blot showcasing GSDMD cleavage of THP-1 cells treated with different concentrations of ATP. GSDMD: Gasdermin D, cGSDMD: cleaved Gasdermin D, ATP: Adenosine triphosphate. Uncleaved GSDMD was found at 53kDa, and cleaved GSDMD at 30kDa. Ratio was calculated by dividing cGSDMD with GSDMD and normalized to the 0mM treatment.

3.2.2 Priming and MCC950

Western blotting was used to assess effective inhibition of pyroptosis by MCC950. GSDMD cleavage was observed in different MCC950 concentrations, along with the priming of THP-1 cells (Figure 9). Cells were either primed with LPS (5ng/mL) for 3 hrs before ATP treatment (3mM) or LPS (5ng/mL) and ATP (3mM) were added at the same time. Figure 9 shows that GSDMD cleavage was more effectively inhibited in primed cells. Primed cells decreased cleavage up to 63.8%, whereas unprimed cells only decreased 35.3%. Moving forward, cells were primed with LPS for all necessary treatments. Concentration of MCC950 used was based on literature, which is 1µM.[77] This concentration was tested and found to be sufficient. The remainder of treatments for this project, adenosine and LPS, were based on previously optimized experiments from our lab.

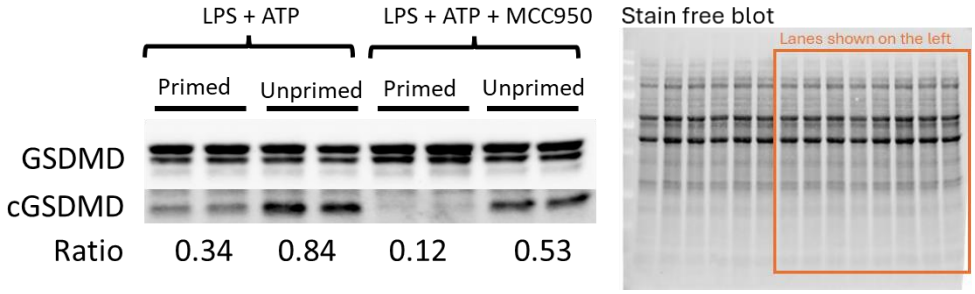

Figure 9: Western blot showcasing GSDMD cleavage of THP-1 cells that were either primed or not primed with LPS and treated with ATP and MCC950. GSDMD: Gasdermin D, cGSDMD:

cleaved Gasdermin D, ATP: adenosine triphosphate. Uncleaved GSDMD was found at 53kDa, and cleaved GSDMD at 30kDa. Ratio was calculated by dividing cGSDMD with GSDMD.

3.3 A_{2B} Knockdown and NLRP3 inhibition

A_{2B} knockdown cells were treated with LPS, Ade, ATP, and MCC950, or a combination of these compounds. Western blotting and ELISA were performed to measure pyroptotic markers. Experiments were repeated three times and data were analyzed using a one-way ANOVA with repeated statistics.

3.3.1 LPS alone increases pyroptotic markers that are inhibited by MCC950

A_{2B} knockdown and scramble THP-1 macrophages were treated with either vehicle, 5ng/mL LPS, or 5ng/mL LPS + 1μM MCC950 and protein expression of pyroptotic markers NLRP3 inflammasome, cleaved GSDMD, cleaved caspase-1 and IL-1β secretion were measured with western blot and ELISA.

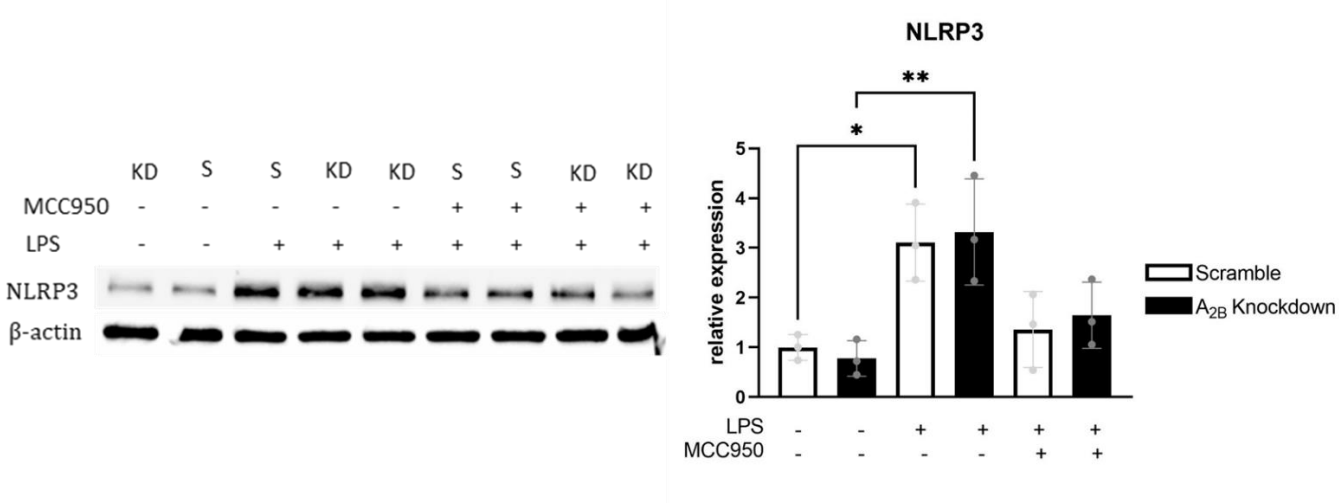

Figure 10: NLRP3 protein expression (118kDa) of scramble and A_{2B} knockdown THP-1 cells as they are treated with vehicle, LPS, and LPS + MCC950. KD: Knockdown, S: Scramble, LPS: Lipopolysaccharide, NLRP3: nucleotide-binding domain, leucine-rich–containing family, pyrin domain–containing-3. Relative expression was calculated by comparing increase of NLRP3 expression to scramble cells treated with vehicle (1.0). Bars represent average expression and error bars represent standard deviation. One way ANOVA analysis with repeated measures was used to compare each individual value with each other to identify significant differences, n= 3.

Figure 10 shows that NLRP3 expression increased with LPS treatment, and MCC950 was not able to inhibit this increase. No significant difference between scramble and knockdown cells were identified for NLRP3 expression. On the other hand, there was a significant increase in caspase-1 cleavage from LPS to LPS + MCC950 treatment for both scramble and knockdown cells (Figure 11), and again, no significant difference between knockdown and scramble cells were identified. For GSDMD (Figure 12), there was a significant increase in cleavage for both scramble and knockdown cells treated with LPS that was successfully inhibited by MCC950. There was more GSDMD cleavage in knockdown cells than scramble cells, indicating a susceptibility of knockdown cells to pyroptosis. Similarly, IL-1β secretion increased with LPS treatment, that was inhibited by the addition of MCC950 in both scramble and knockdown cells, as shown in Figure 13.

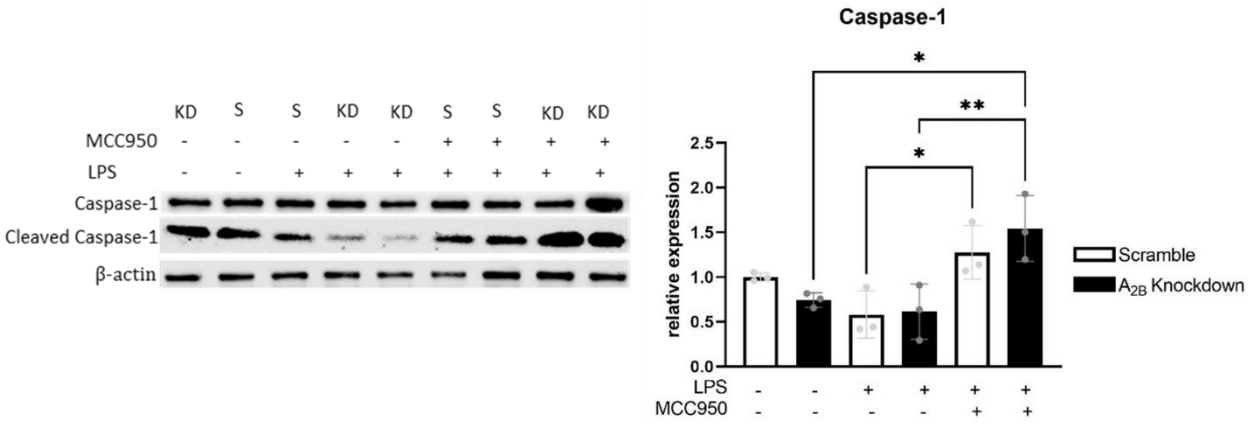

Figure 11: Caspase-1 cleavage ratio of scramble and A_{2B} knockdown THP-1 cells as they are treated with vehicle, LPS, and LPS + MCC950. Caspase-1 is found at 45kDa, whereas cleaved caspase-1 was found at 20kDa. KD: Knockdown cells, S: Scramble cells, LPS: Lipopolysaccharide. Relative expression was calculated by comparing increase of caspase-1 cleavage ratio to ratio identified in scramble cells treated with vehicle (1.0). Bars represent average expression and error bars represent standard deviation. One way ANOVA analysis with repeated measures was used to compare each individual value with each other to identify significant differences, n= 3.

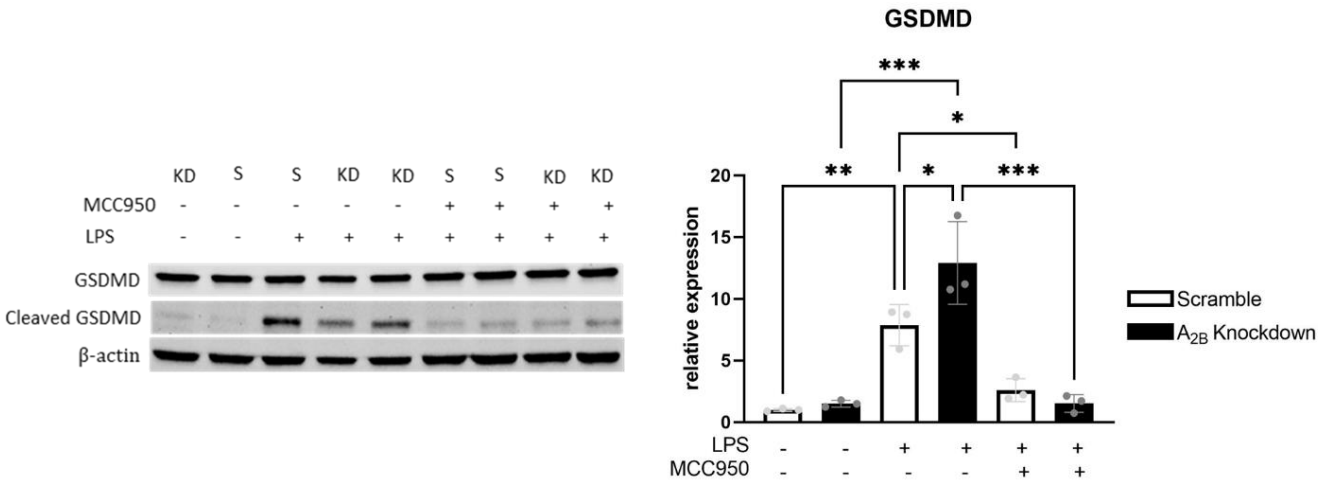

Figure 12: GSDMD cleavage ratio of scramble and A_{2B} knockdown THP-1 cells as they are treated with vehicle, LPS, and LPS + MCC950. GSDMD bands were observed at 53 kDa and cleaved bands observed at 30kDa. KD: Knockdown cells, S: Scramble cells, LPS: Lipopolysaccharide, GSDMD: Gasdermin D. Relative expression was calculated by comparing increase of Gasdermin D cleavage ratio to ratio identified in scramble cells treated with vehicle (1.0). Bars represent average expression and error bars represent standard deviation. One way ANOVA analysis with repeated measures was used to compare each individual value with each other to identify significant differences, n= 3.

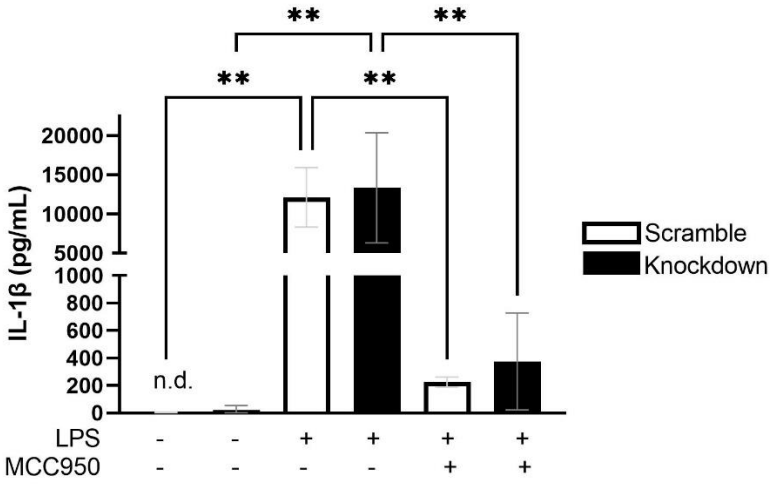

Figure 13: IL-1β secretion of scramble and A_{2B} knockdown THP-1 cells treated with vehicle, LPS, and LPS + MCC950. LPS: Lipopolysaccharide, IL-1β: Interleukin-1β. Bars represent average IL-1β expression and error bars represent standard deviation. One way ANOVA analysis with repeated measures was used to compare each individual value with each other to identify significant differences, n= 3.

This section showed that LPS increased pyroptotic markers NLRP3, GSDMD, and IL-1β for both scramble and knockdown cells. Additionally, MCC950 effectively decreased GSDMD cleavage and IL-1β secretion. A significant difference in GSDMD cleavage was observed between knockdown and scramble cells when treated with LPS, which presents knockdown cells' susceptibility to pyroptosis. It is notable that although there is a significant difference in GSDMD cleavage between knockdown and scramble cells with LPS treatment, this significant difference was not observed with IL-1β and NLRP3 expression where increases were also observed. This data is suggestive of A_{2B} receptor modulating GSDMD cleavage through a mechanism that doesn't influence IL-1β via the NLRP3 inflammasome.

3.3.2. LPS enhances ATP stimulated pyroptosis

Knockdown and scramble THP-1 macrophages were treated with vehicle, 3mM ATP, 5ng/mL LPS + 3mM ATP and 5ng/mL LPS + 3mM ATP + 1μM MCC950. Protein expression of pyroptotic markers NLRP3 inflammasome, cleaved GSDMD, and cleaved caspase-1 were measured with western blot along with ELISA measurements of IL-1β secretions. Figure 14 shows a significant increase of NLRP3 expression for knockdown and scramble cells when treated with LPS + ATP. This decreased in scramble cells with MCC950, whereas knockdown cells did not decrease. On the other hand, caspase-1 cleavage increased for knockdown cells, with ATP alone, and for both scramble and knockdown cells with LPS + ATP treatment (Figure 15). MCC950 was not able to inhibit this increase. GSDMD cleavage significantly increased with the addition of LPS + ATP in both scramble and knockdown cells as shown in Figure 16 and was again successfully inhibited by MCC950. Similarly, Il-1β secretion increased with LPS + ATP treatment and was also inhibited by MCC950 (Figure 17).

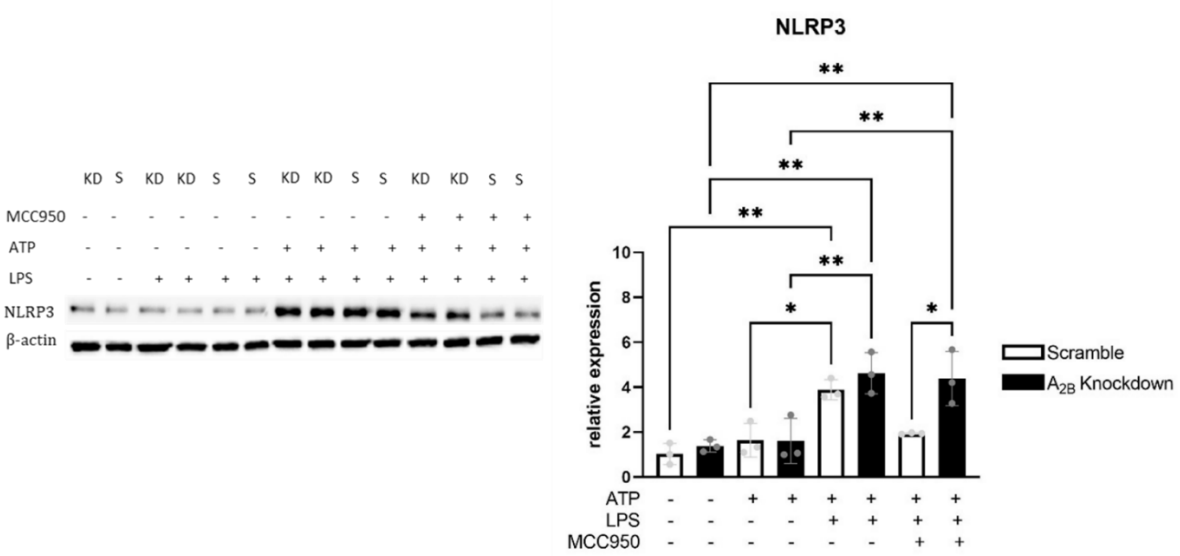

Figure 14: NLRP3 protein expression (118kDa) of scramble and A_{2B} knockdown THP-1 cells as they are treated with vehicle, ATP, LPS + ATP, and LPS + ATP + MCC950. KD: Knockdown cells, S: Scramble cells, LPS: Lipopolysaccharide, NLRP3: nucleotide-binding domain, leucine-rich–containing family, pyrin domain–containing-3, ATP: Adenosine triphosphate. Relative expression was calculated by comparing increase of NLRP3 expression to scramble cells treated with vehicle (1.0). Bars represent average expression and error bars represent standard deviation. One way ANOVA analysis with repeated measures was used to compare each individual value with each other to identify significant differences, n= 3.

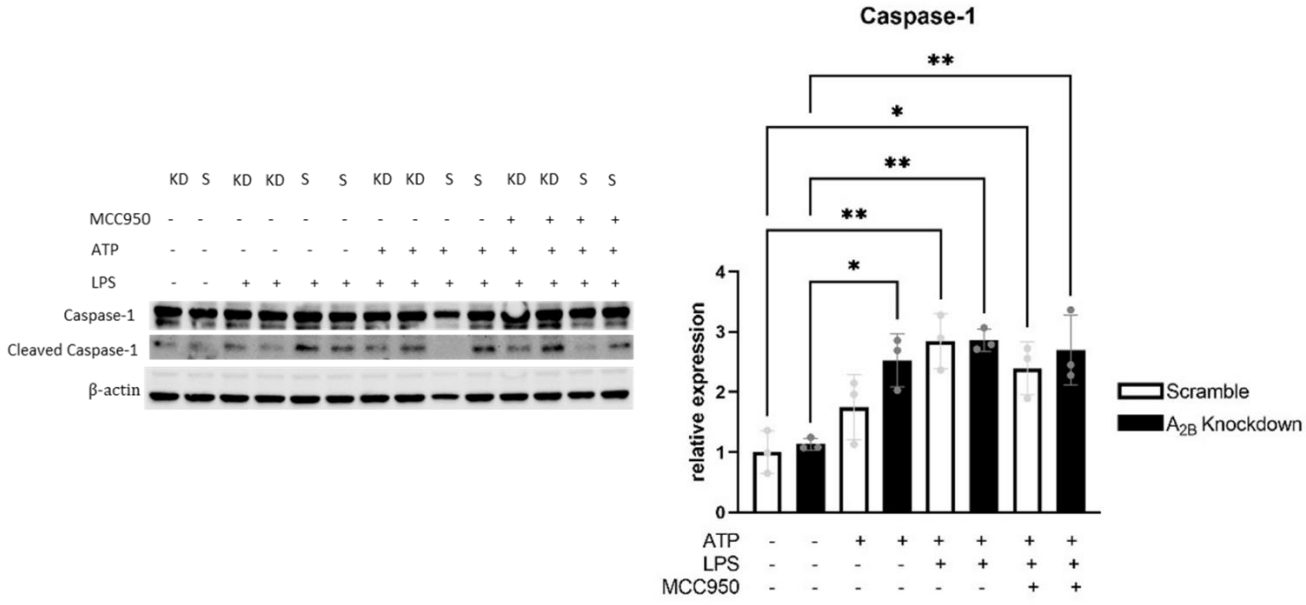

Figure 15: Caspase-1 cleavage ratio of scramble and A_{2B} knockdown THP-1 cells as they are treated with vehicle, ATP, LPS + ATP, and LPS + ATP + MCC950. Caspase-1 is found at 45kDa, whereas cleaved caspase-1 was found at 20kDa. KD: Knockdown cells, S: Scramble cells, LPS: Lipopolysaccharide, ATP: Adenosine Triphosphate. Relative expression was calculated by comparing increase of caspase-1 cleavage ratio to ratio identified in scramble cells treated with vehicle (1.0). Bars represent average expression and error bars represent standard deviation. One

way ANOVA analysis with repeated measures was used to compare each individual value with each other to identify significant differences, n= 3.

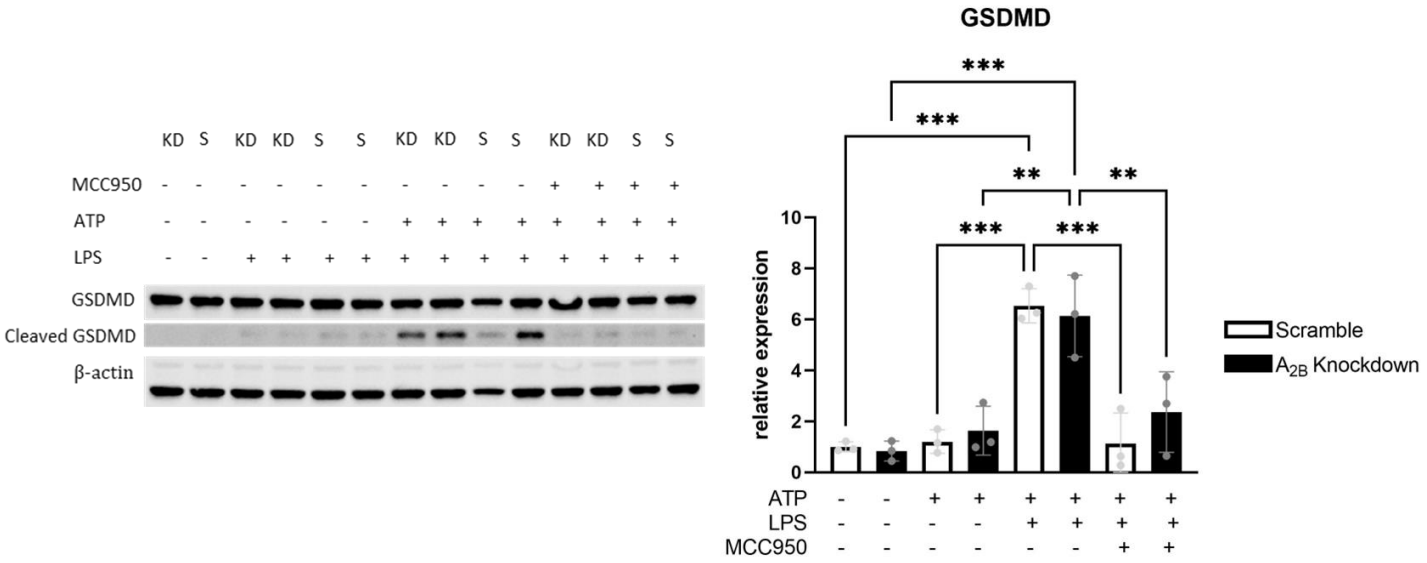

Figure 16: GSDMD cleavage ratio of scramble and A_{2B} knockdown THP-1 cells as they are treated with vehicle, ATP, LPS + ATP, and LPS + ATP + MCC950. GSDMD bands were observed at 53 kDa and cleaved bands observed at 30kDa. KD: Knockdown cells, S: Scramble cells, LPS: Lipopolysaccharide, GSDMD: Gasdermin D, ATP: Adenosine Triphosphate. Relative expression was calculated by comparing increase of Gasdermin D cleavage ratio to ratio identified in scramble cells treated with vehicle (1.0). Bars represent average expression and error bars represent standard deviation. One way ANOVA analysis with repeated measures was used to compare each individual value with each other to identify significant differences, n= 3.

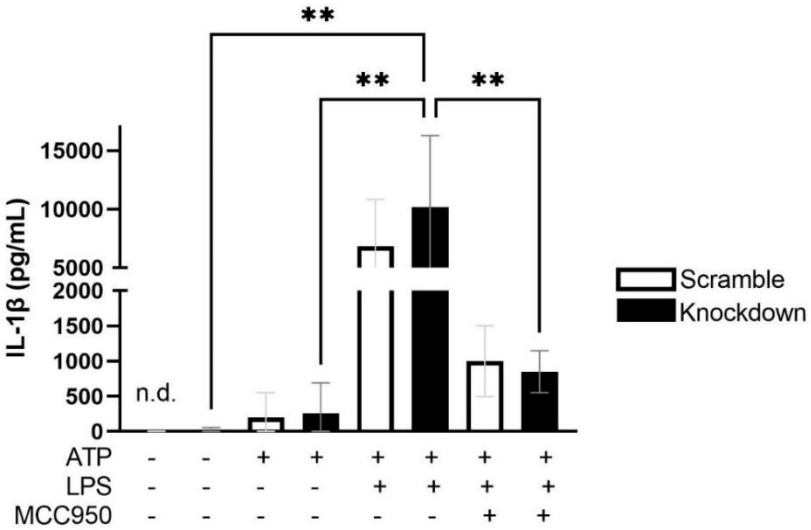

Figure 17: IL-1β secretion of scramble and A_{2B} knockdown THP-1 cells treated with vehicle, ATP, LPS + ATP, and LPS + ATP + MCC950. LPS: Lipopolysaccharide, IL-1β: Interleukin-1β, ATP: Adenosine triphosphate. Bars represent average IL-1β expression and error bars represent standard deviation. One way ANOVA analysis with repeated measures was used to compare each individual value with each other to identify significant differences, n= 3.

In this section, it was observed that ATP alone was not able to increase pyroptotic markers, except for caspase-1 cleavage in knockdown cells. NLRP3, GSDMD, and IL-1β increased only with LPS priming before ATP treatment. It was also observed that MCC950 inhibited GSDMD cleavage and IL-1β secretion. Studies have shown that MCC950 does not inhibit NLRP3 expression, oligomerization, and ASC interactions, but inhibits IL-1β and IL-18 release of cytokines.[100] This is consistent with our studies, as we see IL-1β and GSDMD cleavage decreased with MCC950 treatment, even if NLRP3 and caspase-1 is not decreased. Overall, this section further confirms that MCC950 works as an inhibitor of NLRP3 activity, and we learn that NLRP3 and caspase-1 enzymatic *activity* may not be reflected accurately by the protein expression we observe. The cleavage of GSDMD and IL-1β are better markers of pyroptosis than NLRP3 and caspase-1 activity.

3.3.3. MCC950 is unable to ameliorate GSDMD cleavage induced by adenosine

Knockdown and scramble cells were treated with 1mM adenosine, 5ng/mL LPS + 1mM adenosine and 5ng/mL LPS + 1mM adenosine + 1μM MCC950. Protein expression of pyroptotic markers NLRP3 inflammasome, cleaved GSDMD, and cleaved caspase-1 were measured with western blot along with ELISA measurements of IL-1β secretions.

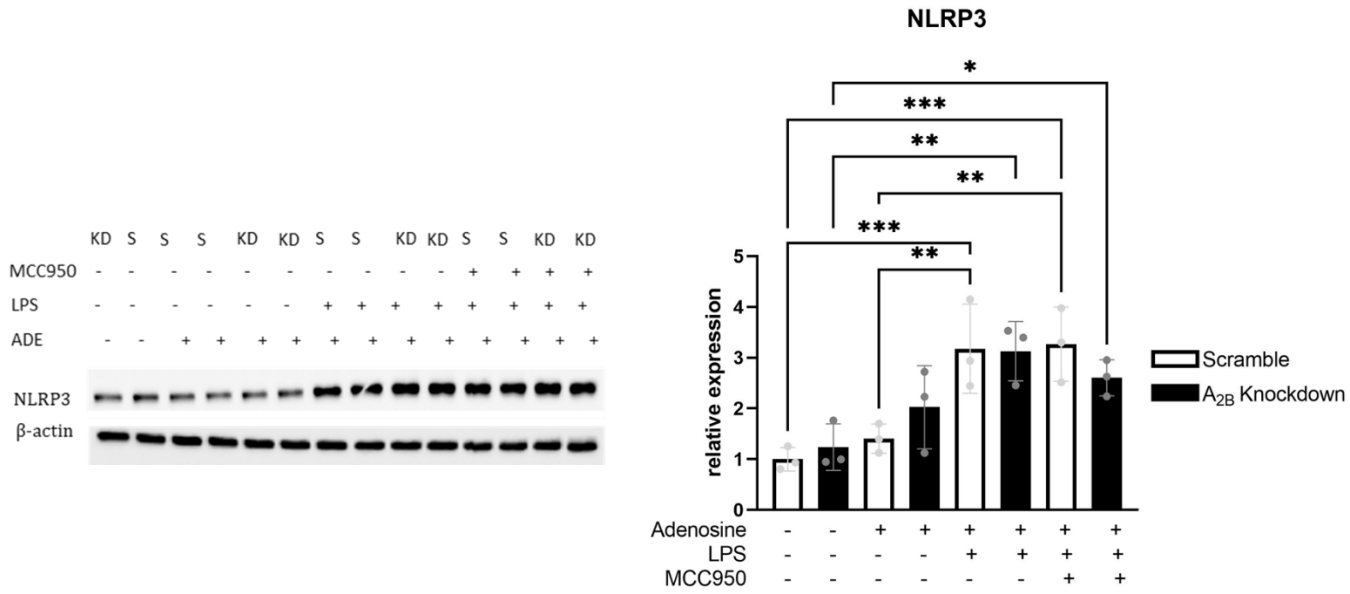

Figure 18: NLRP3 protein expression (118kDa) of scramble and A_{2B} knockdown THP-1 cells as they are treated with vehicle, adenosine, LPS + adenosine, and LPS + adenosine + MCC950. KD: Knockdown cells, S: Scramble cells, LPS: Lipopolysaccharide, NLRP3: nucleotide-binding domain, leucine-rich–containing family, pyrin domain–containing-3, Ade: Adenosine. Relative expression was calculated by comparing increase of NLRP3 expression to scramble cells treated with vehicle (1.0). Bars represent average expression and error bars represent standard deviation. One way ANOVA analysis with repeated measures was used to compare each individual value with each other to identify significant differences, n= 3.

Figure 18 shows NLRP3 expression significantly increased for both scramble and knockdown cells, with the addition of LPS + Adenosine, that was not inhibited by MCC950. On the other hand, caspase-1 cleavage increased in knockdown cells when treated with adenosine, that was successfully inhibited by MCC950 to levels lower than vehicle treated knockdown cells (Figure 19). Furthermore, there was more caspase-1 cleavage in knockdown cells than in scramble cells when treated with adenosine, indicating the A_{2B} knockdown group was more susceptible to pyroptosis. MCC950 decreased caspase-1 cleavage for scramble cells from adenosine treatment to LPS + adenosine + MCC950.

Figure 20 below shows that there is a significant increase in GSDMD cleavage only for knockdown cells when treated with LPS + Adenosine + MCC950. There is also a significant difference between knockdown and scramble groups treated with LPS + Adenosine + MCC950, with more GSDMD cleavage in knockdown cells. Conversely, IL-1β secretion appeared to increase with the addition of LPS + Adenosine for both scramble and knockdown cells but was still significantly inhibited by MCC950 (Figure 21). The different effect of MCC950 on GSDMD and IL-1β secretion indicate that GSDMD cleavage occurs through a signalling mechanism independent of NLRP3 activation in the presence of elevated extracellular adenosine.

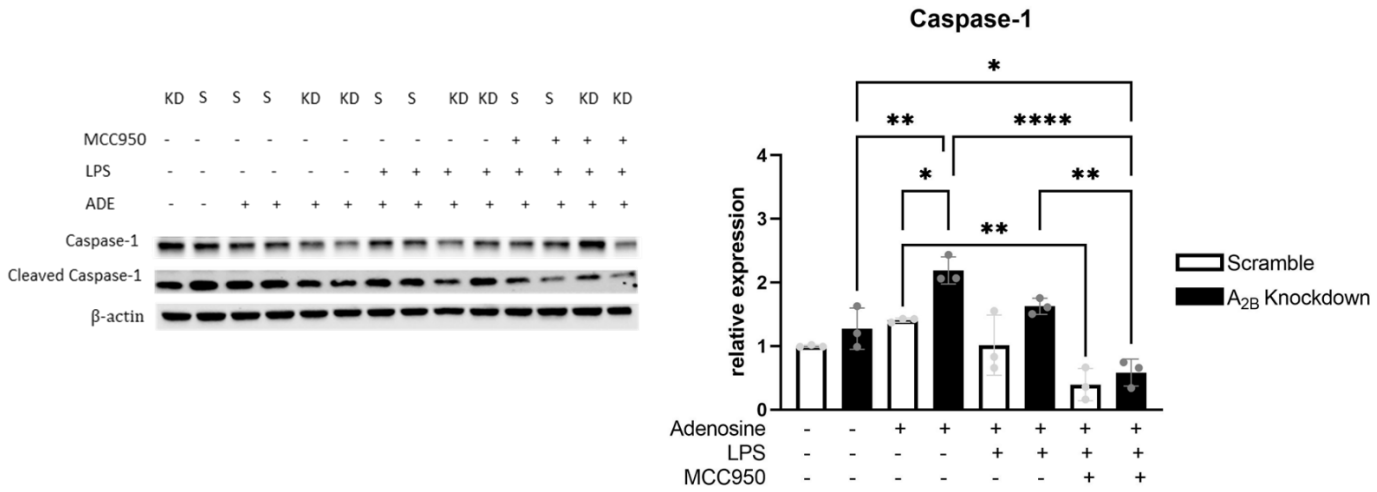

Figure 19: Caspase-1 cleavage ratio of scramble and A_{2B} knockdown THP-1 cells as they are treated with vehicle, adenosine, LPS + adenosine, and LPS + adenosine + MCC950. Caspase-1 is found at 45kDa, whereas cleaved caspase-1 was found at 20kDa. KD: Knockdown cells, S: Scramble cells, LPS: Lipopolysaccharide, Ade: Adenosine. Relative expression was calculated by comparing increase of caspase-1 cleavage ratio to ratio identified in scramble cells treated with vehicle (1.0). Bars represent average expression and error bars represent standard deviation. One way ANOVA analysis with repeated measures was used to compare each individual value with each other to identify significant differences, n= 3.

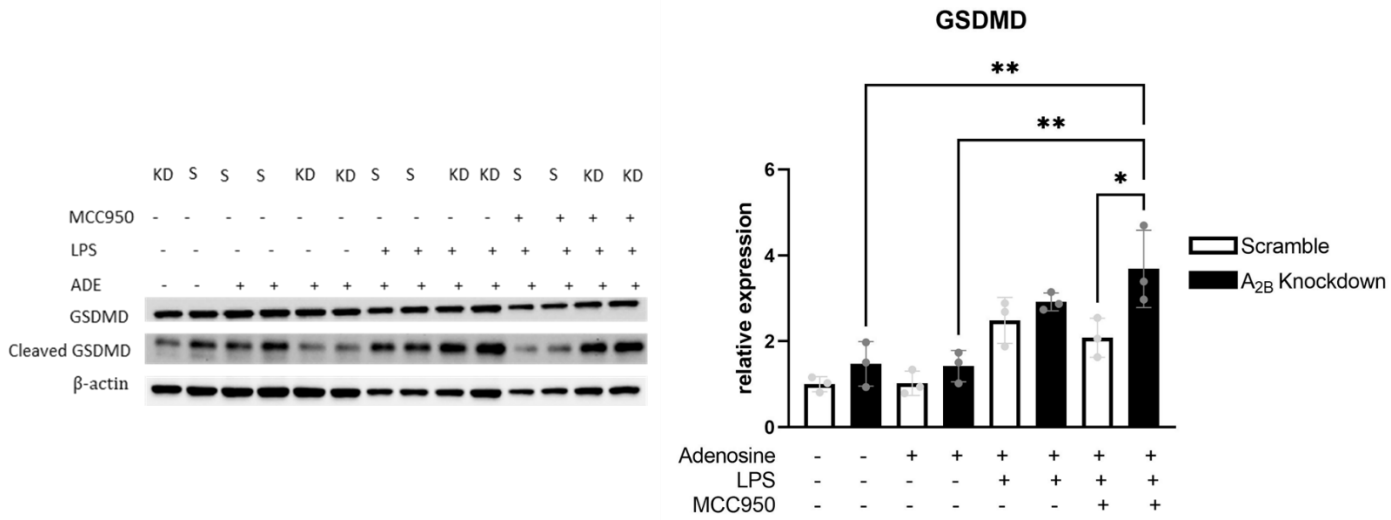

Figure 20: GSDMD cleavage ratio of scramble and A_{2B} knockdown THP-1 cells as they are treated with vehicle, adenosine, LPS + adenosine, and LPS + adenosine + MCC950. GSDMD bands were observed at 53 kDa and cleaved bands observed at 30kDa. KD: Knockdown cells, S: Scramble cells, LPS: Lipopolysaccharide, GSDMD: Gasdermin D, Ade: Adenosine. Relative expression was calculated by comparing increase of Gasdermin D cleavage ratio to ratio identified in scramble cells treated with vehicle (1.0). Bars represent average expression and error bars represent standard deviation. One way ANOVA analysis with repeated measures was used to compare each individual value with each other to identify significant differences, n= 3.

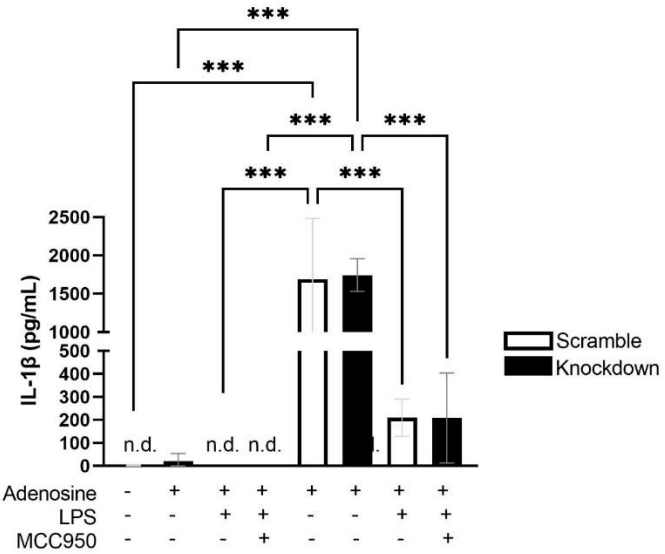

Figure 21: IL-1β secretion of scramble and A_{2B} knockdown THP-1 cells treated with vehicle, adenosine, LPS + adenosine, and LPS + adenosine + MCC950. LPS: Lipopolysaccharide, IL-1β: Interleukin-1β. Bars represent average IL-1β expression and error bars represent standard deviation. One way ANOVA analysis with repeated measures was used to compare each individual value with each other to identify significant differences, n= 3.

In this section, it was observed that MCC950 was able to inhibit caspase-1 and IL-1β, but not NLRP3 and GSDMD. As alluded to in the previous section, NLRP3 and caspase-1 protein expressions do not represent activity accurately. Compared to previous results (section 3.3.1 and 3.3.2) where GSDMD and IL-1β were successfully inhibited by MCC950, here, only IL-1β was inhibited. Consistently in our experiments, MCC950 was able to decrease IL-1β secretion when added, implying that NLRP3 inhibition was working and that IL-1β secretion is directly linked to NLRP3 activity. These results show that GSDMD is activated by a mechanism independent of the NLRP3 inflammasome when treated with adenosine, hence there is no decrease when MCC950 is added. One such possibility where this occurs is the non-canonical pathway of pyroptosis which utilizes caspase-4, not NLRP3, to cleave GSDMD.

3.3.4 Caspase-4 is activated by adenosine

Upon observation that MCC950 does not decrease GSDMD cleavage in LPS + Adenosine + MCC950 treated cells, it was hypothesized that the cleavage of GSDMD is occurring through a mechanism not involving the NLRP3 inflammasome. Therefore, it was presumed that this could be happening through the non-canonical pathway. The non-canonical pathway uses caspase-4 to cleave GSDMD directly instead of using NLRP3 and caspase-1.[121] Samples were then probed with caspase-4 antibody and the resulting blot is shown in Figure 22 below.

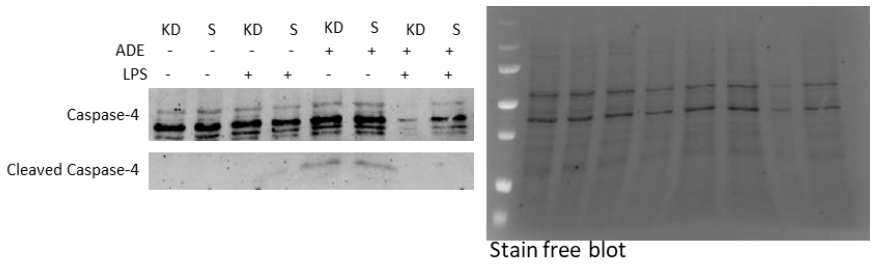

Figure 22: Western blot probed with caspase-4 for adenosine treated cells. Caspase-4 is 45 kDa, and cleavage at 20kDa.

The results show that adenosine alone activates caspase-4, however, as this was only tested on an n=1, these are only preliminary data that requires further investigation. This introduces a possibility of the non-canonical pathway being activated in adenosine treated cells.

3.4 A_{2B} Overexpression

3.4.1 Optimizing Overexpression protocol

Similar to the knockdown procedure, conditions for the overexpression of A_{2B} in THP-1 cells were optimized. Figure 23 shows that 36-hour incubation yielded the best overexpression levels based on mRNA, and for Lipofectamine volume, 2.25µL yielded the best levels of overexpression (Figure 24). These values were used for experiments. We did not note any phenotypic markers of cell deaths throughout the treatments.

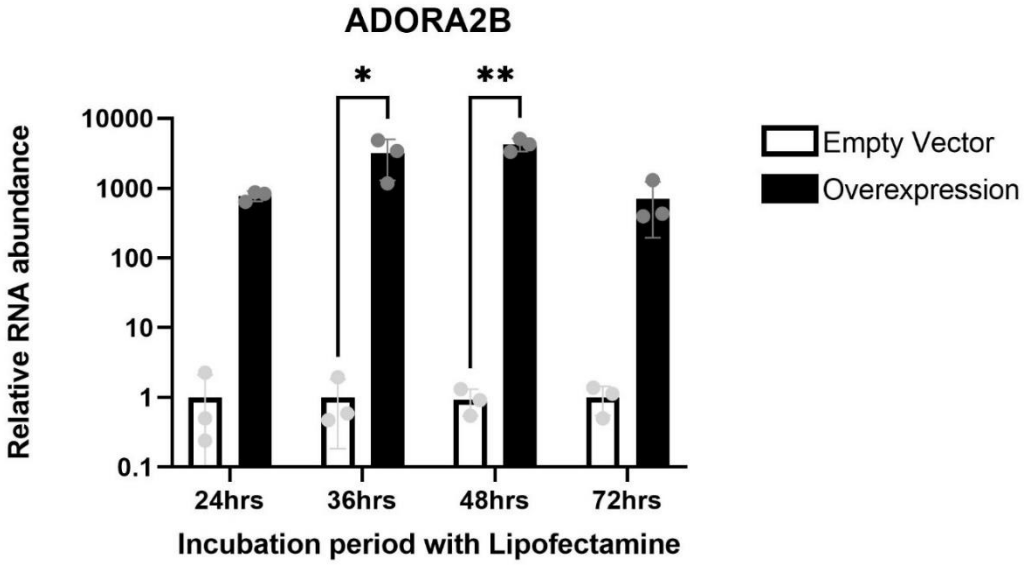

Figure 23: A_{2B} mRNA expression in THP-1 measured by qPCR after overexpression using different time incubations. Bars represent average mRNA expression and error bars represent standard deviation. 2-way ANOVA was performed to identify statistical difference for n=3.

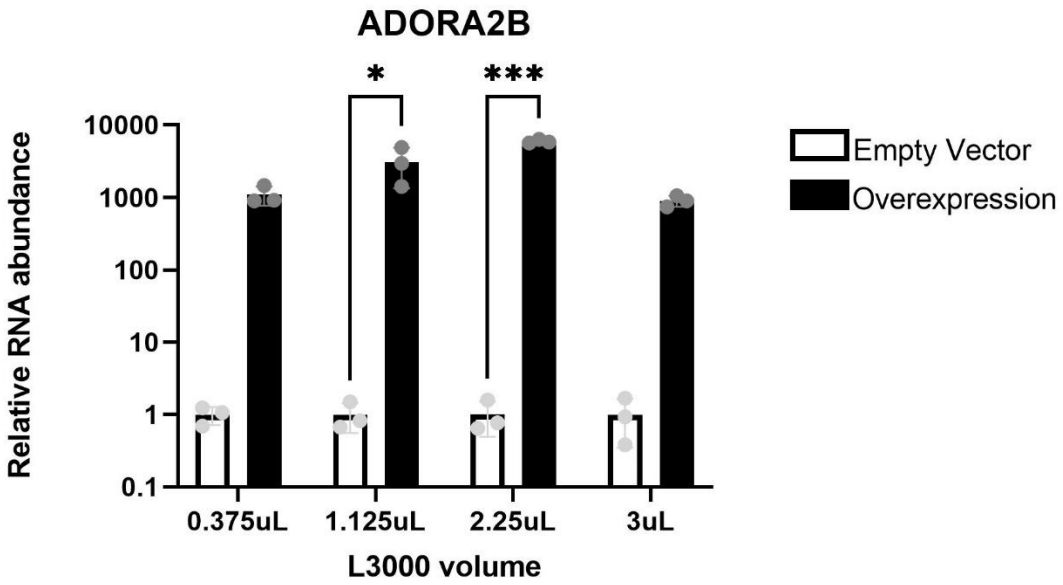

Figure 24: A_{2B} mRNA expression in THP-1 measured by qPCR after overexpression using different Lipofectamine 3000 volumes. Bars represent average mRNA expression and error bars represent standard deviation. 2-way ANOVA was performed to identify statistical difference for n=3.

3.4.2. Proof of A_{2B} Overexpression

The optimized overexpression protocol was performed on both HEK293T cells and THP-1 cells. Shown in Figure 25 below is a western blot ran of immunoprecipitated lysates from HEK293T cells probed with HA-tag antibody. Here, bands were only observed in the second lane for samples treated with HA-tagged A_{2B}. No bands were observed in the first lane for (untagged) stuffer treated samples. This proves that we were able to successfully express HA-tagged A_{2B} proteins in HEK293T cells. The same experiments were run on THP-1 cells, but we were not able to obtain a blot with similar results. No bands were observed on THP-1 cell lysates for both A_{2B} plasmid treated, and stuffer treated cells. This is most likely due to relatively lower transfection efficiency and protein expression by THP-1 cells compared to HEK293T cells.

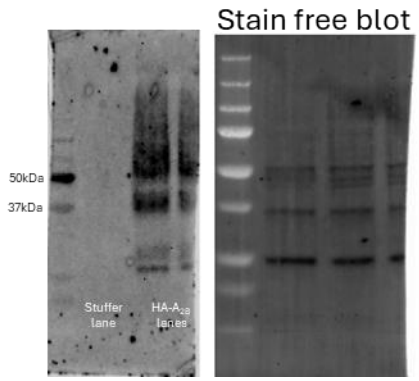

Figure 25: Western blot probed with anti-HA antibody for the A_{2B} and stuffer DNA treated cells. Lane 1 had no visible bands for stuffer treated cells and Lane 2 had numerous bands from the A_{2B} plasmid treated cells.

3.5 Proteomics of overexpressed A_{2B}

3.5.1 Proteomic analysis of A_{2B} in HEK293T cells

HEK293T samples coimmunoprecipitated with anti-HA beads were sent for proteomic analysis as a proof-of-method trial. One sample was treated with HA-A_{2B} plasmid, and one treated with a stuffer plasmid. Protein expression relative to stuffer control were compared to identify proteins that are enriched in the presence of A_{2B}. Proteomic analysis was able to detect over 700 proteins, but only 69 proteins were found to have greater than 5-fold enrichment in the A_{2B} overexpression immunoprecipitate. The resulting STRING network is shown in Figure 26 below.

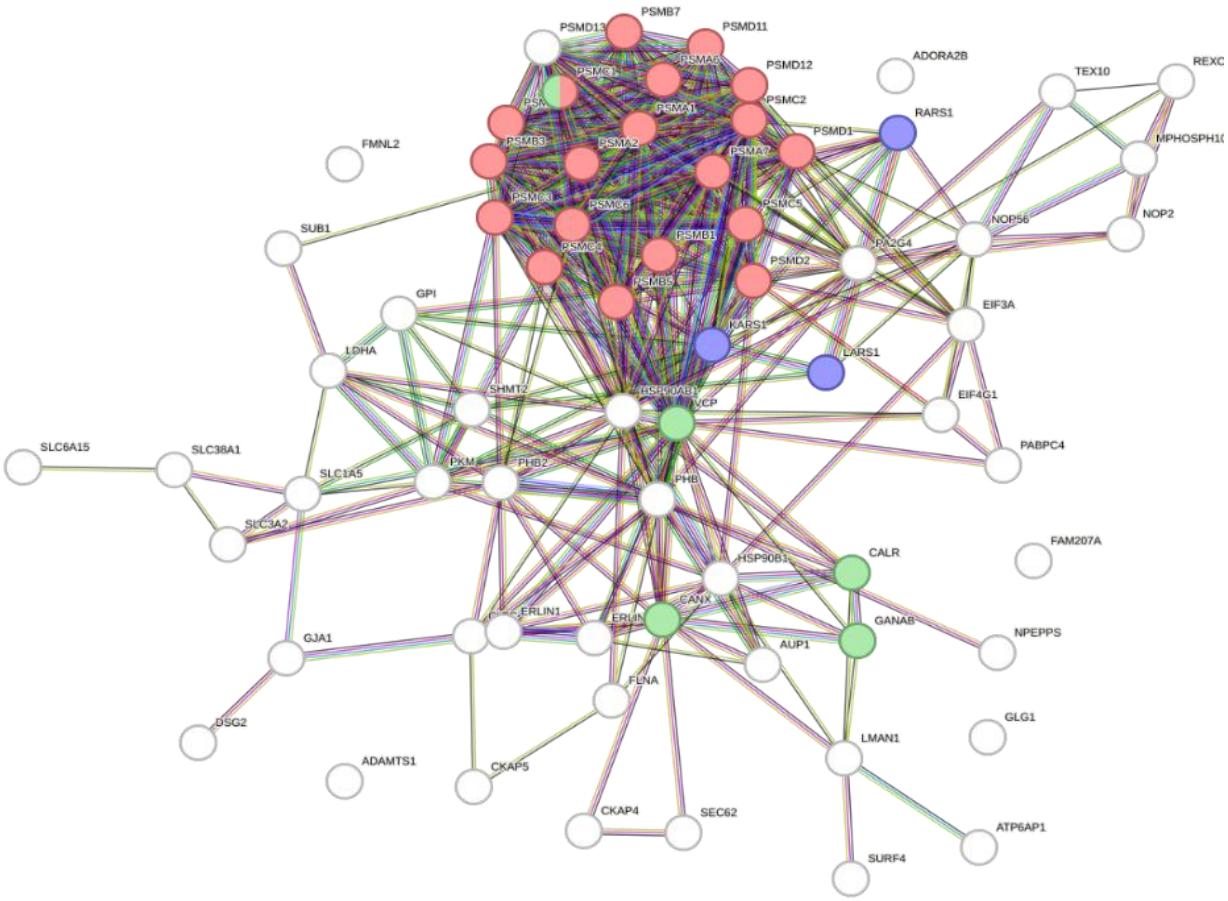

Figure 26: STRING network of proteins coimmunoprecipitated with anti-HA beads linked to A_{2B} receptor in HEK293T cells.

Results from the proteomic analysis show that our transfection experiments were able to capture a large amount of A_{2B} (400-fold) in HEK293T cells, and that this overexpression enriched different types of proteins that are involved in processes such as cellular communication, calcium signaling and gap-junction proteins. Gene Ontology (GO) analysis for biological processes was performed on this gene set and indicated there is an enrichment of proteins associated with pyruvate metabolic process, rRNA processing, viral processes, etc. The raw data acquired from the GO analysis can be found in the Appendix, Table i. GO analysis was also performed to identify proteins from different molecular functions as shown in Appendix

Table ii. Finally, GO analysis of reactome pathways and cellular compartments involving these proteins were done and are presented in Appendix Table iii and iv, respectively. Results of the GO analyses were screened for categories that pertained to immune function, and pyroptotic cell death. Every category selected as relevant to our study was further investigated. The proteasomal and endoplasmic reticulum related proteins identified were linked to protein turnover due to A_{2B} transfection and were filtered out. Using this method, 27 proteins were identified to be of possible interest listed on Table 8.

Table 8: List of proteins identified from HA-A_{2B} coimmunoprecipitation that are of interest from GO analysis of HEK293T A_{2B} overexpression. Where ** indicate proteins that are exclusively found in A_{2B} transfected cells, highlighted in green are proteins that have been linked to pyroptosis.

Gene Code	**Protein Name**	**Relative increase in HA-A_{2B} group compared to control group.**
CANX	Calnexin	199.05
CLTC	Clathrin heavy chain 1	50.27
ERLIN1	ERLIN1	31.7
LMAN1	Protein ERGIC-53	13.88
GPI	Glucose-6-phosphate isomerase	11.60
GANAB	Neutral alpha-glucosidase AB	11.47
PA2G4	Proliferation-associated protein 2G4	9.09
ERLIN2	ERLIN2	8.41
EIF3A	Eukaryotic translation initiation factor 3 subunit A	7.92
HSP90B1	Endoplasmin	7.01
AUP1	Lipid droplet-regulating VLDL assembly factor AUP1	7.00
PKM	Pyruvate kinase PKM	5.97
HSP90AB1	Heat shock protein HSP 90-beta	5.83
SURF4	Surfeit locus protein 4	5.80
SEC62	Translocation protein SEC62	5.49
SLC1A5	Neutral amino acid transporter B(0)	5.39
CKAP4	Cytoskeleton-associated protein 4	5.25
SLC3A2	4F2 cell-surface antigen heavy chain	5.25
CALR	Calreticulin	**
DSG2	Desmoglein-2	**

EIF4G1	Eukaryotic translation initiation factor 4 gamma 1	**
FLNA	Filamin-A	**
GJA1	Gap junction alpha-1 protein	**
PHB1	Prohibitin-1	**
VCP	Transitional endoplasmic reticulum ATPase	**
ATP6AP1	V-type proton ATPase subunit S1	**
PHB-2	Prohibitin-2	**

Each of the protein listed above was investigated for studies linking them to pyroptosis by query of "[protein name] + pyroptosis" on PUBMED. Out of the 27 proteins, CALR (Calreticulin), EIF4G1 (Eukaryotic Initiation Factor 4G), GJA1 (Gap junction protein alpha 1), PHB1 (Prohibitin-1), VCP (Valosin containing protein), ATP6AP1 (ATPase H+ transporting accessory protein 1), LMAN1 (Lectin, Mannose binding 1), GANAB (Glucosidase II alpha subunit), EIF3A (eukaryotic translation initiation factor 3 subunit A), HSP90AB1 (heat shock protein 90 alpha family class B member 1), SURF4 (surfeit 4), and SLC1A5 (Solute carrier family 1 member 5) were linked to pyroptosis in the database; these are highlighted on Table 8 above. Many of these proteins were identified as "pyroptosis related genes" that are used as a marker to indicate pyroptosis. However, a direct link to pyroptosis has not been established. GJA1, EIF4G1, EIF3A, HSP90AB1, and GANAB are a pyroptotic related genes.[110-113] SURF4 and LMAN1 are both related to the cGAS-STING pathway, that is known to activate and mediate inflammasome activation.[98] CALR is a DAMP, similar to ATP, and stimulate the activation of pyroptosis.[97] PHB1 is a mitochondrial membrane associated protein that can activate the release of mitochondrial DNA, another DAMP, that could stimulate different inflammasomes including NLRP3 and AIM2.[92] The last three proteins directly associate with NLRP3: VCP, SLC1A5 and ATP6AP1.

3.5.2 Proteomic analysis of A_{2B} overexpression on THP-1 macrophages

The same coimmunoprecipitation protocol was performed on THP-1 macrophages and samples were sent for proteomic analysis. Unfortunately, proteomic analysis failed to detect A_{2B} protein in immunoprecipitates from the THP-1 cells. As stated in section 3.4, the western blot for THP-1 cells was not able to detect bands in the coimmunoprecipitated samples, most likely due to lower protein expression. We believe this low expression of A_{2B} protein by THP-1 cells contributed to our proteomic results. However, an enrichment of proteins was still observed with A_{2B} overexpression IP beads. Applying the cut-off of 5x more protein expression, 65 proteins were identified. Additionally, some proteins were exclusively observed in immunoprecipitates from A_{2B} overexpression.

Like HEK293T cells, GO analysis was done on the gene set from THP-1 cells for biological processes, molecular function, cellular component, and reactome pathways. These full data sets can be found in the Appendix, tables v-viii. After selecting categories that are relevant to our studies, the proteins identified in this screening are listed in Table 9. These were investigated for links to pyroptosis and out of the 25 proteins, 11 were identified- highlighted in green below. However, while these findings include interesting and pyroptotic targets, we cannot make the conclusion that they are associated with the A_{2B} as the receptor was not identified in our immunoprecipitate.

Table 9: List of proteins identified to be of interest from GO analysis of THP-1 cells ADORA2B overexpression. Where ** indicate proteins that are exclusively found in A_{2B} transfected cells, highlighted in green are proteins that have been linked to pyroptosis.

Gene Code	**Protein name**	**Relative increase in HA-A_{2B} group compared to control group.**
CTSD	Cathepsin D	232.31
CASP14	Caspase-14	37.95

SERPINB3	Serpin B3	30.93
GSDMA	Gasdermin A	27.61
S100A9	Protein S100-A9	21.36
S100A8	Protein S100-A8	16.58
S100A7	Protein S100-A7	14.14
HPSE	Heparanase	8.96
SYNCRIP	Heterogeneous nuclear ribonucleoprotein Q	6.79
SERPINB12	Serpin B12	5.75
ASAH1	Acid ceramidase	**
CTSA	Cathepsin A	**
CTSK	Cathepsin K	**
DDX17	Probable ATP-dependent RNA helicase DDX17	**
ERP44	Endoplasmic reticulum resident protein 44	**
GM_{2A}	Ganglioside GM2 Activator	**
HNRNPR	Heterogeneous nuclear ribonucleoprotein R	**
IGKV4-1	Immunoglobulin kappa variable 4-1	**
LAMP1	Lysosome-associated membrane glycoprotein 1	**
PLRG1	Pleiotropic regulator 1	**
PRKDC	DNA-dependent protein kinase catalytic subunit	**
RALY	RNA-binding protein Raly	**
RBMX	RNA-binding motif protein, X chromosome	**
S100P	Protein S100-P	**
SLU7	Pre-mRNA splicing factor SLU7	**

Unfortunately, because ADORA2B was not detected in the samples, there is no way to tell if the proteins are enriched through A_{2B} overexpression or our transfection procedures. However, it is interesting that among the top 5 detected proteins were caspase-14 and gasdermin-A, which are protein families involved in pyroptosis. Also found in the top 5 enriched proteins was CTSD that has previously been shown to interact with A_{2A} receptors, listed in Table 1 section

1.2 above. CTSD is a cytosolic and lysosomal cathepsin that degrades and activates the pro-apoptotic protein Bid, resulting in the initiation of apoptosis.[91]

For each of the protein listed above, a query for studies linking them to pyroptosis was performed by searching "[protein name] + pyroptosis" on PUBMED. Out of the 25 proteins, CTSA (cathepsin A), CTSK (Cathepsin K), DDX17 (DEAD-box helicase 17), ERP44 (endoplasmic reticulum resident protein 44), S100P (S100 calcium binding protein P), CTSD (Cathepsin-D), CASP14 (Caspase-14), GSDMA (Gasdermin A), S100A9 (S100 calcium binding protein A9), S100A8 (S100 calcium binding protein A8), and S100A7 (S100 calcium binding protein A7) have been linked to pyroptosis. S100P and S100A7 are pyroptotic related genes.[81, 79] CTSA, CTSK, and CTSD are cathepsins; certain cathepsins have been linked to GSDMD activation.[53] Interestingly, CTSD, has been shown to interact with A_{2A} and inactivates proinflammatory chemokines such as inflammatory protein-1α released by macrophages, overall promoting anti-inflammatory effects.[83] DDX17 is linked to NLRC4 inflammasome activation.[99] ERP44 is being investigated for its inhibition of NLRP3 through cisplatin.[109] Finally, sS100A8 and S100A9 are both directly linked to NLRP3 activation.[96, 99]

4.0 Discussion

4.1 An alternative mechanism contributes to A_{2B} knockdown cells' susceptibility to pyroptosis

Increased susceptibility to pyroptosis was described in A_{2B} knockdown cells by Eudy and da Silva in 2020.[46] In our research, we investigated whether NLRP3 activation is linked to this susceptibility. The results are summarized graphically on Figures 27 and 28, presenting the changes of specific pyroptotic markers in THP-1 cells upon treatments. Figure 28 also highlights which markers were affected differently in knockdown cells.

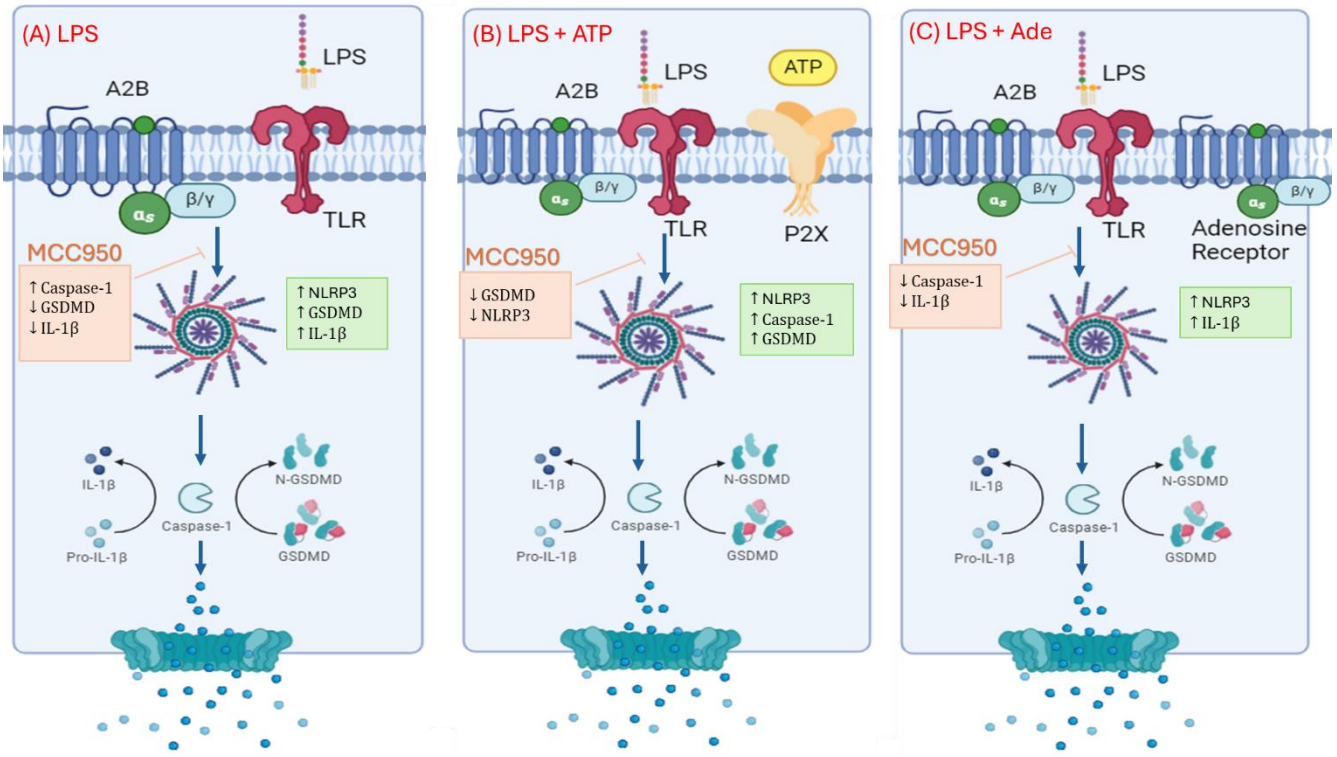

Figure 27: Graphical summary of results in scramble THP-1 cells. Image created in Biorender.

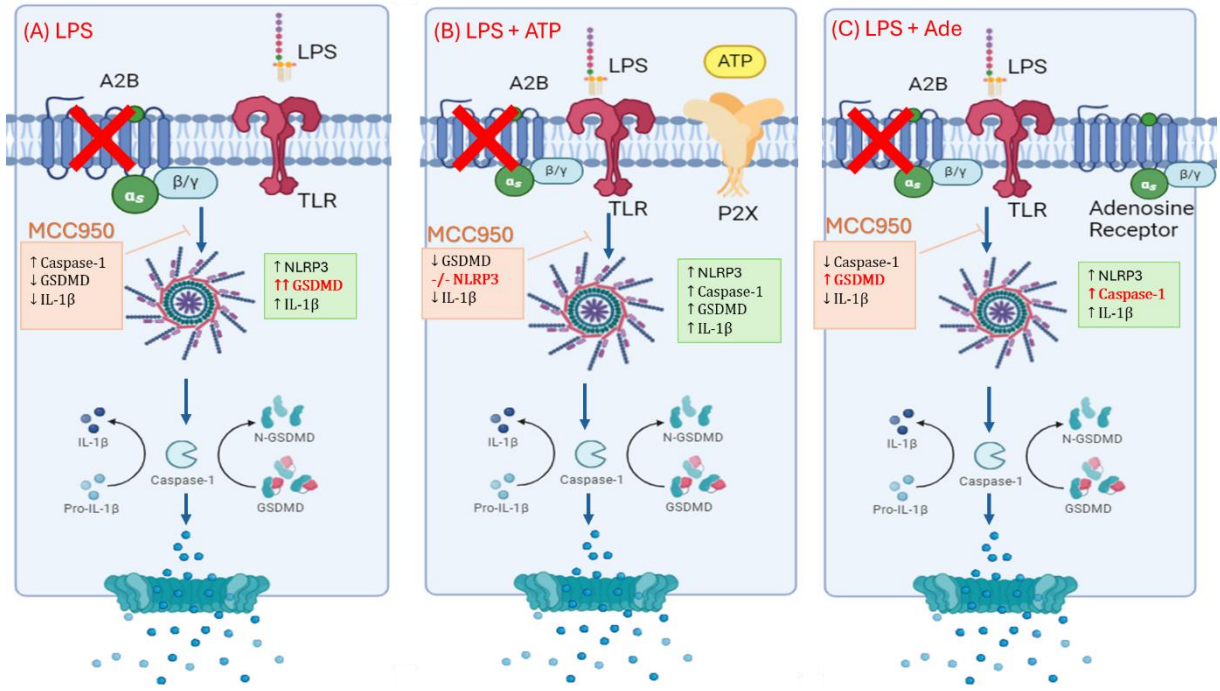

Figure 28: Graphical summary of results in A_{2B} knockdown THP-1 cells. Highlighted in red are pyroptotic markers that were statistically different from scramble cells. Image created in Biorender.

The differences identified between knockdown and scramble cells consistently show increased pyroptotic markers in the A_{2B} knockdown group, confirming Eudy and da Silva's finding that these cells are more prone to pyroptosis.[46] Furthermore, NLRP3 inhibition through MCC950 prevented IL-1β secretion (Figure 13, 17, and 21) in our cells. These results agree with the work of Perrera *et al.* using MCC950 and supports the idea that IL-1β secretion is linked to NLRP3 activity in THP-1 cells.[89] Our knockdown experiments showed that NLRP3 activation is one contributor to A_{2B} deficient macrophages' susceptibility to pyroptosis. However, our results also show that another mechanism may be involved in this susceptibility.

One novel finding from our studies was that LPS-induced GSDMD cleavage was not inhibited by MCC950 in the presence of adenosine (Figure 20). We observed MCC950 inhibition of IL-1β secretion in the same cells, thereby displaying an alternative mechanism that cleaves

GSDMD and is NLRP3 independent. Previous literature suggests that caspase-4 itself binds and cleaves GSDMD,[88] therefore we probed for caspase-4 in our samples.

4.1.1 Adenosine and caspase 4 activation

In our experiments, GSDMD cleavage was not inhibited by MCC950 when treated with adenosine, whereas IL-1β secretion was (Figure 20 and 21), supporting the idea that two independent pathways are occurring simultaneously. Preliminary results suggests that adenosine can induce caspase-4 activation (Figure 22). This poses the possibility of adenosine influencing the non-canonical pathway of pyroptosis. It is known that activated caspase-4 can cleave GSDMD with high affinity.[88] This activation occurs independently from NLRP3 activation; hence this is a plausible explanation to our results in Figures 20 and 21. This has also been observed in a previous study showing adenosine accumulation due to Adenosine Deaminase (ADA) deficiency correlate to increased caspase-4 activation in gastric ulcers and increases inflammation.[106] This finding represents a potential insight into the signalling mechanism through which adenosine can influence pyroptosis and needs further investigation. There is no difference in the intensity of caspase-4 activation between scramble and knockdown cells suggesting that this process is not impacted by the presence of A_{2B} receptor and that a different AR may be involved in this mechanism. Alternatively, an A_{2B} – AR interaction could also be occurring.

Adenosine functions are affected by changes in expression of ARs in the surface and by AR-AR interactions. There are a few examples where AR-AR interaction change ligand binding affinity and alters the resulting cellular response. A_{2A}- A_{2B} receptor interaction studies by Hinz *et al.* showed that when the two receptors are interacting, ligands have less affinity to A_{2A} and changes the sensitivity of the receptor.[90] Furthermore, some studies in the brain indicate that an

A_1-A_{2A} heterodimer preferentially signals through the A_1 receptor at basal, or low levels, of adenosine but increased adenosine concentration changed signalling to go through the A_{2A} receptor.[96, 103] In our studies, perhaps changes in A_{2B} expression or an A_{2B}-AR interaction is regulating pyroptotic response. An increased A_{2B} expression could be protective of pyroptosis while decreased A_{2B} would favor pyroptosis.

4.2 A_{2B} interacting proteins are connected to mechanisms of pyroptosis

4.2.1 A_{2B} interacting proteins in HEK293T cells

In HEK293T cells, proteins related to the pathway of pyroptosis were coimmunoprecipitated with A_{2B} receptors. There were 12 proteins of interest, but most were "pyroptotic related genes". Interestingly, VCP, SLC1A5, and ATP6AP1, have all been shown to affect NLRP3 activity. A previous study showed that symptoms of myopathy, a VCP associated disease, was ameliorated by MCC950.[93, 94] SLC1A5 has been strongly associated in the symptoms of Parkinson's disease and it was shown that inflammation through the activation of NLRP3 by direct binding of SLC1A5 induces these symptoms.[95] Finally, in epithelial lung cells, a part of the SARS-COV-2 (COVID-19) virus binds ATP6AP1, which causes an autophagic flux that activates NLRP3 and contributes to the severity of the signs and symptoms of the infection.[96]

Other proteins identified in Table 8 were related to other mechanisms that may lead to pyroptosis such as cGAS-STING pathway, DAMP signalling, mitochondrial DNA release, and IL-1β secretion; namely, SURF4, PHB1 HSP90AB1, HSP90B1, and SEC62. In THP-1 cells, SURF4 was shown to inhibit apoptosis and caspase-3/caspase-9 activation.[124] Caspase-3 can also activate pyroptosis through cleavage of GSDME, similar to caspase-1 cleaving GSDMD.[125-127]

Furthermore, in macrophages, knockdown of PHB1 affected mitochondrial integrity, thereby increasing IL-1β secretion.[128] Finally, HSP90 is also involved in IL-1β secretion of HEK293T cells, along with SEC61, a protein translocator.[123] Interestingly, our coimmunoprecipitation and proteomic analysis has identified HSP90B1 and HSP90AB1, and although we did not find SEC61, another protein translocator was identified, SEC62. It is possible that A_{2B} performs its protective measures by interacting with these proteins. A_{2B} can interact with SURF4 to inhibit caspase-3 activation, or with PHB1 to protect mitochondrial integrity, or with HSP90 and SEC62 to inhibit IL-1β secretion, thereby decreasing pyroptosis.

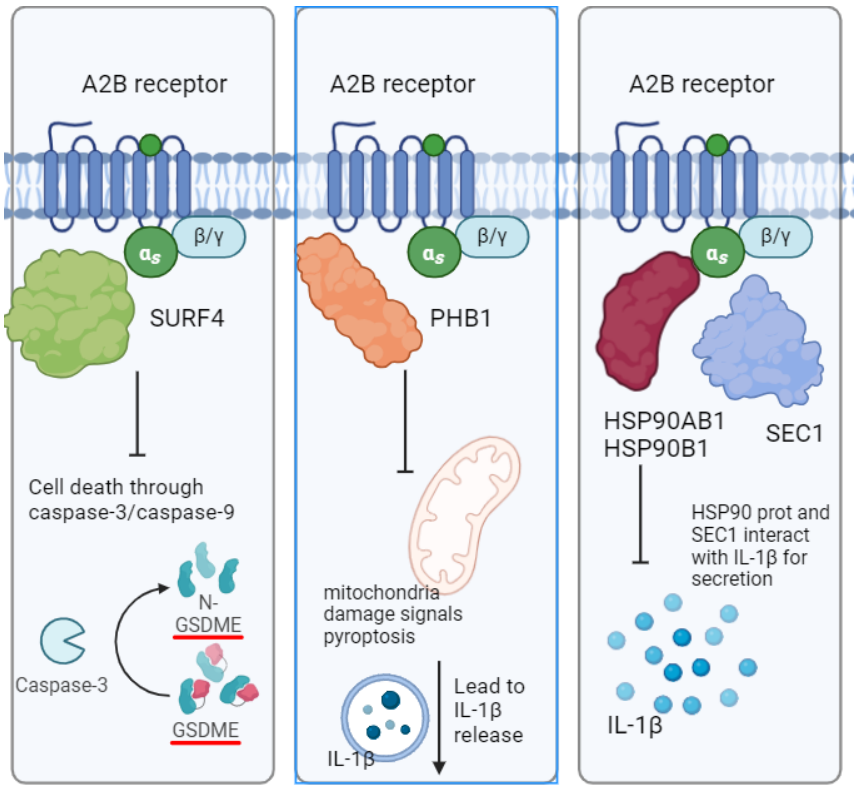

Figure 29: A_{2B} interacting proteins in HEK293T cells, and links to pyroptosis. Image created in Biorender.

It was interesting to find A_{2B} coimmunoprecipitated with proteins that have protective effects in cell survival and linked to pyroptotic processes like caspase-3 activation and IL-1β secretion. These results are encouraging and displays how A_{2B} interacts with many proteins that are related to pyroptosis and could be regulating pyroptosis through these protein-receptor interactions.

4.2.2 A_{2B} interacting proteins in THP-1 cells

In THP-1 cells, the A_{2B} receptor was not detected in proteomic analysis. However, we did detect the vector after transfection through qPCR. The lack of protein detection may have been due to low levels of protein expression, ion suppression of A_{2B} fragments caused by abundance of other proteins in the samples, or a combination of both phenomena. Low protein abundance can be due to high protein degradation or loss of stability. At high levels of mRNA, folding and stability can also interfere with the translation process, preventing the formation of the A_{2B} receptor. A study by Kudla *et al.,* shows that during overexpression, mRNA folding can prevent ribosomal binding thereby affecting protein translation.[122] Despite this fact, we did observe an alteration of protein expression in THP-1 cells treated with the A_{2B} plasmid compared to those treated with stuffer plasmid. 11 of these proteins were identified to be of interest and linked to pyroptosis.

As A_{2B} was not detected in the samples, results cannot be confirmed as due to A_{2B} overexpression, and nothing can be inferred in confidence. However, I will endeavor to postulate on potential roles for some interesting proteins immunoprecipitated from THP-1 cells that contained the A_{2B} vector. As seen in Table 9, some proteins identified in our coimmunoprecipitation studies: CTSK, S100P, S100A7, S100A8, and S100A9, affect TLR signalling, which is linked to the noncanonical pathway of pyroptosis.[110, 87, 108, 120, 107]

Furthermore, DDX17 that was also pulled down, has been identified as a sensor leading to the assembly of an inflammasome comprised of NLRC4, NLRP3, and ASC.[101] Finally, caspase-14 and GSDMA were also identified. Caspase-14 has not been implicated in pyroptosis, though upon discovery in 1998, it used to be called "MICE": mini-interleukin converting-enzyme, based on its similarity to caspase-1 (named ICE at the time).[105] Caspase-14 has been shown to associate with caspase-1 and caspase-4 among other caspases.[105] On the other hand, GSDMA is known to induce pyroptosis through formation of pores on the plasma membrane.[117, 118] Thus far, the protease that cleaves GSDMA has not been identified,[118] but one study has shown that caspase-14 cleaves GSDMA in skin cells of HSV-1 infected mice.[114] Again, though links to pyroptosis were identified here, we cannot conclude that these proteins interact with the A_{2B} protein in THP-1 cells. These theories have limitations, further investigations are required to make conclusions.

4.3 Limitations

Some limitations of this studies include: (a) use of *in vitro* cell lines which may not reflect *in vivo* conditions. Furthermore, these experiments used a cancer cell line, THP-1, which may react differently from primary cells. To accommodate for these limitations, the studies presented in this thesis should be conducted using primary cells.

(b) A_{2B} was not found in proteomic analysis of THP-1 cells which brings about the question of whether the identified proteins are indeed interacting with A_{2B}. It is observable that there is an enrichment of proteins in the IP samples that contain the HA-A_{2B} vector and so it is possible that the HA-tagged A_{2B} expression is too low to detect. There may also have been issues with solubility, stability, mRNA folding and/or localization.

(c) Although HEK293T cells were able to overexpress A_{2B} receptor, this cell line is not an immune cell line and the interacting proteins identified in proteomics may have different purposes outside of immune response.

(d) We hypothesized that an alternate signalling mechanism, apart from AR GPCR function, regulates A_{2B} knockdown pyroptosis which is why we chose to examine protein-protein interactions through proteomics. We chose to use an antibody bound to magnetic bead technology to perform immunoprecipitation, and looked for targets that interact with A_{2B} but could also potentially interact with pyroptotic proteins. Non-specific binding of protein to the beads can be a concern causing high background readings. Because of this, a negative control vector with a non-transcribed scrambled sequence was used.

With these limitations and mitigations in mind, we aimed to elucidate how A_{2B} receptor affects macrophages during inflammation and discover potential mechanisms through which adenosine signalling can influence macrophage pyroptosis.

4.4 Conclusion

In conclusion, this study has confirmed the previous finding that A_{2B} knockdown increases pyroptosis in THP-1 cells[46] and now show that this is largely reduced by NLRP3 inhibition, but we also provide the novel finding that adenosine can activate an alternative mechanism of GSDMD cleavage independent of NLRP3 activation. Based on our results, TLR signalling, noncanonical pyroptosis and AR-AR interactions may be involved. Preliminary results show that caspase-4 was activated by adenosine. Proteomic analysis identified possible targets of protein-protein interactions that affect pyroptosis. Some further studies to compliment the results of this project could be: probing targets in the non-canonical pathway like TLR4, caspase-5; and performing the experiments in primary cell lines as identified in limitations. It

might also be helpful to do a double knockdown of A_{2B} with other adenosine receptors to determine if another AR is responsible for the exacerbation of GSDMD cleavage.

Pyroptotic cell death is an inflammatory mechanism that has evolved to protect the body from pathogens. Researchers are studying how to limit this cell death, as well as how to initiate it for therapeutic purposes. Eudy and da Silva identified A_{2B} as a novel regulator of pyroptosis which inhibits this cell death in macrophages. Our research provided insight into the possible mechanisms by which A_{2B} performs pyroptotic inhibition, and a potential novel role of adenosine in triggering pyroptosis was discovered. However, further research is necessary to investigate these findings.

5.0 References

1. Chen, L., Deng, H., Cui, H., Fang, J., Zuo, Z., Deng, J., Li, Y., Wang, X., & Zhao, L. (2018). Inflammatory responses and inflammation-associated diseases in organs. *Oncotarget*, *9*(6), 7204–7218. https://doi.org/10.18632/oncotarget.23208
2. Janeway, C. A. Jr, Travers, P., Walport, M., & Mark J. Schlomchik. (2001). Immunobiology: The Immune System in Health and Disease (5th ed.). New York: Garland Science. Retrieved from https://www.ncbi.nlm.nih.gov/books/NBK10757/
3. Martín-Orozco, N., Isibasi, A., & Ortiz-Navarrete, V. (2001). Macrophages present exogenous antigens by class I major histocompatibility complex molecules via a secretory pathway as a consequence of interferon-γ activation. *Immunology*, *103*(1), 41–48. https://doi.org/10.1046/j.0019-2805.2001.01226.x
4. Ardura, J. A., Rackov, G., Izquierdo, E., Alonso, V., Gortazar, A. R., & Escribese, M. M. (2019). Targeting macrophages: Friends or foes in disease? *Frontiers in Pharmacology*, *10*, 1255–1255. https://doi.org/10.3389/fphar.2019.01255
5. Tabas, I., & Bornfeldt, K. E. (2016). Macrophage Phenotype and Function in Different Stages of Atherosclerosis. *Circulation Research*, *118*(4), 653–667. https://doi.org/10.1161/CIRCRESAHA.115.306256
6. Steen, E. H., Wang, X., Balaji, S., Butte, M. J., Bollyky, P. L., & Keswani, S. G. (2020). The Role of the Anti-Inflammatory Cytokine Interleukin-10 in Tissue Fibrosis. *Advances in wound care*, *9*(4), 184–198. https://doi.org/10.1089/wound.2019.1032
7. Galluzzi, L., Aaronson, S. A., Abrams, J. M., Alnemri, E. S., Amelio, I., Andrews, D. W., Annicchiarico-Petruzzelli, M., Antonov, A. V., Arama, E., Barlev, N. A., Bazan, N. G., Bianchi, K., Blagosklonny, M. V., Boya, P., Brenner, C., Campanella, M., Candi, E., Carmona-Gutierrez, D., Cecconi, F., … Kroemer, G. (2018). Molecular mechanisms of cell death: Recommendations of the Nomenclature Committee on Cell Death 2018. *Cell Death and Differentiation*, *25*(3), 486–541. https://doi.org/10.1038/s41418-017-0012-4
8. Tang, D., Kang, R., Berghe, T. V., Vandenabeele, P., & Kroemer, G. (2019). The molecular machinery of regulated cell death. *Cell Research*, *29*(5), 347–364. https://doi.org/10.1038/s41422-019-0164-5
9. Wei, X., Xie, F., Zhou, X., Wu, Y., Yan, H., Liu, T., Huang, J., Wang, F., Zhou, F., & Zhang, L. (2022). Role of pyroptosis in inflammation and cancer. *Cellular & Molecular Immunology*, *19*(9), 971–992. https://doi.org/10.1038/s41423-022-00905-x

10. Yu, P., Zhang, X., Liu, N., Tang, L., Peng, C., & Chen, X. (2021). Pyroptosis: mechanisms and diseases. *Signal Transduction and Targeted Therapy*, *6*(1), 128–21. https://doi.org/10.1038/s41392-021-00507-5

11. Zheng, X., Chen, W., Gong, F., Chen, Y., & Chen, E. (2021). The Role and Mechanism of Pyroptosis and Potential Therapeutic Targets in Sepsis: A Review. *Frontiers in Immunology*, *12*, 711939–711939. https://doi.org/10.3389/fimmu.2021.711939

12. Man, S. M., Karki, R., & Kanneganti, T. (2017). Molecular mechanisms and functions of pyroptosis, inflammatory caspases and inflammasomes in infectious diseases. *Immunological Reviews*, *277*(1), 61–75. https://doi.org/10.1111/imr.12534

13. Downs, K. P., Nguyen, H., Dorfleutner, A., & Stehlik, C. (2020). An overview of the non-canonical inflammasome. *Molecular Aspects of Medicine*, *76*, 100924–100924. https://doi.org/10.1016/j.mam.2020.100924

14. van de Veerdonk, F. L., Netea, M. G., Dinarello, C. A., & Joosten, L. A. B. (2011). Inflammasome activation and IL-1β and IL-18 processing during infection. *Trends in Immunology*, *32*(3), 110–116. https://doi.org/10.1016/j.it.2011.01.003

15. Okamoto, M., Liu, W., Luo, Y., Tanaka, A., Cai, X., Norris, D. A., Dinarello, C. A., & Fujita, M. (2010). Constitutively Active Inflammasome in Human Melanoma Cells Mediating Autoinflammation via Caspase-1 Processing and Secretion of Interleukin-1β. *The Journal of Biological Chemistry*, *285*(9), 6477–6488. https://doi.org/10.1074/jbc.M109.064907

16. Wu, J., Lin, S., Wan, B., Velani, B., & Zhu, Y. (2019). Pyroptosis in liver disease: New insights into disease mechanisms. *Aging and Disease*, *10*(5), 1094–1108. https://doi.org/10.14336/AD.2019.0116

17. Zeng, C., Wang, R., & Tan, H. (2019). Role of pyroptosis in cardiovascular diseases and its therapeutic implications. *International Journal of Biological Sciences*, *15*(7), 1345–1357. https://doi.org/10.7150/ijbs.33568

18. Coll, R. C., Schroder, K., & Pelegrín, P. (2022). NLRP3 and pyroptosis blockers for treating inflammatory diseases. *Trends in Pharmacological Sciences (Regular Ed.)*, *43*(8), 653–668. https://doi.org/10.1016/j.tips.2022.04.003

19. Sheth, S., Brito, R., Mukherjea, D., Rybak, L. P., & Ramkumar, V. (2014). Adenosine receptors: Expression, function and regulation. *International Journal of Molecular Sciences*, *15*(2), 2024–2052. https://doi.org/10.3390/ijms15022024

20. Fredholm, B. B., Arslan, G., Halldner, L., Kull, B., Schulte, G., & Wasserman, W. (2000). Structure and function of adenosine receptors and their genes. *Naunyn-Schmiedeberg's Archives of Pharmacology*, *362*(4–5), 364–374. https://doi.org/10.1007/s002100000313

21. Jacobson, K. A., & Gao, Z.-G. (2006). Adenosine receptors as therapeutic targets. *Nature Reviews. Drug Discovery*, *5*(3), 247–264. https://doi.org/10.1038/nrd1983

22. Rosenbaum, D. M., Rasmussen, S. G. F., & Kobilka, B. K. (2009). The structure and function of G-protein-coupled receptors. *Nature*, *459*(7245), 356–363. https://doi.org/10.1038/nature08144

23. Patra C, Foster K, Corley JE, et al. Biochemistry, cAMP. [Updated 2023 Jul 25]. In: StatPearls [Internet]. Treasure Island (FL): StatPearls Publishing; 2024 Jan-. Available from: https://www.ncbi.nlm.nih.gov/books/NBK535431/

24. Zhang, T., Yu-Jing, L., & Ma, T. (2022). The immunomodulatory function of adenosine in sepsis. *Frontiers in Immunology*, *13*, 936547–936547. https://doi.org/10.3389/fimmu.2022.936547

25. Keshwani, M. M., Kanter, J. R., Ma, Y., Wilderman, A., Darshi, M., Insel, P. A., & Taylor, S. S. (2015). Mechanisms of cyclic AMP/protein kinase A- and glucocorticoid-mediated apoptosis using S49 lymphoma cells as a model system. *Proceedings of the National Academy of Sciences - PNAS*, *112*(41), 12681–12686. https://doi.org/10.1073/pnas.1516057112

26. "Protein Kinase C Signaling." Cell Signalling Technology, Cell Signalling Technology, 14 Jan. 2020, www.cellsignal.com/pathways/protein-kinase-c-signaling.

27. Haskó, G., & Pacher, P. (2012). Regulation of Macrophage Function by Adenosine. *Arteriosclerosis, Thrombosis, and Vascular Biology*, *32*(4), 865–869. https://doi.org/10.1161/ATVBAHA.111.226852

28. Haskó, G., Pacher, P., Deitch, E. A., & Vizi, E. S. (2007). Shaping of monocyte and macrophage function by adenosine receptors. *Pharmacology & Therapeutics (Oxford)*, *113*(2), 264–275. https://doi.org/10.1016/j.pharmthera.2006.08.003

29. Pinhal-Enfield, G., Ramanathan, M., Hasko, G., Vogel, S., Salzman, A., Boons, G., & Leibovich, S. (2003). An angiogenic switch in macrophages involving synergy between toll-like receptors 2, 4, 7, and 9 and adenosine A(2A) receptors. *The American Journal of Pathology*, *163*(2), 711–721. https://doi.org/10.1016/S0002-9440(10)63698-X

30. Vergauwen, L., Hespel, P., & Richter, E. A. (1994). Adenosine receptors mediate synergistic stimulation of glucose uptake and transport by insulin and by contractions in rat skeletal muscle. *The Journal of Clinical Investigation*, *93*(3), 974–981. https://doi.org/10.1172/JCI117104

31. Zhong, H., Belardinelli, L., Maa, T., & Zeng, D. (2005). Synergy between A2B adenosine receptors and hypoxia in activating human lung fibroblasts. *American journal of respiratory cell and molecular biology*, *32*(1), 2–8. https://doi.org/10.1165/rcmb.2004-0103OC

32. Ferré, S., Karcz-Kubicha, M., Hope, B. T., Popoli, P., Burgueño, J., Gutiérrez, M. A., Casadó, V., Fuxe, K., Goldberg, S. R., Lluis, C., Franco, R., & Ciruela, F. (2002).

Synergistic Interaction between Adenosine A2A and Glutamate mGlu5 Receptors: Implications for Striatal Neuronal Function. *Proceedings of the National Academy of Sciences - PNAS*, *99*(18), 11940–11945. https://doi.org/10.1073/pnas.172393799

33. Olah, M. E., & Caldwell, C. C. (2003). Adenosine Receptors and Mammalian Toll-Like Receptors: Synergism in Macrophages. *Molecular Interventions*, *3*(7), 370–374. https://doi.org/10.1124/mi.3.7.370

34. Ciruela, F., Albergaria, C., Soriano, A., Cuffí, L., Carbonell, L., Sánchez, S., Gandía, J., & Fernández-Dueñas, V. (2010). Adenosine receptors interacting proteins (ARIPs): Behind the biology of adenosine signaling. *BIOCHIMICA ET BIOPHYSICA ACTA-BIOMEMBRANES*, *1798*(1), 9–20. https://doi.org/10.1016/j.bbamem.2009.10.016

35. Tian, D., Shi, X., & Zhao, Y. (2020). The Effect of A1 Adenosine Receptor in Diabetic Megalin Loss with Caspase-1/IL18 Signaling (vol 12, pg 1583, 2019). *Diabetes, Metabolic Syndrome and Obesity*, *13*, 775–776. https://doi.org/10.2147/DMSO.S250600

36. Bai, H., Zhang, Z., Liu, L., Wang, X., Song, X., & Gao, L. (2022). Activation of adenosine A3 receptor attenuates progression of osteoarthritis through inhibiting the NLRP3/caspase-1/GSDMD induced signalling. *Journal of Cellular and Molecular Medicine*, *26*(15), 4230–4243. https://doi.org/10.1111/jcmm.17438

37. Merighi, S., Nigro, M., Travagli, A., Pasquini, S., Borea, P. A., Varani, K., Vincenzi, F., & Gessi, S. (2022). A2A Adenosine Receptor: A Possible Therapeutic Target for Alzheimer's Disease by Regulating NLRP3 Inflammasome Activity? *International Journal of Molecular Sciences*, *23*(9), 5056-. https://doi.org/10.3390/ijms23095056

38. Xu, S., Wang, J., Zhong, J., Shao, M., Jiang, J., Song, J., Zhu, W., Zhang, F., Xu, H., Xu, G., Zhang, Y., Ma, X., & Lyu, F. (2021). CD73 alleviates GSDMD-mediated microglia pyroptosis in spinal cord injury through PI3K/AKT/Foxo1 signaling. *Clinical and Translational Medicine*, *11*(1), e269-n/a. https://doi.org/10.1002/ctm2.269

39. Thapa, A., Abdelbaset-Ismail, A., Chumak, V., Adamiak, M., Brzezniakiewicz-Janus, K., Ratajczak, J., Kucia, M., & Ratajczak, M. Z. (2022). Extracellular Adenosine (eAdo) - A2B Receptor Axis Inhibits in Nlrp3 Inflammasome-dependent Manner Trafficking of Hematopoietic Stem/progenitor Cells. *Stem Cell Reviews*, *18*(8), 2893–2911. https://doi.org/10.1007/s12015-022-10417-w

40. Xiao, P., Lv, M., Chen, W., Tian, T., & Ren, T. (2021). Adenosine A3 receptor interacts with Gasdermin D to modulate intestinal epithelial cell pyroptosis in ulcerative colitis. *Gastroenterology (New York, N.Y. 1943)*, *160*(3), S31–S31. https://doi.org/10.1053/j.gastro.2021.01.095

41. Eckle, T., Krahn, T., Eltzschig, H. K., Grenz, A., Kohler, D., Mittelbronn, M., Ledent, C., Jacobson, M. A., Osswald, H., Thompson, L. F., & Unertl, K. (2007). Cardioprotection by ecto-5′-nucleotidase (CD73) and A2B adenosine receptors.

Circulation (New York, N.Y.), *115*(12), 1581–1590. https://doi.org/10.1161/CIRCULATIONAHA.106.669697

42. Rao, V. S., Srinivas, K., Sujini, G. N., & Kumar, G. N. S. (2014). Protein-Protein Interaction Detection: Methods and Analysis. *International Journal of Proteomics*, *2014*, 147648–12. https://doi.org/10.1155/2014/147648

43. Sitaraman, S. V., Wang, L., Wong, M., Bruewer, M., Hobert, M., Yun, C.-H., Merlin, D., & Madara, J. L. (2002). The Adenosine 2b Receptor Is Recruited to the Plasma Membrane and Associates with E3KARP and Ezrin upon Agonist Stimulation. *The Journal of Biological Chemistry*, *277*(36), 33188–33195. https://doi.org/10.1074/jbc.M202522200

44. Movsesyan, V. A., Stoica, B. A., & Faden, A. I. (2004). MGLuR5 activation reduces beta-amyloid-induced cell death in primary neuronal cultures and attenuates translocation of cytochrome c and apoptosis-inducing factor. *Journal of neurochemistry*, *89*(6), 1528–1536. https://doi.org/10.1111/j.1471-4159.2004.02451.x

45. Li, G., Zhou, T., Liu, L., Chen, J., Zhao, Z., Peng, Y., Li, P., & Gao, N. (2013). Ezrin dephosphorylation/downregulation contributes to ursolic acid-mediated cell death in human leukemia cells. *Blood Cancer Journal (New York)*, *3*(4), e108–e108. https://doi.org/10.1038/bcj.2013.7

46. Eudy, B. J., & da Silva, R. P. (2021). Systematic deletion of adenosine receptors reveals novel roles in inflammation and pyroptosis in THP-1 macrophages. *Molecular Immunology*, *132*, 1–7. https://doi.org/10.1016/j.molimm.2021.01.018

47. Stutz, A., Kolbe, C. C., Stahl, R., Horvath, G. L., Franklin, B. S., van Ray, O., Brinkschulte, R., Geyer, M., Meissner, F., & Latz, E. (2017). NLRP3 inflammasome assembly is regulated by phosphorylation of the pyrin domain. *The Journal of experimental medicine*, *214*(6), 1725–1736. https://doi.org/10.1084/jem.20160933

48. Italiani, P., & Boraschi, D. (2014). From Monocytes to M1/M2 Macrophages: Phenotypical vs. Functional Differentiation. *Frontiers in immunology*, *5*, 514. https://doi.org/10.3389/fimmu.2014.00514

49. Ameisen, J. C. (2002). On the origin, evolution, and nature of programmed cell death: A timeline of four billion years. *Cell Death and Differentiation*, *9*(4), 367–393. https://doi.org/10.1038/sj.cdd.4400950

50. Kasama, H., Sakamoto, Y., Kasamatsu, A., Okamoto, A., Koyama, T., Minakawa, Y., Ogawara, K., Yokoe, H., Shiiba, M., Tanzawa, H., & Uzawa, K. (2015). Adenosine A2b receptor promotes progression of human oral cancer. *BMC Cancer*, *15*(1), 563–563. https://doi.org/10.1186/s12885-015-1577-2

51. Coll, R. C., Hill, J. R., Day, C. J., Zamoshnikova, A., Boucher, D., Massey, N. L., Chitty, J. L., Fraser, J. A., Jennings, M. P., Robertson, A. A. B., & Schroder, K. (2019). MCC950 directly targets the NLRP3 ATP-hydrolysis motif for inflammasome

inhibition. *Nature Chemical Biology*, *15*(6), 556–559. https://doi.org/10.1038/s41589-019-0277-7

52. Ouyang, X., Ghani, A., Malik, A., Wilder, T., Colegio, O. R., Flavell, R. A., Cronstein, B. N., & Mehal, W. Z. (2013). Adenosine is required for sustained inflammasome activation via the A_2A receptor and the HIF-1α pathway. *Nature Communications*, *4*(1), 2909–2909. https://doi.org/10.1038/ncomms3909

53. Branco, L. M., Amaral, M. P., Boekhoff, H., de Lima, A. B. F., Farias, I. S., Lage, S. L., Pereira, G. J. S., Franklin, B. S., & Bortoluci, K. R. (2022). Lysosomal cathepsins act in concert with Gasdermin-D during NAIP/NLRC4-dependent IL-1β secretion. *Cell Death & Disease*, *13*(12), 1029–10. https://doi.org/10.1038/s41419-022-05476-3

54. Zhou, Y., Zeng, X., Li, G., Yang, Q., Xu, J., Zhang, M., Mao, X., Cao, Y., Wang, L., Xu, Y., Wang, Y., Zhang, Y., Xu, Z., Wu, C., Chen, J., Hoda, M. N., Liu, Z., Hong, M., & Huo, Y. (2019). Inactivation of endothelial adenosine A2A receptors protects mice from cerebral ischaemia-induced brain injury. *British Journal of Pharmacology*, *176*(13), 2250–2263. https://doi.org/10.1111/bph.14673

55. Chambers, E. D., White, A., Vang, A., Wang, Z., Ayala, A., Weng, T., Blackburn, M., Choudhary, G., Rounds, S., & Lu, Q. (2020). Blockade of equilibrative nucleoside transporter 1/2 protects against Pseudomonas aeruginosa–induced acute lung injury and NLRP3 inflammasome activation. *The FASEB Journal*, *34*(1), 1516–1531. https://doi.org/10.1096/fj.201902286R

56. Yuan, X., Mills, T., Doursout, M.-F., Evans, S. E., Vidal Melo, M. F., & Eltzschig, H. K. (2022). Alternative adenosine Receptor activation: The netrin-Adora2b link. *Frontiers in Pharmacology*, *13*, 944994–944994. https://doi.org/10.3389/fphar.2022.944994

57. Fan, Y., Li, J., Huang, L., Wang, K., & Zhao, M. (2022). 7-Methylxanthine Influences the Behavior of ADORA2A-DRD2 Heterodimers in Human Retinal Pigment Epithelial Cells. *Ophthalmic Research*, *65*(6), 678–684. https://doi.org/10.1159/000525563

58. Agustin Leon-Navarro, D., Luis Albasanz, J., & Martin, M. (2019). Functional Cross-Talk between Adenosine and Metabotropic Glutamate Receptors. *Current Neuropharmacology*, *17*(5), 422–437. https://doi.org/10.2174/1570159X16666180416093717

59. Zhang, J. G., Hepburn, L., Cruz, G., Borman, R. A., & Clark, K. L. (2005). The role of adenosine A2A and A2B receptors in the regulation of TNF-α production by human monocytes. *Biochemical Pharmacology*, *69*(6), 883–889. https://doi.org/10.1016/j.bcp.2004.12.008

60. Ferré, S., Quiroz, C., Woods, A. S., Cunha, R., Popoli, P., Ciruela, F., Lluis, C., Franco, R., Azdad, K., & Schiffmann, S. N. (2008). An Update on Adenosine A2A-Dopamine D2 Receptor Interactions: Implications for the Function of G Protein-Coupled

Receptors. *Current Pharmaceutical Design*, *14*(15), 1468–1474. https://doi.org/10.2174/138161208784480108

61. Ferre, S., Ciruela, F., Borycz, J., Solinas, M., Quarta, D., Antoniou, K., Quiroz, C., Justinova, Z., Lluis, C., Franco, R., & Goldberg, S. R. (2008). Adenosine A1-A2A receptor heteromers: new targets for caffeine in the brain. Frontiers in bioscience : a journal and virtual library, 13, 2391–2399. https://doi.org/10.2741/2852

62. Skopál, A., Kéki, T., Tóth, P. Á., Csóka, B., Koscsó, B., Németh, Z. H., Antonioli, L., Ivessa, A., Ciruela, F., Virág, L., Haskó, G., & Kókai, E. (2022). Cathepsin D interacts with adenosine A2A receptors in mouse macrophages to modulate cell surface localization and inflammatory signaling. *The Journal of Biological Chemistry*, *298*(5), 101888–101888. https://doi.org/10.1016/j.jbc.2022.101888

63. Sun, Y., Duan, Y., Eisenstein, A. S., Hu, W., Quintana, A., Lam, W. K., Wang, Y., Wu, Z., Ravid, K., & Huang, P. (2012). A novel mechanism of control of NFκB activation and inflammation involving A2B adenosine receptors. *Journal of Cell Science*, *125*(19), 4507–4517. https://doi.org/10.1242/jcs.105023

64. Lim, B., Jung, K., Gwon, Y., Oh, J. G., Roh, J. il, Hong, S. H., Kho, C., Park, W. J., Lee, H. W., Bae, J. W., & Jung, Y. K. (2019). Cardioprotective role of APIP in myocardial infarction through ADORA2B. *Cell Death & Disease*, *10*(7), 511–513. https://doi.org/10.1038/s41419-019-1746-3

65. Borea, P. A., Gessi, S., Merighi, S., Vincenzi, F., & Varani, K. (2018). Pharmacology of adenosine receptors: The state of the art. *Physiological Reviews*, *98*(3), 1591–1625. https://doi.org/10.1152/physrev.00049.2017

66. Saggu, S., Chen, Y., Chen, L., Pizarro, D., Pati, S., Law, W. J., McMahon, L., Jiao, K., & Wang, Q. (2022). A peptide blocking the ADORA1-neurabin interaction is anticonvulsant and inhibits epilepsy in an Alzheimer's model. *JCI insight*, *7*(11), e155002. https://doi.org/10.1172/jci.insight.155002

67. Milojević, T., Reiterer, V., Stefan, E., Korkhov, V. M., Dorostkar, M. M., Ducza, E., Ogris, E., Boehm, S., Freissmuth, M., & Nanoff, C. (2006). The Ubiquitin-Specific Protease Usp4 Regulates the Cell Surface Level of the A2a Receptor. *Molecular Pharmacology*, *69*(4), 1083–1094. https://doi.org/10.1124/mol.105.015818

68. Hasko, Gyorgy., Cronstein, B. N., & Szabo, C. (2007). *Adenosine receptors : therapeutic aspects for inflammatory and immune diseases*. CRC/Taylor & Francis. https://doi.org/10.1201/9781420005776

69. Ingwersen, J., Wingerath, B., Graf, J., Lepka, K., Hofrichter, M., Schröter, F., Wedekind, F., Bauer, A., Schrader, J., Hartung, H. P., Prozorovski, T., & Aktas, O. (2016). Dual roles of the adenosine A2a receptor in autoimmune neuroinflammation. *Journal of Neuroinflammation*, *13*(1), 48–48. https://doi.org/10.1186/s12974-016-0512-z

70. Haskó, G., Csóka, B., Németh, Z. H., Vizi, E. S., & Pacher, P. (2009). A2B adenosine receptors in immunity and inflammation. *Trends in Immunology*, *30*(6), 263–270. https://doi.org/10.1016/j.it.2009.04.001

71. Italiani, P., & Boraschi, D. (2015). New Insights Into Tissue Macrophages: From Their Origin to the Development of Memory. *Immune network*, *15*(4), 167–176. https://doi.org/10.4110/in.2015.15.4.167

72. Mosser, D. M., & Edwards, J. P. (2008). Exploring the full spectrum of macrophage activation. *Nature reviews. Immunology*, *8*(12), 958–969. https://doi.org/10.1038/nri2448

73. Antonioli, L., Pacher, P., Vizi, E. S., & Haskó, G. (2013). CD39 and CD73 in immunity and inflammation. *Trends in molecular medicine*, *19*(6), 355–367. https://doi.org/10.1016/j.molmed.2013.03.005

74. Fritsch, M., Günther, S. D., Schwarzer, R., Albert, M. C., Schorn, F., Werthenbach, J. P., Schiffmann, L. M., Stair, N., Stocks, H., Seeger, J. M., Lamkanfi, M., Krönke, M., Pasparakis, M., & Kashkar, H. (2019). Caspase-8 is the molecular switch for apoptosis, necroptosis and pyroptosis. *Nature (London)*, *575*(7784), 683–687. https://doi.org/10.1038/s41586-019-1770-6

75. Sarhan, J., Liu, B. C., Muendlein, H. I., Li, P., Nilson, R., Tang, A. Y., Rongvaux, A., Bunnell, S. C., Shao, F., Green, D. R., & Poltorak, A. (2018). Caspase-8 induces cleavage of gasdermin D to elicit pyroptosis during Yersinia infection. *Proceedings of the National Academy of Sciences - PNAS*, *115*(46), E10888–E10897. https://doi.org/10.1073/pnas.1809548115

76. Broz, P., Pelegrín, P., & Shao, F. (2020). The gasdermins, a protein family executing cell death and inflammation. *Nature Reviews. Immunology*, *20*(3), 143–157. https://doi.org/10.1038/s41577-019-0228-2

77. Csóka, Németh, Z. H., Virág, L., Gergely, P., Leibovich, S. J., Pacher, P., Sun, C.-X., Blackburn, M. R., Vizi, E. S., Deitch, E. A., & Haskó, G. (2007). A2A adenosine receptors and C/EBPβ are crucially required for IL-10 production by macrophages exposed to Escherichia coli. Blood, 110(7), 2685–2695. https://doi.org/10.1182/blood-2007-01-065870

78. Haskó, & Cronstein, B. (2013). Regulation of inflammation by adenosine. Frontiers in Immunology, 4, 85–85. https://doi.org/10.3389/fimmu.2013.00085

79. Wang, Z., Bao, A., Liu, S., Dai, F., Gong, Y., & Cheng, Y. (2022). A Pyroptosis-Related Gene Signature Predicts Prognosis and Immune Microenvironment for Breast Cancer Based on Computational Biology Techniques. *Frontiers in genetics*, *13*, 801056. https://doi.org/10.3389/fgene.2022.801056

80. Haas, B., Leonard, F., Ernens, I., Rodius, S., Vausort, M., Rolland-Turner, M., Devaux, Y., & Wagner, D. R. (2011). Adenosine reduces cell surface expression of toll-like

receptor 4 and inflammation in response to lipopolysaccharide and matrix products. *Journal of cardiovascular translational research*, *4*(6), 790–800. https://doi.org/10.1007/s12265-011-9279-x

81. El-Kenawi, A., Berglund, A., Estrella, V., Zhang, Y., Liu, M., Putney, R. M., Yoder, S. J., Johnson, J., Brown, J., & Gatenby, R. (2023). Elevated Methionine Flux Drives Pyroptosis Evasion in Persister Cancer Cells. *Cancer research*, *83*(5), 720–734. https://doi.org/10.1158/0008-5472.CAN-22-1002

82. Kawaguchi, K., & Asano, S. (2022). Pathophysiological Roles of Actin-Binding Scaffold Protein, Ezrin. *International journal of molecular sciences*, *23*(6), 3246. https://doi.org/10.3390/ijms23063246

83. Wolf, M., Clark-Lewis, I., Buri, C., Langen, H., Lis, M., & Mazzucchelli, L. (2003). Cathepsin D specifically cleaves the chemokines macrophage inflammatory protein-1 alpha, macrophage inflammatory protein-1 beta, and SLC that are expressed in human breast cancer. *The American journal of pathology*, *162*(4), 1183–1190. https://doi.org/10.1016/s0002-9440(10)63914-4

84. Souza, C. O. S., Ketelut-Carneiro, N., Milanezi, C. M., Faccioli, L. H., Gardinassi, L. G., & Silva, J. S. (2021). NLRC4 inhibits NLRP3 inflammasome and abrogates effective antifungal CD8+ T cell responses. *iScience*, *24*(6), 102548–102548. https://doi.org/10.1016/j.isci.2021.102548

85. Eckhart, L., & Tschachler, E. (2018). Control of cell death-associated danger signals during cornification prevents autoinflammation of the skin. *Experimental Dermatology*, *27*(8), 884–891. https://doi.org/10.1111/exd.13700

86. Hoste, E., Kemperman, P., Devos, M., Denecker, G., Kezic, S., Yau, N., Gilbert, B., Lippens, S., De Groote, P., Roelandt, R., Van Damme, P., Gevaert, K., Presland, R. B., Takahara, H., Puppels, G., Caspers, P., Vandenabeele, P., & Declercq, W. (2011). Caspase-14 is required for filaggrin degradation to natural moisturizing factors in the skin. *The Journal of investigative dermatology*, *131*(11), 2233–2241. https://doi.org/10.1038/jid.2011.153

87. Wei, W., Ren, J., Yin, W., Ding, H., Lu, Q., Tan, L., Deng, S., Liu, J., Yang, Q., Wang, J., Wang, M., Yue, Y., & Hao, L. (2020). Inhibition of Ctsk modulates periodontitis with arthritis via downregulation of TLR9 and autophagy. Cell proliferation, 53(1), e12722. https://doi.org/10.1111/cpr.12722

88. Wang, K., Sun, Q., Zhong, X., Zeng, M., Zeng, H., Shi, X., Li, Z., Wang, Y., Zhao, Q., Shao, F., & Ding, J. (2020). Structural Mechanism for GSDMD Targeting by Autoprocessed Caspases in Pyroptosis. *Cell*, *180*(5), 941-955.e20. https://doi.org/10.1016/j.cell.2020.02.002

89. Perera, A. P., Fernando, R., Shinde, T., Gundamaraju, R., Southam, B., Sohal, S. S., Robertson, A. A. B., Schroder, K., Kunde, D., & Eri, R. (2018). MCC950, a specific

small molecule inhibitor of NLRP3 inflammasome attenuates colonic inflammation in spontaneous colitis mice. *Scientific Reports*, *8*(1), 8618–15. https://doi.org/10.1038/s41598-018-26775-w

90. Hinz, S., Navarro, G., Borroto-Escuela, D., Seibt, B. F., Ammon, Y. C., de Filippo, E., Danish, A., Lacher, S. K., Červinková, B., Rafehi, M., Fuxe, K., Schiedel, A. C., Franco, R., & Müller, C. E. (2018). Adenosine A2A receptor ligand recognition and signaling is blocked by A2B receptors. *Oncotarget*, *9*(17), 13593–13611. https://doi.org/10.18632/oncotarget.24423

91. Yadati, T., Houben, T., Bitorina, A., & Shiri-Sverdlov, R. (2020). *The Ins and Outs of Cathepsins*: Physiological Function and Role in Disease Management. *Cells*, *9*(7), 1679. https://doi.org/10.3390/cells9071679

92. Liu, H., Fan, H., He, P., Zhuang, H., Liu, X., Chen, M., Zhong, W., Zhang, Y., Zhen, C., Li, Y., Jiang, H., Meng, T., Xu, Y., Zhao, G., & Feng, D. (2022). Prohibitin 1 regulates mtDNA release and downstream inflammatory responses. *The EMBO journal*, *41*(24), e111173. https://doi.org/10.15252/embj.2022111173

93. Nalbandian, A., Khan, A. A., Srivastava, R., Llewellyn, K. J., Tan, B., Shukr, N., Fazli, Y., Kimonis, V. E., & BenMohamed, L. (2017). Activation of the NLRP3 Inflammasome Is Associated with Valosin-Containing Protein Myopathy. *Inflammation*, *40*(1), 21–41. https://doi.org/10.1007/s10753-016-0449-5

94. Liu, Y., Wang, D., Li, T., Yang, F., Li, Z., Bai, X., & Wang, Y. (2022). The role of NLRP3 inflammasome in inflammation-related skeletal muscle atrophy. *Frontiers in Immunology*, *13*, 1035709–1035709. https://doi.org/10.3389/fimmu.2022.1035709

95. Liu, Y., Liu, T., Zhou, Y., Li, W., Wang, M., Song, N., Zhang, W., Jiang, J., Yuan, S., Ding, J., Hu, G., & Lu, M. (2023). Impeding the combination of astrocytic ASCT2 and NLRP3 by talniflumate alleviates neuroinflammation in experimental models of Parkinson's disease. *Acta pharmaceutica Sinica. B*, *13*(2), 662–677. https://doi.org/10.1016/j.apsb.2022.07.021

96. Sun, X., Liu, Y., Huang, Z., Xu, W., Hu, W., Yi, L., Liu, Z., Chan, H., Zeng, J., Liu, X., Chen, H., Yu, J., Chan, F. K. L., Ng, S. C., Wong, S. H., Wang, M. H., Gin, T., Joynt, G. M., Hui, D. S. C., … Wu, W. K. K. (2022). SARS-CoV-2 non-structural protein 6 triggers NLRP3-dependent pyroptosis by targeting ATP6AP1. *Cell Death and Differentiation*, *29*(6), 1240–1254. https://doi.org/10.1038/s41418-021-00916-7

97. Tsuchiya K. (2021). Switching from Apoptosis to Pyroptosis: Gasdermin-Elicited Inflammation and Antitumor Immunity. *International journal of molecular sciences*, *22*(1), 426. https://doi.org/10.3390/ijms22010426

98. Liu, J., Zhou, J., Luan, Y., Li, X., Meng, X., Liao, W., Tang, J., & Wang, Z. (2024). cGAS-STING, inflammasomes and pyroptosis: an overview of crosstalk mechanism of

activation and regulation. *Cell communication and signaling : CCS*, *22*(1), 22. https://doi.org/10.1186/s12964-023-01466-w

99. Netea, M. G., Nold-Petry, C. A., Nold, M. F., Joosten, L. A. B., Opitz, B., van der Meer, J. H. M., van de Veerdonk, F. L., Ferwerda, G., Heinhuis, B., Devesa, I., Funk, C. J., Mason, R. J., Kullberg, B. J., Rubartelli, A., van der Meer, J. W. M., & Dinarello, C. A. (2009). Differential requirement for the activation of the inflammasome for processing and release of IL-1β in monocytes and macrophages. *Blood*, *113*(10), 2324–2335. https://doi.org/10.1182/blood-2008-03-146720

100. Coll, R. C., Robertson, A. A. B., Chae, J. J., Higgins, S. C., Muñoz-Planillo, R., Inserra, M. C., Vetter, I., Dungan, L. S., Monks, B. G., Stutz, A., Croker, D. E., Butler, M. S., Haneklaus, M., Sutton, C. E., Núñez, G., Latz, E., Kastner, D. L., Mills, K. H. G., Masters, S. L., … O'Neill, L. A. J. (2015). A small-molecule inhibitor of the NLRP3 inflammasome for the treatment of inflammatory diseases. *Nature Medicine*, *21*(3), 248–255. https://doi.org/10.1038/nm.3806

101. Wang, S. B., Narendran, S., Hirahara, S., Varshney, A., Pereira, F., Apicella, I., Ambati, M., Ambati, V. L., Yerramothu, P., Ambati, K., Nagasaka, Y., Argyle, D., Huang, P., Baker, K. L., Marion, K. M., Gupta, K., Liu, B., Hinton, D. R., Canna, S. W., Sallam, T., … Ambati, J. (2021). DDX17 is an essential mediator of sterile NLRC4 inflammasome activation by retrotransposon RNAs. *Science immunology*, *6*(66), eabi4493. https://doi.org/10.1126/sciimmunol.abi4493

102. Gurung, P., & Kanneganti, T. D. (2015). Novel roles for caspase-8 in IL-1β and inflammasome regulation. *The American journal of pathology*, *185*(1), 17–25. https://doi.org/10.1016/j.ajpath.2014.08.025

103. Ciruela, F., Casadó, V., Rodrigues, R. J., Luján, R., Burgueño, J., Canals, M., Borycz, J., Rebola, N., Goldberg, S. R., Mallol, J., Cortés, A., Canela, E. I., López-Giménez, J. F., Milligan, G., Lluis, C., Cunha, R. A., Ferré, S., & Franco, R. (2006). Presynaptic control of striatal glutamatergic neurotransmission by adenosine A1-A2A receptor heteromers. *The Journal of neuroscience : the official journal of the Society for Neuroscience*, *26*(7), 2080–2087. https://doi.org/10.1523/JNEUROSCI.3574-05.2006

104. Sroussi, H. Y., Lu, Y., Zhang, Q. L., Villines, D., & Marucha, P. T. (2010). S100A8 and S100A9 inhibit neutrophil oxidative metabolism in-vitro: involvement of adenosine metabolites. *Free radical research*, *44*(4), 389–396. https://doi.org/10.3109/10715760903431434

105. Hu, S., Snipas, S. J., Vincenz, C., Salvesen, G., & Dixit, V. M. (1998). Caspase-14 Is a Novel Developmentally Regulated Protease. *The Journal of Biological Chemistry*, *273*(45), 29648–29653. https://doi.org/10.1074/jbc.273.45.29648

106. Yaguchi, T., Saito, M., Yasuda, Y., & Nishizaki, T. (2010). Caspase-4 activation in association with decreased adenosine deaminase activity may be a factor for gastric ulcer. *Digestion*, *81*(1), 62–67. https://doi.org/10.1159/000252771

107. Liu, T., Zhang, L., Joo, D., & Sun, S. C. (2017). NF-κB signaling in inflammation. *Signal Transduction and Targeted Therapy*, *2*(1), 17023-. https://doi.org/10.1038/sigtrans.2017.23

108. Asagiri, M., Hirai, T., Kunigami, T., Kamano, S., Gober, H.-J., Okamoto, K., Nishikawa, K., Latz, E., Golenbock, D. T., Aoki, K., Ohya, K., Imai, Y., Morishita, Y., Miyazono, K., Kato, S., Saftig, P., & Takayanagi, H. (2008). Cathepsin K-Dependent Toll-Like Receptor 9 Signaling Revealed in Experimental Arthritis. *Science (American Association for the Advancement of Science)*, *319*(5863), 624–627. https://doi.org/10.1126/science.1150110

109. Xia, T., Tian, H., Zhang, K., Zhang, S., Chen, W., Shi, S., & You, Y. (2021). Exosomal ERp44 derived from ER-stressed cells strengthens cisplatin resistance of nasopharyngeal carcinoma. *BMC cancer*, *21*(1), 1003. https://doi.org/10.1186/s12885-021-08712-9

110. Zuo, J., Yi, C., Chen, Z., Zhou, B., Yang, T., & Lin, J. (2022). A novel refined pyroptosis and inflammasome-related genes signature for predicting prognosis and immune microenvironment in pancreatic ductal adenocarcinoma. *Scientific reports*, *12*(1), 18384. https://doi.org/10.1038/s41598-022-22864-z

111. Murao, A., Aziz, M., Wang, H., Brenner, M., & Wang, P. (2021). Release mechanisms of major DAMPs. *Apoptosis : an international journal on programmed cell death*, *26*(3-4), 152–162. https://doi.org/10.1007/s10495-021-01663-3

112. Yu, H., Fu, Y., Tang, Z., Jiang, L., Qu, C., Li, H., Tan, Z., Shu, D., Peng, Y., & Liu, S. (2022). A novel pyroptosis-related signature predicts prognosis and response to treatment in breast carcinoma. *Aging*, *14*(2), 989–1013. https://doi.org/10.18632/aging.203855

113. Wang, B., Shi, M., Yu, C., Pan, H., Shen, H., Du, Y., Zhang, Y., Liu, B., Xi, D., Sheng, J., Huang, H., & Ding, G. (2023). NLRP3 Inflammasome-dependent Pathway is Involved in the Pathogenesis of Polycystic Ovary Syndrome. *Reproductive sciences (Thousand Oaks, Calif.)*, 10.1007/s43032-023-01348-z. Advance online publication. https://doi.org/10.1007/s43032-023-01348-z

114. Li, L., Kovacs, S. B., Jørgensen, I., Larson, H. N., Lazear, H. M., & Miao, E. A. (2022). Role of Caspases and Gasdermin A during HSV-1 Infection in Mice. *Viruses*, *14*(9), 2034-. https://doi.org/10.3390/v14092034

115. Schmid-Burgk, J. L., Gaidt, M. M., Schmidt, T., Ebert, T. S., Bartok, E., & Hornung, V. (2015). Caspase-4 mediates non-canonical activation of the NLRP3 inflammasome in human myeloid cells. *European Journal of Immunology*, *45*(10), 2911–2917. https://doi.org/10.1002/eji.201545523

116. Shalini, S., Dorstyn, L., Dawar, S., & Kumar, S. (2015). Old, new and emerging functions of caspases. *Cell Death and Differentiation*, *22*(4), 526–539. https://doi.org/10.1038/cdd.2014.216

117. Chen, Q., Shi, P., Wang, Y., Zou, D., Wu, X., Wang, D., Hu, Q., Zou, Y., Huang, Z., Ren, J., Lin, Z., & Gao, X. (2019). GSDMB promotes non-canonical pyroptosis by enhancing caspase-4 activity. *Journal of Molecular Cell Biology*, *11*(6), 496–508. https://doi.org/10.1093/jmcb/mjy056

118. Mari, S. A., Pluhackova, K., Pipercevic, J., Leipner, M., Hiller, S., Engel, A., & Müller, D. J. (2022). Gasdermin-A3 pore formation propagates along variable pathways. *Nature Communications*, *13*(1), 2609–2609. https://doi.org/10.1038/s41467-022-30232-8

119. Klijn, C., Durinck, S., Stawiski, E. W., Haverty, P. M., Jiang, Z., Liu, H., Degenhardt, J., Mayba, O., Gnad, F., Liu, J., Pau, G., Reeder, J., Cao, Y., Mukhyala, K., Selvaraj, S. K., Yu, M., Zynda, G. J., Brauer, M. J., Wu, T. D., Gentleman, R. C., … Zhang, Z. (2015). A comprehensive transcriptional portrait of human cancer cell lines. *Nature biotechnology*, *33*(3), 306–312. https://doi.org/10.1038/nbt.3080

120. Yadati, T., Houben, T., Bitorina, A., & Shiri-Sverdlov, R. (2020). *The Ins and Outs of Cathepsins*: Physiological Function and Role in Disease Management. *Cells*, *9*(7), 1679. https://doi.org/10.3390/cells9071679

121. Kayagaki, N., Stowe, I. B., Lee, B. L., O'Rourke, K., Anderson, K., Warming, S., Cuellar, T., Haley, B., Roose-Girma, M., Phung, Q. T., Liu, P. S., Lill, J. R., Li, H., Wu, J., Kummerfeld, S., Zhang, J., Lee, W. P., Snipas, S. J., Salvesen, G. S., … Dixit, V. M. (2015). Caspase-11 cleaves gasdermin D for non-canonical inflammasome signalling. *Nature (London)*, *526*(7575), 666–671. https://doi.org/10.1038/nature15541

122. Kudla, G., Murray, A. W., Tollervey, D., & Plotkin, J. B. (2009). Coding-Sequence Determinants of Gene Expression in Escherichia coli. *Science (American Association for the Advancement of Science)*, *324*(5924), 255–258. https://doi.org/10.1126/science.1170160

123. Zhang, M., Kenny, S. J., Ge, L., Xu, K., & Schekman, R. (2015). Translocation of interleukin-1β into a vesicle intermediate in autophagy-mediated secretion. *eLife*, *4*. https://doi.org/10.7554/eLife.11205

124. Kim, J., Lee, H., Hong, C. M., Nam, J. H., Yeo, H. J., Cho, W. H., Kim, H., Hong, C., Kim, Y. H., & Lee, D. (2023). Novel endogenous endoplasmic reticulum transmembrane protein SURF4 suppresses cell death by negatively regulating the STING-STAT6 axis in myeloid leukemia. *Cancer Communications (London, England)*, *43*(3), 395–399. https://doi.org/10.1002/cac2.12390

125. Jiang, M., Qi, L., Li, L., & Li, Y. (2020). The caspase-3/GSDME signal pathway as a switch between apoptosis and pyroptosis in cancer. *Cell Death Discovery*, *6*(1), 112–112. https://doi.org/10.1038/s41420-020-00349-0

126. Shen, X., Wang, H., Weng, C., Jiang, H., & Chen, J. (2021). Caspase 3/GSDME-dependent pyroptosis contributes to chemotherapy drug-induced nephrotoxicity. *Cell Death & Disease*, *12*(2), 186–16. https://doi.org/10.1038/s41419-021-03458-5

127. Bhat, A. A., Thapa, R., Afzal, O., Agrawal, N., Almalki, W. H., Kazmi, I., Alzarea, S. I., Altamimi, A. S. A., Prasher, P., Singh, S. K., Dua, K., & Gupta, G. (2023). The

pyroptotic role of Caspase-3/GSDME signalling pathway among various cancer: A Review. *International Journal of Biological Macromolecules*, *242*(Pt 2), 124832–124832. https://doi.org/10.1016/j.ijbiomac.2023.124832

128. Liu, H., Fan, H., He, P., Zhuang, H., Liu, X., Chen, M., Zhong, W., Zhang, Y., Zhen, C., Li, Y., Jiang, H., Meng, T., Xu, Y., Zhao, G., & Feng, D. (2022). Prohibitin 1 regulates mtDNA release and downstream inflammatory responses. *The EMBO Journal*, *41*(24), e111173-n/a. https://doi.org/10.15252/embj.2022111173
129. Wu, D., Chen, Y., Sun, Y., Gao, Q., Li, H., Yang, Z., Wang, Y., Jiang, X., & Yu, B. (2020). Target of MCC950 in Inhibition of NLRP3 Inflammasome Activation: a Literature Review. *Inflammation*, *43*(1), 17–23. https://doi.org/10.1007/s10753-019-01098-8
130. Kennedy, C. R., Goya Grocin, A., Kovačič, T., Singh, R., Ward, J. A., Shenoy, A. R., & Tate, E. W. (2021). A Probe for NLRP3 Inflammasome Inhibitor MCC950 Identifies Carbonic Anhydrase 2 as a Novel Target. *ACS Chemical Biology*, *16*(6), 982–990. https://doi.org/10.1021/acschembio.1c00218

6.0 Appendix

The following Tables in this section are raw data acquired from the research.

Table i. Biological processes identified from GO analysis of proteomic analysis of coimmunoprecipitation samples from HEK293T cells transfected with HA-tagged A_{2B} vector and probed with anti-HA beads.

GO biological process complete	Homo sapiens - REFLIST (20592)	# of proteins identified related	expected expression	over/ under	Fold enrichment	raw P-value	FDR
protein folding in endoplasmic reticulum (GO:0034975)	11	3	0.04	+	80.23	1.32E-05	6.14E-03
retrograde protein transport, ER to cytosol (GO:0030970)	18	3	0.06	+	49.03	4.74E-05	1.82E-02
endoplasmic reticulum to cytosol transport (GO:1903513)	18	3	0.06	+	49.03	4.74E-05	1.78E-02
protein exit from endoplasmic reticulum (GO:0032527)	26	3	0.09	+	33.94	1.28E-04	4.00E-02
ubiquitin-dependent ERAD pathway (GO:0030433)	79	8	0.27	+	29.79	5.43E-10	3.97E-07
ERAD pathway (GO:0036503)	98	8	0.33	+	24.01	2.66E-09	1.86E-06
proteasome-mediated ubiquitin-dependent protein catabolic process (GO:0043161)	355	27	1.21	+	22.37	5.66E-29	8.68E-25
neutral amino acid transport (GO:0015804)	54	4	0.18	+	21.79	4.46E-05	1.76E-02
proteasomal protein catabolic process (GO:0010498)	390	27	1.33	+	20.37	6.09E-28	4.67E-24
positive regulation of proteasomal protein catabolic process (GO:1901800)	119	7	0.4	+	17.3	2.31E-07	1.48E-04
pyruvate metabolic process (GO:0006090)	72	4	0.24	+	16.34	1.29E-04	3.96E-02
ubiquitin-dependent protein catabolic process (GO:0006511)	527	27	1.79	+	15.07	1.22E-24	6.26E-21
modification-dependent protein catabolic process (GO:0019941)	538	27	1.83	+	14.76	2.06E-24	7.90E-21
positive regulation of proteolysis involved in protein catabolic process (GO:1903052)	141	7	0.48	+	14.6	6.90E-07	3.92E-04
modification-dependent macromolecule catabolic process (GO:0043632)	549	27	1.87	+	14.47	3.43E-24	1.05E-20
proteolysis involved in protein catabolic process (GO:0051603)	601	27	2.04	+	13.22	3.35E-23	8.56E-20

regulation of proteasomal protein catabolic process (GO:0061136)	198	8	0.67	+	11.89	4.74E-07	2.80E-04
amino acid transport (GO:0006865)	124	5	0.42	+	11.86	7.67E-05	2.74E-02
response to endoplasmic reticulum stress (GO:0034976)	231	9	0.79	+	11.46	1.16E-07	7.77E-05
protein catabolic process (GO:0030163)	715	27	2.43	+	11.11	2.61E-21	5.72E-18
regulation of protein catabolic process (GO:0042176)	373	13	1.27	+	10.25	5.01E-10	3.84E-07
regulation of proteolysis involved in protein catabolic process (GO:1903050)	238	8	0.81	+	9.89	1.80E-06	9.87E-04
positive regulation of protein catabolic process (GO:0045732)	217	7	0.74	+	9.49	1.08E-05	5.51E-03
rRNA processing (GO:0006364)	218	7	0.74	+	9.45	1.11E-05	5.48E-03
macromolecule catabolic process (GO:0009057)	947	29	3.22	+	9.01	1.51E-20	2.90E-17
rRNA metabolic process (GO:0016072)	249	7	0.85	+	8.27	2.55E-05	1.12E-02
organonitrogen compound catabolic process (GO:1901565)	1060	29	3.6	+	8.05	3.02E-19	5.15E-16
viral process (GO:0016032)	256	7	0.87	+	8.04	3.02E-05	1.22E-02
proteolysis (GO:0006508)	1187	30	4.04	+	7.43	5.06E-19	7.07E-16
ribosome biogenesis (GO:0042254)	317	7	1.08	+	6.5	1.12E-04	3.59E-02
organic substance catabolic process (GO:1901575)	1654	34	5.62	+	6.05	4.48E-19	6.89E-16
ribonucleoprotein complex biogenesis (GO:0022613)	462	9	1.57	+	5.73	2.92E-05	1.21E-02
ncRNA processing (GO:0034470)	420	8	1.43	+	5.6	9.75E-05	3.25E-02
ncRNA metabolic process (GO:0034660)	530	10	1.8	+	5.55	1.33E-05	6.00E-03
catabolic process (GO:0009056)	1930	36	6.56	+	5.49	5.31E-19	6.79E-16
regulation of catabolic process (GO:0009894)	1026	16	3.49	+	4.59	2.96E-07	1.82E-04
response to nitrogen compound (GO:1901698)	1060	14	3.6	+	3.89	1.22E-05	5.84E-03
response to organonitrogen compound (GO:0010243)	988	13	3.36	+	3.87	2.72E-05	1.16E-02

protein metabolic process (GO:0019538)	3620	42	12.31	+	3.41	3.28E-15	3.88E-12
regulation of protein metabolic process (GO:0051246)	2230	22	7.58	+	2.9	2.85E-06	1.51E-03
nitrogen compound transport (GO:0071705)	1642	16	5.58	+	2.87	1.06E-04	3.46E-02
organonitrogen compound metabolic process (GO:1901564)	4684	44	15.92	+	2.76	9.27E-13	7.49E-10
macromolecule metabolic process (GO:0043170)	5672	50	19.28	+	2.59	3.41E-14	3.49E-11
gene expression (GO:0010467)	2464	21	8.38	+	2.51	4.79E-05	1.75E-02
response to organic substance (GO:0010033)	2585	21	8.79	+	2.39	9.62E-05	3.28E-02
nitrogen compound metabolic process (GO:0006807)	6402	52	21.76	+	2.39	1.54E-13	1.31E-10
primary metabolic process (GO:0044238)	6966	56	23.68	+	2.36	3.34E-15	3.66E-12
macromolecule biosynthetic process (GO:0009059)	2923	23	9.94	+	2.31	8.50E-05	2.96E-02
organic substance metabolic process (GO:0071704)	7478	56	25.42	+	2.2	1.19E-13	1.07E-10
metabolic process (GO:0008152)	8001	58	27.2	+	2.13	9.66E-14	9.27E-11

Table ii. Molecular functions identified from GO analysis of proteomic analysis from HEK293T cell lysates treated with HA-tagged A_{2B} receptor and probed with anti-HA beads.

GO molecular function complete	Homo sapiens - REFLIST (20592)	# of proteins identified related	expected expression	over/ under	Fold enrichment	raw P-value	FDR
proteasome-activating activity (GO:0036402)	6	6	0.02	+	> 100	1.10E-12	5.60E-09
neutral L-amino acid transmembrane transporter activity (GO:0015175)	46	4	0.16	+	25.58	2.47E-05	1.39E-02
unfolded protein binding (GO:0051082)	122	5	0.41	+	12.06	7.13E-05	3.61E-02
ubiquitin protein ligase binding (GO:0031625)	312	9	1.06	+	8.49	1.33E-06	1.69E-03
cadherin binding (GO:0045296)	326	9	1.11	+	8.12	1.90E-06	1.92E-03
ubiquitin-like protein ligase binding (GO:0044389)	331	9	1.13	+	8	2.14E-06	1.81E-03

ATP hydrolysis activity (GO:0016887)	416	9	1.41	+	6.36	1.30E-05	8.23E-03
cell adhesion molecule binding (GO:0050839)	554	11	1.88	+	5.84	2.91E-06	2.11E-03
RNA binding (GO:0003723)	1682	26	5.72	+	4.55	1.83E-11	4.65E-08
protein binding (GO:0005515)	14435	67	49.07	+	1.37	1.19E-07	2.01E-04
binding (GO:0005488)	16632	68	56.54	+	1.2	9.47E-05	4.37E-02

Table iii. Reactome pathways identified from GO analysis of proteomic analysis from HEK293T cell lysates treated with HA-tagged A_{2B} receptor and probed with anti-HA beads.

Reactome pathways	Homo sapiens - REFLIST (20592)	# of proteins identified related	expected expression	over/ under	Fold enrichment	raw P-value	FDR
Assembly of Viral Components at the Budding Site (R-HSA-168316)	2	2	0.01	+	> 100	6.76E-05	1.07E-03
Virus Assembly and Release (R-HSA-168268)	2	2	0.01	+	> 100	6.76E-05	1.07E-03
Cross-presentation of soluble exogenous antigens (endosomes) (R-HSA-1236978)	49	20	0.17	+	> 100	2.04E-34	6.57E-32
Regulation of activated PAK-2p34 by proteasome mediated degradation (R-HSA-211733)	49	20	0.17	+	> 100	2.04E-34	5.84E-32
Maturation of spike protein (R-HSA-9683686)	5	2	0.02	+	> 100	2.35E-04	3.65E-03
Regulation of ornithine decarboxylase (ODC) (R-HSA-350562)	50	20	0.17	+	> 100	2.85E-34	7.34E-32
AUF1 (hnRNP D0) binds and destabilizes mRNA (R-HSA-450408)	53	21	0.18	+	> 100	6.43E-36	5.52E-33
Autodegradation of the E3 ubiquitin ligase COP1 (R-HSA-349425)	51	20	0.17	+	> 100	3.96E-34	9.27E-32
Vpu mediated degradation of CD4 (R-HSA-180534)	51	20	0.17	+	> 100	3.96E-34	8.50E-32
Ubiquitin-dependent degradation of Cyclin D (R-HSA-75815)	51	20	0.17	+	> 100	3.96E-34	7.84E-32

GSK3B and BTRC:CUL1-mediated-degradation of NFE2L2 (R-HSA-9762114)	51	20	0.17	+	> 100	3.96E-34	7.28E-32
p53-Independent G1/S DNA damage checkpoint (R-HSA-69613)	51	20	0.17	+	> 100	3.96E-34	6.80E-32
p53-Independent DNA Damage Response (R-HSA-69610)	51	20	0.17	+	> 100	3.96E-34	6.37E-32
Ubiquitin Mediated Degradation of Phosphorylated Cdc25A (R-HSA-69601)	51	20	0.17	+	> 100	3.96E-34	6.00E-32
Negative regulation of NOTCH4 signaling (R-HSA-9604323)	52	20	0.18	+	> 100	5.47E-34	7.83E-32
Vif-mediated degradation of APOBEC3G (R-HSA-180585)	52	20	0.18	+	> 100	5.47E-34	7.41E-32
Regulation of Apoptosis (R-HSA-169911)	52	20	0.18	+	> 100	5.47E-34	7.04E-32
Defective CFTR causes cystic fibrosis (R-HSA-5678895)	60	23	0.2	+	> 100	4.25E-39	1.10E-35
Hh mutants are degraded by ERAD (R-HSA-5362768)	55	21	0.19	+	> 100	1.23E-35	7.91E-33
Regulation of RUNX3 expression and activity (R-HSA-8941858)	53	20	0.18	+	> 100	7.52E-34	9.22E-32
FBXL7 down-regulates AURKA during mitotic entry and in early mitosis (R-HSA-8854050)	54	20	0.18	+	> 100	1.03E-33	1.20E-31
Somitogenesis (R-HSA-9824272)	54	20	0.18	+	> 100	1.03E-33	1.15E-31
SCF-beta-TrCP mediated degradation of Emi1 (R-HSA-174113)	54	20	0.18	+	> 100	1.03E-33	1.10E-31
Degradation of AXIN (R-HSA-4641257)	54	20	0.18	+	> 100	1.03E-33	1.06E-31
Stabilization of p53 (R-HSA-69541)	55	20	0.19	+	> 100	1.40E-33	1.38E-31

Hh mutants abrogate ligand secretion (R-HSA-5387390)	58	21	0.2	+	> 100	3.13E-35	1.61E-32
Degradation of DVL (R-HSA-4641258)	56	20	0.19	+	> 100	1.89E-33	1.81E-31
Metabolism of polyamines (R-HSA-351202)	57	20	0.19	+	> 100	2.55E-33	2.35E-31
NIK-->noncanonical NF-kB signaling (R-HSA-5676590)	58	20	0.2	+	> 100	3.42E-33	3.04E-31
SCF(Skp2)-mediated degradation of p27/p21 (R-HSA-187577)	59	20	0.2	+	99.72	4.57E-33	3.93E-31
GLI3 is processed to GLI3R by the proteasome (R-HSA-5610785)	59	20	0.2	+	99.72	4.57E-33	3.80E-31
Degradation of GLI2 by the proteasome (R-HSA-5610783)	59	20	0.2	+	99.72	4.57E-33	3.68E-31
Degradation of GLI1 by the proteasome (R-HSA-5610780)	59	20	0.2	+	99.72	4.57E-33	3.57E-31
Dectin-1 mediated noncanonical NF-kB signaling (R-HSA-5607761)	59	20	0.2	+	99.72	4.57E-33	3.46E-31
Hedgehog ligand biogenesis (R-HSA-5358346)	64	21	0.22	+	96.52	1.80E-34	6.62E-32
Asymmetric localization of PCP proteins (R-HSA-4608870)	63	20	0.21	+	93.39	1.40E-32	1.00E-30
Autodegradation of Cdh1 by Cdh1:APC/C (R-HSA-174084)	63	20	0.21	+	93.39	1.40E-32	9.73E-31
p53-Dependent G1/S DNA damage checkpoint (R-HSA-69580)	64	20	0.22	+	91.93	1.83E-32	1.24E-30
p53-Dependent G1 DNA Damage Response (R-HSA-69563)	64	20	0.22	+	91.93	1.83E-32	1.21E-30

Oxygen-dependent proline hydroxylation of Hypoxia-inducible Factor Alpha (R-HSA-1234176)	65	20	0.22	+	90.51	2.39E-32	1.54E-30
Regulation of RAS by GAPs (R-HSA-5658442)	66	20	0.22	+	89.14	3.10E-32	1.95E-30
Activation of NF-kappaB in B cells (R-HSA-1169091)	66	20	0.22	+	89.14	3.10E-32	1.90E-30
G1/S DNA Damage Checkpoints (R-HSA-69615)	66	20	0.22	+	89.14	3.10E-32	1.86E-30
ABC transporter disorders (R-HSA-5619084)	77	23	0.26	+	87.87	5.55E-37	7.15E-34
APC/C:Cdc20 mediated degradation of Securin (R-HSA-174154)	67	20	0.23	+	87.81	4.02E-32	2.30E-30
Regulation of PTEN stability and activity (R-HSA-8948751)	68	20	0.23	+	86.52	5.19E-32	2.91E-30
Formation of paraxial mesoderm (R-HSA-9793380)	68	20	0.23	+	86.52	5.19E-32	2.85E-30
Orc1 removal from chromatin (R-HSA-68949)	70	20	0.24	+	84.05	8.57E-32	4.60E-30
Regulation of RUNX2 expression and activity (R-HSA-8939902)	70	20	0.24	+	84.05	8.57E-32	4.51E-30
CDK-mediated phosphorylation and removal of Cdc6 (R-HSA-69017)	72	20	0.24	+	81.71	1.40E-31	6.92E-30
Cdc20:Phospho-APC/C mediated degradation of Cyclin A (R-HSA-174184)	72	20	0.24	+	81.71	1.40E-31	6.79E-30

APC:Cdc20 mediated degradation of cell cycle proteins prior to satisfation of the cell cycle checkpoint (R-HSA-179419)	73	20	0.25	+	80.59	1.78E-31	8.47E-30
APC/C:Cdh1 mediated degradation of Cdc20 and other APC/C:Cdh1 targeted proteins in late mitosis/early G1 (R-HSA-174178)	73	20	0.25	+	80.59	1.78E-31	8.32E-30
Cellular response to hypoxia (R-HSA-1234174)	74	20	0.25	+	79.51	2.25E-31	1.02E-29
The role of GTSE1 in G2/M progression after G2 checkpoint (R-HSA-8852276)	78	21	0.27	+	79.2	6.47E-33	4.76E-31
APC/C:Cdc20 mediated degradation of mitotic proteins (R-HSA-176409)	75	20	0.25	+	78.45	2.84E-31	1.26E-29
Activation of APC/C and APC/C:Cdc20 mediated degradation of mitotic proteins (R-HSA-176814)	76	20	0.26	+	77.41	3.58E-31	1.56E-29
Nuclear events mediated by NFE2L2 (R-HSA-9759194)	76	20	0.26	+	77.41	3.58E-31	1.54E-29
Downstream signaling events of B Cell Receptor (BCR) (R-HSA-1168372)	79	20	0.27	+	74.47	7.06E-31	2.98E-29
Regulation of APC/C activators between G1/S and early anaphase (R-HSA-176408)	80	20	0.27	+	73.54	8.80E-31	3.66E-29

Signaling by NOTCH4 (R-HSA-9013694)	80	20	0.27	+	73.54	8.80E-31	3.60E-29
Regulation of mRNA stability by proteins that bind AU-rich elements (R-HSA-450531)	85	21	0.29	+	72.68	3.14E-32	1.84E-30
Degradation of beta-catenin by the destruction complex (R-HSA-195253)	82	20	0.28	+	71.75	1.36E-30	5.39E-29
Cyclin E associated events during G1/S transition (R-HSA-69202)	82	20	0.28	+	71.75	1.36E-30	5.30E-29
Hedgehog 'on' state (R-HSA-5632684)	84	20	0.29	+	70.04	2.08E-30	7.87E-29
Cyclin A:Cdk2-associated events at S phase entry (R-HSA-69656)	84	20	0.29	+	70.04	2.08E-30	7.76E-29
ER-Phagosome pathway (R-HSA-1236974)	90	21	0.31	+	68.64	9.06E-32	4.67E-30
PCP/CE pathway (R-HSA-4086400)	91	21	0.31	+	67.89	1.11E-31	5.62E-30
Regulation of mitotic cell cycle (R-HSA-453276)	87	20	0.3	+	67.63	3.87E-30	1.42E-28
APC/C-mediated degradation of cell cycle proteins (R-HSA-174143)	87	20	0.3	+	67.63	3.87E-30	1.40E-28
MAPK6/MAPK4 signaling (R-HSA-5687128)	88	20	0.3	+	66.86	4.73E-30	1.69E-28
ABC-family proteins mediated transport (R-HSA-382556)	102	23	0.35	+	66.33	1.60E-34	6.87E-32
ATF6 (ATF6-alpha) activates chaperone genes (R-HSA-381183)	9	2	0.03	+	65.37	6.10E-04	9.30E-03

Switching of origins to a post-replicative state (R-HSA-69052)	91	20	0.31	+	64.65	8.58E-30	3.03E-28
Transcriptional regulation by RUNX3 (R-HSA-8878159)	93	20	0.32	+	63.26	1.26E-29	4.40E-28
UCH proteinases (R-HSA-5689603)	95	20	0.32	+	61.93	1.85E-29	6.34E-28
CLEC7A (Dectin-1) signaling (R-HSA-5607764)	96	20	0.33	+	61.29	2.23E-29	7.54E-28
RUNX1 regulates transcription of genes involved in differentiation of HSCs (R-HSA-8939236)	97	20	0.33	+	60.65	2.68E-29	8.96E-28
TNFR2 non-canonical NF-kB pathway (R-HSA-5668541)	98	20	0.33	+	60.03	3.22E-29	1.06E-27
KEAP1-NFE2L2 pathway (R-HSA-9755511)	104	21	0.35	+	59.4	1.35E-30	5.44E-29
Antigen processing-Cross presentation (R-HSA-1236975)	106	21	0.36	+	58.28	1.94E-30	7.44E-29
Downstream TCR signaling (R-HSA-202424)	102	20	0.35	+	57.68	6.59E-29	2.15E-27
Gastrulation (R-HSA-9758941)	104	20	0.35	+	56.57	9.34E-29	3.01E-27
Assembly of the pre-replicative complex (R-HSA-68867)	110	20	0.37	+	53.49	2.56E-28	8.15E-27
ATF6 (ATF6-alpha) activates chaperones (R-HSA-381033)	11	2	0.04	+	53.49	8.61E-04	1.30E-02
Formation of annular gap junctions (R-HSA-196025)	11	2	0.04	+	53.49	8.61E-04	1.29E-02
Interleukin-1 signaling (R-HSA-9020702)	112	20	0.38	+	52.53	3.55E-28	1.12E-26
Hedgehog 'off' state (R-HSA-5610787)	112	20	0.38	+	52.53	3.55E-28	1.10E-26

Transcriptional regulation by RUNX2 (R-HSA-8878166)	117	20	0.4	+	50.29	7.82E-28	2.37E-26
Gap junction degradation (R-HSA-190873)	12	2	0.04	+	49.03	1.00E-03	1.49E-02
HSF1 activation (R-HSA-3371511)	12	2	0.04	+	49.03	1.00E-03	1.48E-02
Synthesis of DNA (R-HSA-69239)	120	20	0.41	+	49.03	1.24E-27	3.67E-26
TCR signaling (R-HSA-202403)	124	20	0.42	+	47.45	2.25E-27	6.58E-26
Host Interactions of HIV factors (R-HSA-162909)	125	20	0.42	+	47.07	2.60E-27	7.53E-26
DNA Replication Pre-Initiation (R-HSA-69002)	127	20	0.43	+	46.33	3.47E-27	9.93E-26
G1/S Transition (R-HSA-69206)	130	20	0.44	+	45.26	5.31E-27	1.50E-25
Beta-catenin independent WNT signaling (R-HSA-3858494)	142	21	0.48	+	43.5	5.04E-28	1.55E-26
PTEN Regulation (R-HSA-6807070)	137	20	0.47	+	42.94	1.38E-26	3.79E-25
C-type lectin receptors (CLRs) (R-HSA-5621481)	138	20	0.47	+	42.63	1.58E-26	4.29E-25
N-glycan trimming in the ER and Calnexin/Calreticulin cycle (R-HSA-532668)	35	5	0.12	+	42.02	2.32E-07	3.80E-06
Signaling by Hedgehog (R-HSA-5358351)	148	21	0.5	+	41.74	1.12E-27	3.35E-26
FCERI mediated NF-kB activation (R-HSA-2871837)	141	20	0.48	+	41.73	2.34E-26	6.10E-25
Disorders of transmembrane transporters (R-HSA-5619115)	173	24	0.59	+	40.81	1.81E-31	8.34E-30
Mitotic G1 phase and G1/S transition (R-HSA-453279)	147	20	0.5	+	40.02	5.03E-26	1.30E-24
G2/M Checkpoints (R-HSA-69481)	149	20	0.51	+	39.49	6.45E-26	1.64E-24

Interleukin-1 family signaling (R-HSA-446652)	150	20	0.51	+	39.22	7.29E-26	1.84E-24
DNA Replication (R-HSA-69306)	155	20	0.53	+	37.96	1.33E-25	3.30E-24
Amino acid transport across the plasma membrane (R-HSA-352230)	32	4	0.11	+	36.77	6.56E-06	1.05E-04
Cytosolic tRNA aminoacylation (R-HSA-379716)	24	3	0.08	+	36.77	1.03E-04	1.61E-03
Processing of SMDT1 (R-HSA-8949664)	16	2	0.05	+	36.77	1.67E-03	2.43E-02
Regulation of expression of SLITs and ROBOs (R-HSA-9010553)	170	21	0.58	+	36.34	1.62E-26	4.35E-25
S Phase (R-HSA-69242)	162	20	0.55	+	36.32	3.00E-25	7.30E-24
Apoptosis (R-HSA-109581)	173	21	0.59	+	35.71	2.27E-26	5.98E-25
Signaling by the B Cell Receptor (BCR) (R-HSA-983705)	169	20	0.57	+	34.81	6.55E-25	1.56E-23
Calnexin/calreticulin cycle (R-HSA-901042)	26	3	0.09	+	33.94	1.28E-04	1.99E-03
G2/M Transition (R-HSA-69275)	195	22	0.66	+	33.19	5.48E-27	1.54E-25
Separation of Sister Chromatids (R-HSA-2467813)	187	21	0.64	+	33.04	1.03E-25	2.57E-24
Mitotic G2-G2/M phases (R-HSA-453274)	197	22	0.67	+	32.85	6.75E-27	1.87E-25
Cellular response to chemical stress (R-HSA-9711123)	193	21	0.66	+	32.01	1.90E-25	4.66E-24
Fc epsilon receptor (FCERI) signaling (R-HSA-2454202)	187	20	0.64	+	31.46	4.26E-24	9.88E-23
Scavenging by Class A Receptors (R-HSA-3000480)	19	2	0.06	+	30.97	2.28E-03	3.28E-02

Programmed Cell Death (R-HSA-5357801)	205	21	0.7	+	30.13	6.15E-25	1.48E-23
TCF dependent signaling in response to WNT (R-HSA-201681)	200	20	0.68	+	29.42	1.48E-23	3.34E-22
Signaling by NOTCH (R-HSA-157118)	200	20	0.68	+	29.42	1.48E-23	3.31E-22
Transcriptional regulation by RUNX1 (R-HSA-8878171)	202	20	0.69	+	29.13	1.78E-23	3.95E-22
Ub-specific processing proteases (R-HSA-5689880)	204	20	0.69	+	28.84	2.14E-23	4.66E-22
Signaling by ROBO receptors (R-HSA-376176)	216	21	0.73	+	28.6	1.70E-24	4.03E-23
Mitotic Anaphase (R-HSA-68882)	227	21	0.77	+	27.21	4.49E-24	1.03E-22
Mitotic Metaphase and Anaphase (R-HSA-2555396)	228	21	0.78	+	27.09	4.89E-24	1.12E-22
HIV Infection (R-HSA-162906)	225	20	0.76	+	26.15	1.32E-22	2.79E-21
Mitochondrial calcium ion transport (R-HSA-8949215)	23	2	0.08	+	25.58	3.23E-03	4.62E-02
Neddylation (R-HSA-8951664)	244	21	0.83	+	25.32	1.84E-23	4.05E-22
RAF/MAP kinase cascade (R-HSA-5673001)	264	21	0.9	+	23.4	8.59E-23	1.84E-21
PIP3 activates AKT signaling (R-HSA-1257604)	252	20	0.86	+	23.35	1.09E-21	2.20E-20
MAPK1/MAPK3 signaling (R-HSA-5684996)	269	21	0.91	+	22.97	1.24E-22	2.64E-21
Cell Cycle Checkpoints (R-HSA-69620)	270	21	0.92	+	22.88	1.33E-22	2.79E-21
Deubiquitination (R-HSA-5688426)	282	21	0.96	+	21.91	3.12E-22	6.44E-21
tRNA Aminoacylation (R-HSA-379724)	42	3	0.14	+	21.01	4.77E-04	7.36E-03

Signaling by WNT (R-HSA-195721)	296	21	1.01	+	20.87	8.06E-22	1.65E-20
Intracellular signaling by second messengers (R-HSA-9006925)	292	20	0.99	+	20.15	1.69E-20	3.35E-19
MAPK family signaling cascades (R-HSA-5683057)	308	21	1.05	+	20.06	1.76E-21	3.53E-20
Antigen processing: Ubiquitination & Proteasome degradation (R-HSA-983168)	308	21	1.05	+	20.06	1.76E-21	3.50E-20
Metabolism of amino acids and derivatives (R-HSA-71291)	370	24	1.26	+	19.08	4.18E-24	9.79E-23
Class I MHC mediated antigen processing & presentation (R-HSA-983169)	382	23	1.3	+	17.71	2.18E-22	4.54E-21
Diseases of signal transduction by growth factor receptors and second messengers (R-HSA-5663202)	418	24	1.42	+	16.89	6.43E-23	1.39E-21
M Phase (R-HSA-68886)	374	21	1.27	+	16.52	7.83E-20	1.53E-18
rRNA modification in the nucleus and cytosol (R-HSA-6790901)	60	3	0.2	+	14.71	1.28E-03	1.88E-02
Signaling by Interleukins (R-HSA-449147)	459	22	1.56	+	14.1	2.25E-19	4.36E-18
Transport of small molecules (R-HSA-382551)	717	31	2.44	+	12.72	2.14E-26	5.68E-25
Cell Cycle, Mitotic (R-HSA-69278)	516	22	1.75	+	12.54	2.45E-18	4.57E-17
Axon guidance (R-HSA-422475)	550	23	1.87	+	12.3	5.31E-19	1.01E-17
RHOG GTPase cycle (R-HSA-9013408)	73	3	0.25	+	12.09	2.19E-03	3.17E-02
Nervous system development (R-HSA-9675108)	575	23	1.95	+	11.77	1.37E-18	2.57E-17

Transport of inorganic cations/anions and amino acids/oligopeptides (R-HSA-425393)	105	4	0.36	+	11.21	5.14E-04	7.88E-03
Neutrophil degranulation (R-HSA-6798695)	478	18	1.62	+	11.08	3.78E-14	6.50E-13
Metabolism of RNA (R-HSA-8953854)	703	25	2.39	+	10.46	4.55E-19	8.69E-18
Viral Infection Pathways (R-HSA-9824446)	784	27	2.67	+	10.13	2.60E-20	5.11E-19
Cell Cycle (R-HSA-1640170)	647	22	2.2	+	10	2.39E-16	4.24E-15
Cytokine Signaling in Immune system (R-HSA-1280215)	714	24	2.43	+	9.89	9.58E-18	1.76E-16
Cellular responses to stress (R-HSA-2262752)	751	24	2.55	+	9.4	2.91E-17	5.24E-16
Cellular responses to stimuli (R-HSA-8953897)	765	24	2.6	+	9.23	4.36E-17	7.80E-16
Adaptive Immune System (R-HSA-1280218)	830	24	2.82	+	8.51	2.59E-16	4.58E-15
Infectious disease (R-HSA-5663205)	975	28	3.31	+	8.45	4.46E-19	8.58E-18
SARS-CoV-1 Infection (R-HSA-9678108)	141	4	0.48	+	8.35	1.49E-03	2.18E-02
Innate Immune System (R-HSA-168249)	1114	28	3.79	+	7.39	1.33E-17	2.43E-16
RHO GTPase cycle (R-HSA-9012999)	448	11	1.52	+	7.22	3.84E-07	6.25E-06
Developmental Biology (R-HSA-1266738)	1143	24	3.89	+	6.18	2.53E-13	4.31E-12
Post-translational protein modification (R-HSA-597592)	1402	28	4.77	+	5.88	4.24E-15	7.32E-14
Asparagine N-linked glycosylation (R-HSA-446203)	305	6	1.04	+	5.79	6.47E-04	9.81E-03
Signaling by Rho GTPases (R-HSA-194315)	669	13	2.27	+	5.72	4.14E-07	6.70E-06

Signaling by Rho GTPases, Miro GTPases and RHOBTB3 (R-HSA-9716542)	684	13	2.33	+	5.59	5.29E-07	8.52E-06
Disease (R-HSA-1643685)	1750	33	5.95	+	5.55	2.46E-17	4.46E-16
Metabolism of proteins (R-HSA-392499)	1918	35	6.52	+	5.37	4.30E-18	7.97E-17
Generic Transcription Pathway (R-HSA-212436)	1209	22	4.11	+	5.35	5.11E-11	8.55E-10
SARS-CoV-2 Infection (R-HSA-9694516)	293	5	1	+	5.02	3.40E-03	4.84E-02
Translation (R-HSA-72766)	294	5	1	+	5	3.45E-03	4.88E-02
RNA Polymerase II Transcription (R-HSA-73857)	1331	22	4.52	+	4.86	3.12E-10	5.19E-09
Immune System (R-HSA-168256)	2068	34	7.03	+	4.84	3.86E-16	6.76E-15
Gene expression (Transcription) (R-HSA-74160)	1494	22	5.08	+	4.33	2.64E-09	4.36E-08
Signal Transduction (R-HSA-162582)	2521	36	8.57	+	4.2	2.56E-15	4.45E-14
Metabolism (R-HSA-1430728)	2086	29	7.09	+	4.09	9.96E-12	1.69E-10
Unclassified (UNCLASSIFIED)	9630	7	32.74	-	0.21	5.09E-11	8.56E-10

Table iv: Cellular components identified from GO analysis of proteomic analysis from HEK293T cell lysates treated with HA-tagged A_{2B} receptor and probed with anti-HA beads.

GO cellular component complete	Homo sapiens - REFLIST (20592)	upload_1 (70)	upload_1 (expected)	upload_1 (over/under)	upload_1 (fold Enrichment)	upload_1 (raw P-value)	upload_1 (FDR)
mitochondrial prohibitin complex (GO:0035632)	2	2	0.01	+	> 100	6.76E-05	2.65E-03
proteasome storage granule (GO:0034515)	2	2	0.01	+	> 100	6.76E-05	2.60E-03

proteasome regulatory particle, base subcomplex (GO:0008540)	12	8	0.04	+	> 100	1.40E-15	1.86E-13
proteasome regulatory particle (GO:0005838)	22	12	0.07	+	> 100	4.37E-22	2.18E-19
proteasome core complex, alpha-subunit complex (GO:0019773)	8	4	0.03	+	> 100	5.86E-08	3.08E-06
proteasome regulatory particle, lid subcomplex (GO:0008541)	8	4	0.03	+	> 100	5.86E-08	3.00E-06
proteasome accessory complex (GO:0022624)	25	12	0.08	+	> 100	1.47E-21	3.25E-19
proteasome core complex (GO:0005839)	20	8	0.07	+	> 100	3.38E-14	3.38E-12
proteasome core complex, beta-subunit complex (GO:0019774)	11	4	0.04	+	> 100	1.60E-07	7.62E-06
proteasome complex (GO:0000502)	64	21	0.22	+	96.52	1.80E-34	3.59E-31
aminoacyl-tRNA synthetase multienzyme complex (GO:0017101)	11	3	0.04	+	80.23	1.32E-05	5.73E-04
endopeptidase complex (GO:1905369)	88	21	0.3	+	70.2	5.97E-32	5.96E-29
sarcoplasmic reticulum lumen (GO:0033018)	10	2	0.03	+	58.83	7.31E-04	2.11E-02
peptidase complex (GO:1905368)	124	21	0.42	+	49.82	3.78E-29	2.51E-26

endoplasmic reticulum quality control compartment (GO:0044322)	15	2	0.05	+	39.22	1.49E-03	4.02E-02
ficolin-1-rich granule lumen (GO:1904813)	124	14	0.42	+	33.21	2.52E-17	3.87E-15
ficolin-1-rich granule (GO:0101002)	185	14	0.63	+	22.26	4.49E-15	5.60E-13
melanosome (GO:0042470)	112	7	0.38	+	18.39	1.56E-07	7.80E-06
pigment granule (GO:0048770)	112	7	0.38	+	18.39	1.56E-07	7.61E-06
polysome (GO:0005844)	73	4	0.25	+	16.12	1.36E-04	5.11E-03
rough endoplasmic reticulum (GO:0005791)	58	3	0.2	+	15.22	1.16E-03	3.23E-02
secretory granule lumen (GO:0034774)	321	16	1.09	+	14.66	1.97E-14	2.31E-12
endoplasmic reticulum-Golgi intermediate compartment membrane (GO:0033116)	81	4	0.28	+	14.53	1.99E-04	6.85E-03
cytoplasmic vesicle lumen (GO:0060205)	324	16	1.1	+	14.53	2.26E-14	2.50E-12
vesicle lumen (GO:0031983)	325	16	1.1	+	14.48	2.36E-14	2.48E-12
P-body (GO:0000932)	100	4	0.34	+	11.77	4.30E-04	1.28E-02
preribosome (GO:0030684)	110	4	0.37	+	10.7	6.09E-04	1.79E-02
azurophil granule (GO:0042582)	154	5	0.52	+	9.55	2.05E-04	6.94E-03
primary lysosome (GO:0005766)	154	5	0.52	+	9.55	2.05E-04	6.82E-03
endoplasmic reticulum protein-containing	127	4	0.43	+	9.27	1.02E-03	2.92E-02

complex (GO:0140534)							
endoplasmic reticulum-Golgi intermediate compartment (GO:0005793)	135	4	0.46	+	8.72	1.28E-03	3.49E-02
intracellular protein-containing complex (GO:0140535)	934	26	3.18	+	8.19	2.51E-17	4.18E-15
cytoplasmic ribonucleoprotein granule (GO:0036464)	255	7	0.87	+	8.08	2.95E-05	1.25E-03
ribonucleoprotein granule (GO:0035770)	272	7	0.92	+	7.57	4.40E-05	1.79E-03
secretory granule (GO:0030141)	904	19	3.07	+	6.18	1.37E-10	9.43E-09
extracellular exosome (GO:0070062)	2101	40	7.14	+	5.6	7.15E-22	2.86E-19
extracellular vesicle (GO:1903561)	2124	40	7.22	+	5.54	1.06E-21	3.53E-19
extracellular organelle (GO:0043230)	2125	40	7.22	+	5.54	1.08E-21	3.08E-19
extracellular membrane-bounded organelle (GO:0065010)	2125	40	7.22	+	5.54	1.08E-21	2.70E-19
secretory vesicle (GO:0099503)	1079	20	3.67	+	5.45	3.53E-10	2.27E-08
catalytic complex (GO:1902494)	1771	29	6.02	+	4.82	1.74E-13	1.65E-11
ribonucleoprotein complex (GO:1990904)	748	11	2.54	+	4.33	4.58E-05	1.83E-03
lytic vacuole (GO:0000323)	757	10	2.57	+	3.89	2.48E-04	7.98E-03
lysosome (GO:0005764)	757	10	2.57	+	3.89	2.48E-04	7.86E-03

vacuole (GO:0005773)	853	11	2.9	+	3.79	1.45E-04	5.37E-03
nucleolus (GO:0005730)	1020	13	3.47	+	3.75	3.77E-05	1.57E-03
cytoplasmic vesicle (GO:0031410)	2523	32	8.58	+	3.73	5.46E-12	4.19E-10
intracellular vesicle (GO:0097708)	2528	32	8.59	+	3.72	5.75E-12	4.25E-10
extracellular space (GO:0005615)	3325	41	11.3	+	3.63	1.13E-15	1.61E-13
vesicle (GO:0031982)	4005	49	13.61	+	3.6	7.98E-20	1.59E-17
extracellular region (GO:0005576)	4281	48	14.55	+	3.3	1.23E-17	2.24E-15
endoplasmic reticulum membrane (GO:0005789)	1196	13	4.07	+	3.2	1.85E-04	6.59E-03
endoplasmic reticulum subcompartment (GO:0098827)	1202	13	4.09	+	3.18	1.94E-04	6.80E-03
nuclear outer membrane-endoplasmic reticulum membrane network (GO:0042175)	1219	13	4.14	+	3.14	2.23E-04	7.28E-03
organelle subcompartment (GO:0031984)	1526	15	5.19	+	2.89	1.66E-04	6.01E-03
supramolecular complex (GO:0099080)	1434	13	4.87	+	2.67	1.03E-03	2.88E-02
nuclear lumen (GO:0031981)	4520	40	15.37	+	2.6	2.04E-10	1.36E-08
organelle lumen (GO:0043233)	5648	49	19.2	+	2.55	1.80E-13	1.64E-11
intracellular organelle lumen (GO:0070013)	5648	49	19.2	+	2.55	1.80E-13	1.57E-11

membrane-enclosed lumen (GO:0031974)	5648	49	19.2	+	2.55	1.80E-13	1.50E-11
nucleoplasm (GO:0005654)	4153	35	14.12	+	2.48	2.75E-08	1.53E-06
cytosol (GO:0005829)	5534	44	18.81	+	2.34	6.09E-10	3.80E-08
protein-containing complex (GO:0032991)	6529	51	22.19	+	2.3	2.16E-12	1.73E-10
endomembrane system (GO:0012505)	4781	34	16.25	+	2.09	5.38E-06	2.39E-04
nucleus (GO:0005634)	7658	51	26.03	+	1.96	2.32E-09	1.36E-07
intracellular non-membrane-bounded organelle (GO:0043232)	5330	32	18.12	+	1.77	3.33E-04	1.02E-02
non-membrane-bounded organelle (GO:0043228)	5331	32	18.12	+	1.77	3.33E-04	1.01E-02
intracellular membrane-bounded organelle (GO:0043231)	12165	66	41.35	+	1.6	4.66E-11	3.32E-09
membrane-bounded organelle (GO:0043227)	13247	67	45.03	+	1.49	6.34E-10	3.83E-08
cytoplasm (GO:0005737)	12158	61	41.33	+	1.48	5.15E-07	2.39E-05
intracellular organelle (GO:0043229)	13299	66	45.21	+	1.46	8.49E-09	4.84E-07
membrane (GO:0016020)	9929	49	33.75	+	1.45	2.80E-04	8.73E-03
organelle (GO:0043226)	14098	67	47.92	+	1.4	3.44E-08	1.86E-06
intracellular anatomical structure (GO:0005622)	14943	67	50.8	+	1.32	1.14E-06	5.18E-05

Table v: Biological processes identified from GO analysis of proteomic analysis from THP-1 cell lysates treated with HA-tagged A_{2B} receptor and probed with anti-HA beads.

GO biological process complete	Homo sapiens - REFLIST (20592)	upload_1 (68)	upload_1 (expected)	upload_1 (over/under)	upload_1 (fold Enrichment)	upload_1 (raw P-value)	upload_1 (FDR)
neutrophil aggregation (GO:0070488)	2	2	0.01	+	> 100	6.38E-05	2.80E-02
sequestering of zinc ion (GO:0032119)	2	2	0.01	+	> 100	6.38E-05	2.72E-02
autocrine signaling (GO:0035425)	7	3	0.02	+	> 100	4.03E-06	4.12E-03
CRD-mediated mRNA stabilization (GO:0070934)	11	3	0.04	+	82.59	1.21E-05	8.07E-03
keratinization (GO:0031424)	83	5	0.27	+	18.24	1.05E-05	7.71E-03
keratinocyte differentiation (GO:0030216)	145	8	0.48	+	16.71	3.82E-08	1.95E-04
rRNA processing (GO:0006364)	218	9	0.72	+	12.5	5.59E-08	1.72E-04
negative regulation of peptidase activity (GO:0010466)	126	5	0.42	+	12.02	7.19E-05	2.90E-02
epidermal cell differentiation (GO:0009913)	211	8	0.7	+	11.48	6.00E-07	1.15E-03
regulation of peptidase activity (GO:0052547)	301	11	0.99	+	11.07	5.57E-09	4.28E-05
rRNA metabolic process (GO:0016072)	249	9	0.82	+	10.95	1.67E-07	3.65E-04
positive regulation of peptidase activity (GO:0010952)	168	6	0.55	+	10.82	2.33E-05	1.19E-02
ribosome biogenesis (GO:0042254)	317	10	1.05	+	9.55	1.11E-07	2.84E-04

regulation of endopeptidase activity (GO:0052548)	278	8	0.92	+	8.71	4.40E-06	4.22E-03
skin development (GO:0043588)	283	8	0.93	+	8.56	5.00E-06	4.27E-03
mRNA splicing, via spliceosome (GO:0000398)	249	7	0.82	+	8.51	2.10E-05	1.20E-02
RNA splicing, via transesterification reactions with bulged adenosine as nucleophile (GO:0000377)	249	7	0.82	+	8.51	2.10E-05	1.15E-02
RNA splicing, via transesterification reactions (GO:0000375)	253	7	0.84	+	8.38	2.32E-05	1.23E-02
ribonucleoprotein complex biogenesis (GO:0022613)	462	12	1.53	+	7.87	4.21E-08	1.62E-04
ncRNA processing (GO:0034470)	420	10	1.39	+	7.21	1.36E-06	1.90E-03
epidermis development (GO:0008544)	345	8	1.14	+	7.02	2.03E-05	1.20E-02
RNA processing (GO:0006396)	882	17	2.91	+	5.84	3.44E-09	5.28E-05
ncRNA metabolic process (GO:0034660)	530	10	1.75	+	5.71	1.02E-05	7.84E-03
regulation of proteolysis (GO:0030162)	605	11	2	+	5.51	4.96E-06	4.48E-03
regulation of hydrolase activity (GO:0051336)	755	11	2.49	+	4.41	3.77E-05	1.76E-02
negative regulation of protein metabolic process (GO:0051248)	874	11	2.89	+	3.81	1.37E-04	4.90E-02
RNA metabolic process (GO:0016070)	1508	18	4.98	+	3.61	1.40E-06	1.79E-03

gene expression (GO:0010467)	2464	23	8.14	+	2.83	2.26E-06	2.67E-03
nucleic acid metabolic process (GO:0090304)	2164	20	7.15	+	2.8	1.53E-05	9.76E-03
negative regulation of macromolecule metabolic process (GO:0010605)	2685	23	8.87	+	2.59	9.64E-06	7.79E-03
regulation of protein metabolic process (GO:0051246)	2230	19	7.36	+	2.58	8.10E-05	3.11E-02
negative regulation of nitrogen compound metabolic process (GO:0051172)	2294	19	7.58	+	2.51	1.18E-04	4.32E-02
negative regulation of metabolic process (GO:0009892)	2902	23	9.58	+	2.4	3.42E-05	1.64E-02
macromolecule biosynthetic process (GO:0009059)	2923	23	9.65	+	2.38	3.84E-05	1.73E-02
nucleobase-containing compound metabolic process (GO:0006139)	2682	21	8.86	+	2.37	1.03E-04	3.85E-02
cellular aromatic compound metabolic process (GO:0006725)	2906	22	9.6	+	2.29	1.39E-04	4.85E-02
cellular nitrogen compound metabolic process (GO:0034641)	3232	24	10.67	+	2.25	7.09E-05	2.94E-02
cellular developmental process (GO:0048869)	3651	27	12.06	+	2.24	1.94E-05	1.19E-02

cell differentiation (GO:0030154)	3648	26	12.05	+	2.16	7.89E-05	3.11E-02
macromolecule metabolic process (GO:0043170)	5672	38	18.73	+	2.03	9.74E-07	1.66E-03
nitrogen compound metabolic process (GO:0006807)	6402	41	21.14	+	1.94	1.03E-06	1.57E-03
primary metabolic process (GO:0044238)	6966	42	23	+	1.83	3.79E-06	4.15E-03
organic substance metabolic process (GO:0071704)	7478	43	24.69	+	1.74	1.07E-05	7.47E-03
metabolic process (GO:0008152)	8001	44	26.42	+	1.67	2.63E-05	1.30E-02

Table vi: Molecular functions identified from GO analysis of proteomic analysis from THP-1 cell lysates treated with HA-tagged A_{2B} receptor and probed with anti-HA beads.

GO molecular function complete	Homo sapiens - REFLIST (20592)	upload_1 (68)	upload_1 (expected)	upload_1 (over/under)	upload_1 (fold Enrichment)	upload_1 (raw P-value)	upload_1 (FDR)
RAGE receptor binding (GO:0050786)	11	3	0.04	+	82.59	1.21E-05	1.53E-02
snoRNA binding (GO:0030515)	32	4	0.11	+	37.85	5.84E-06	1.48E-02
structural molecule activity (GO:0005198)	794	12	2.62	+	4.58	1.12E-05	1.89E-02
RNA binding (GO:0003723)	1682	23	5.55	+	4.14	2.19E-09	1.11E-05
protein binding (GO:0005515)	14435	62	47.67	+	1.3	4.76E-05	4.83E-02

Table vii: Cellular components identified from GO analysis of proteomic analysis from THP-1 cell lysates treated with HA-tagged A_{2B} receptor and probed with anti-HA beads.

GO cellular component complete	Homo sapiens -	upload_1 (68)	upload_1 (expected)	upload_1 (over/under)	upload_1 (fold Enrichment)	upload_1 (raw P-value)	upload_1 (FDR)

	REFLIST (20592)						
mCRD-mediated mRNA stability complex (GO:0106002)	5	2	0.02	+	> 100	2.22E-04	1.01E-02
lamin filament (GO:0005638)	5	2	0.02	+	> 100	2.22E-04	9.84E-03
nuclear lamina (GO:0005652)	13	2	0.04	+	46.59	1.09E-03	3.89E-02
90S preribosome (GO:0030686)	29	3	0.1	+	31.33	1.58E-04	8.30E-03
cornified envelope (GO:0001533)	60	5	0.2	+	25.24	2.36E-06	2.05E-04
catalytic step 2 spliceosome (GO:0071013)	91	6	0.3	+	19.97	7.93E-07	8.33E-05
lysosomal lumen (GO:0043202)	98	6	0.32	+	18.54	1.20E-06	1.19E-04
preribosome (GO:0030684)	110	6	0.36	+	16.52	2.27E-06	2.06E-04
small-subunit processome (GO:0032040)	74	4	0.24	+	16.37	1.27E-04	6.88E-03
specific granule lumen (GO:0035580)	62	3	0.2	+	14.65	1.29E-03	4.51E-02
vacuolar lumen (GO:0005775)	175	8	0.58	+	13.84	1.53E-07	2.03E-05
azurophil granule lumen (GO:0035578)	90	4	0.3	+	13.46	2.62E-04	1.14E-02
SWI/SNF superfamily-type complex (GO:0070603)	94	4	0.31	+	12.89	3.07E-04	1.31E-02
secretory granule lumen (GO:0034774)	321	13	1.06	+	12.26	5.76E-11	2.30E-08
cytoplasmic vesicle lumen (GO:0060205)	324	13	1.07	+	12.15	6.43E-11	2.14E-08
vesicle lumen (GO:0031983)	325	13	1.07	+	12.11	6.68E-11	1.90E-08

keratin filament (GO:0045095)	102	4	0.34	+	11.88	4.14E-04	1.69E-02
azurophil granule (GO:0042582)	154	5	0.51	+	9.83	1.79E-04	8.92E-03
primary lysosome (GO:0005766)	154	5	0.51	+	9.83	1.79E-04	8.71E-03
nuclear matrix (GO:0016363)	128	4	0.42	+	9.46	9.45E-04	3.43E-02
spliceosomal complex (GO:0005681)	208	6	0.69	+	8.74	7.38E-05	4.34E-03
ficolin-1-rich granule (GO:0101002)	185	5	0.61	+	8.18	4.07E-04	1.69E-02
intermediate filament cytoskeleton (GO:0045111)	263	7	0.87	+	8.06	2.96E-05	1.97E-03
intermediate filament (GO:0005882)	227	6	0.75	+	8	1.18E-04	6.53E-03
ribonucleoprotein complex (GO:1990904)	748	16	2.47	+	6.48	2.55E-09	3.92E-07
secretory granule (GO:0030141)	904	16	2.99	+	5.36	3.50E-08	4.99E-06
collagen-containing extracellular matrix (GO:0062023)	429	7	1.42	+	4.94	5.68E-04	2.14E-02
secretory vesicle (GO:0099503)	1079	16	3.56	+	4.49	3.76E-07	4.42E-05
extracellular matrix (GO:0031012)	563	8	1.86	+	4.3	5.58E-04	2.18E-02
external encapsulating structure (GO:0030312)	564	8	1.86	+	4.3	5.64E-04	2.17E-02
nucleolus (GO:0005730)	1020	14	3.37	+	4.16	5.55E-06	4.43E-04
lytic vacuole (GO:0000323)	757	10	2.5	+	4	1.94E-04	9.24E-03
lysosome (GO:0005764)	757	10	2.5	+	4	1.94E-04	9.02E-03

extracellular vesicle (GO:1903561)	2124	28	7.01	+	3.99	4.08E-11	4.08E-08
extracellular organelle (GO:0043230)	2125	28	7.02	+	3.99	4.13E-11	2.75E-08
extracellular membrane-bounded organelle (GO:0065010)	2125	28	7.02	+	3.99	4.13E-11	2.06E-08
extracellular exosome (GO:0070062)	2101	27	6.94	+	3.89	1.90E-10	4.75E-08
vacuole (GO:0005773)	853	10	2.82	+	3.55	4.96E-04	1.98E-02
nuclear protein-containing complex (GO:0140513)	1282	15	4.23	+	3.54	1.62E-05	1.15E-03
extracellular space (GO:0005615)	3325	37	10.98	+	3.37	6.27E-13	1.25E-09
extracellular region (GO:0005576)	4281	37	14.14	+	2.62	1.26E-09	2.10E-07
catalytic complex (GO:1902494)	1771	15	5.85	+	2.56	5.81E-04	2.15E-02
vesicle (GO:0031982)	4005	32	13.23	+	2.42	2.64E-07	3.30E-05
organelle lumen (GO:0043233)	5648	43	18.65	+	2.31	1.12E-09	2.49E-07
intracellular organelle lumen (GO:0070013)	5648	43	18.65	+	2.31	1.12E-09	2.24E-07
membrane-enclosed lumen (GO:0031974)	5648	43	18.65	+	2.31	1.12E-09	2.04E-07
nucleoplasm (GO:0005654)	4153	28	13.71	+	2.04	9.86E-05	5.63E-03
nuclear lumen (GO:0031981)	4520	30	14.93	+	2.01	4.85E-05	3.13E-03
cytosol (GO:0005829)	5534	36	18.27	+	1.97	6.35E-06	4.88E-04
intracellular non-membrane-bounded	5330	33	17.6	+	1.87	7.16E-05	4.47E-03

organelle (GO:0043232)							
non-membrane-bounded organelle (GO:0043228)	5331	33	17.6	+	1.87	7.17E-05	4.34E-03
nucleus (GO:0005634)	7658	44	25.29	+	1.74	6.40E-06	4.73E-04
membrane-bounded organelle (GO:0043227)	13247	62	43.74	+	1.42	6.42E-07	7.13E-05
intracellular membrane-bounded organelle (GO:0043231)	12165	55	40.17	+	1.37	1.74E-04	8.92E-03
intracellular organelle (GO:0043229)	13299	60	43.92	+	1.37	1.78E-05	1.23E-03
organelle (GO:0043226)	14098	63	46.56	+	1.35	2.60E-06	2.16E-04
intracellular anatomical structure (GO:0005622)	14943	65	49.35	+	1.32	1.73E-06	1.65E-04

Table viii: Reactome pathways identified from GO analysis of proteomic analysis from THP-1 cell lysates treated with HA-tagged A_{2B} receptor and probed with anti-HA beads.

Reactome pathways	Homo sapiens - REFLIST (20592)	upload_1 (68)	upload_1 (expected)	upload_1 (over/under)	upload_1 (fold Enrichment)	upload_1 (raw P-value)	upload_1 (FDR)
Metal sequestration by antimicrobial proteins (R-HSA-6799990)	6	3	0.02	+	> 100	2.82E-06	1.46E-03
Formation of the cornified envelope (R-HSA-6809371)	129	6	0.43	+	14.08	5.47E-06	2.35E-03

Neutrophil degranulation (R-HSA-6798695)	478	14	1.58	+	8.87	5.97E-10	1.54E-06
Keratinization (R-HSA-6805567)	217	6	0.72	+	8.37	9.26E-05	2.98E-02
Metabolism of RNA (R-HSA-8953854)	703	13	2.32	+	5.6	5.05E-07	3.25E-04
Innate Immune System (R-HSA-168249)	1114	17	3.68	+	4.62	1.00E-07	1.29E-04
Immune System (R-HSA-168256)	2068	20	6.83	+	2.93	7.80E-06	2.87E-03
Unclassified (UNCLASSIFIED)	9630	11	31.8	-	0.35	1.47E-07	1.27E-04